Schweizerische Eidgenossenschaft
Confédération suisse
Confederazione Svizzera
Confederaziun svizra

Eidgenössisches Departement für Umwelt, Verkehr, Energie und Kommunikation UVEK
Département fédéral de l'environnement, des transports, de l'énergie et de la communication DETEC
Dipartimento federale dell'ambiente, dei trasporti, dell'energia e delle comunicazioni DATEC

Bundesamt für Strassen
Office fédéral des routes
Ufficio federale delle Strade

Improving the durability of low-noise SDA through a multi-scale optimization

Verbesserung der Dauerhaftigkeit von lärmarmen Belägen mit einer multi-skalen Optimierung

Amélioration de la durabilité des enrobés phonoabsorbants SDA grâce à une optimisation multi-échelle

Empa
Lily, D. Poulikakos
Peter Mikhailenko

Grolimund+Partner AG
Erik Bühlmann
Felix Schlatter
Peter Mikhailenko

IMP
Christian Angst
Liliane Huber

Forschungsprojekt TRU_20_01D_01 auf Antrag der Arbeitsgruppe Trassee und Umwelt (TRU)

February 2025 **1788**

Schweizerische Eidgenossenschaft
Confédération suisse
Confederazione Svizzera
Confederaziun svizra

Eidgenössisches Departement für Umwelt, Verkehr, Energie und Kommunikation UVEK
Département fédéral de l'environnement, des transports, de l'énergie et de la communication DETEC
Dipartimento federale dell'ambiente, dei trasporti, dell'energia e delle comunicazioni DATEC

Bundesamt für Strassen
Office fédéral des routes
Ufficio federale delle Strade

Improving the durability of low-noise SDA through a multi-scale optimization

Verbesserung der Dauerhaftigkeit von lärmarmen Belägen mit einer multi-skalen Optimierung

Amélioration de la durabilité des enrobés phonoabsorbants SDA grâce à une optimisation multi-échelle

Empa
Lily, D. Poulikakos
Peter Mikhailenko

Grolimund+Partner AG
Erik Bühlmann
Felix Schlatter
Peter Mikhailenko

IMP
Christian Angst
Liliane Huber

Forschungsprojekt TRU_20_01D_01 auf Antrag der Arbeitsgruppe Trassee und Umwelt (TRU)

February 2025 **1788**

Impressum

Forschungsstelle und Projektteam

Projektleitung
Lily D. Poulikakos, Empa

Mitglieder
Peter Mikhailenko, Empa (bis April 2023), G+P (ab Juni 2023)
Erik Bühlmann, G+P
Felix Schlatter, G+P
Christian Angst, IMP
Liliane Huber, IMP
Pietro Luraschi, IMP (bis August 2023)

Begleitkommission

Präsident
Nicolas Bueche, BFH

Mitglieder
Tobias Balmer, Weibel AG
Hanspeter Gloor, Ehemalige Abteilung Tiefbau Kanton Aargau
Martin Horat, Tiefbauamt ZH
Olga Paperna, Abteilung Tiefbau Kanton Aargau
Fabian Traber, ASTRA
Simon Steiner, BAFU
Michael Strickler, Abteilung Tiefbau Kanton Aargau

Antragsteller

Arbeitsgruppe Trassee und Umwelt (TRU)

Bezugsquelle

Das Dokument kann kostenlos von http://www.mobilityplatform.ch heruntergeladen werden.

Inhaltsverzeichnis

Summary

Introduction
Semi Dense Asphalt (SDA) pavements, known for their effectiveness in reducing noise, are gap graded mixtures widely used for noise abatement. Despite their proven efficacy, there's a pressing need to enhance their mechanical and acoustic durability to ensure cost-effectiveness throughout their shorter life cycle compared to dense mixtures. In Switzerland, SDA pavements serve as established noise mitigation measures. These mixtures, with lower porosity than porous asphalt (PA), offer a promising balance of noise reduction and improved mechanical durability. Switzerland has witnessed the construction of over 1'000 low-noise pavements since 2010, reflecting the practical adoption of SDA technology. Ongoing research and practical experiences have led to advancements in both the mechanical and acoustic performance of these asphalt mixtures. However, concerns persist regarding the long-term durability of these pavements, requiring further investigation into their mechanical and acoustic properties.

Objectives
A recent scientific research carried out under the D-A-CH initiative, specifically showed the importance of the correct selection of the amount and type of the binder for the acoustic durability of the material [33]. However, the D-A-CH project did not provide specific solutions for increasing the durability of SDA. This project was therefore devised for bridging this gap in the knowledge, focusing on the Swiss traffic, climatic and constructive conditions. Having this in mind, the specific goals of this work were:

- Improving the acoustic and mechanical durability of the main SDA used in Switzerland, namely SDA 4, SDA 6 and SDA 8, by optimizing and adapting the mixtures to different traffic and climatic conditions present on the Swiss national and main road network using a multi-scale approach
- Addressing two priority research focuses of ASTRA «TRU 1 - Erhöhung der mechanischen Dauerhaftigkeit und Lärmreduktion von Belägen» as well as «TRU 3-Alterung von Bitumen: Mikrostruktur sowie chemische Zusammensetzung».

Methodology
In order to reach the desired outcome, the work was organized as outlined in Fig. 3, combining the know-how and strengths of the partners involved in the project: Empa, IMP and G+P. The first step was to define the mixtures to be studied, which were selected based on the current state of in-situ performance of low noise pavements as they are known for their good performance in Switzerland. These mixtures were tested for their mechanical and acoustic performance in non-aged and aged states using a multi-scale approach. Thereafter a systematic optimization protocol was applied to these mixtures. Thereby, the best performing mixtures were selected and optimization parameters were identified. The project could uniquely combine knowledge from in-situ long term performance and laboratory performance of low noise pavements. These mixtures as well as the corresponding mastic (filler + bitumen + additive) were tested for their mechanical and acoustic performance partially in non-aged and aged states using a multi-scale approach (mm to km). Thereafter a systematic optimization protocol was applied to these mastics and promising results were applied to the mixture scale. As a result, the best performing mixtures were selected and optimization parameters were identified. These parameters were applied in the m-scale slabs in order to determine the mechanical and acoustic performance. The proposed project could uniquely combine knowledge from in-situ long term performance and laboratory performance of low noise pavements. To this end five work packages (WP) were conceived to reach the project goals.

- In "WP1: Characterization of unaged and aged SDA 4, SDA 6, SDA 8 (cm scale)", the mechanical properties of benchmark mastics and mixtures were examined. Mechanical performance of aged materials were determined and used as a benchmark. Aging was

performed with short-term oven aging (STOA), which replicates in the laboratory the aging that the mixture experiences during production, by exposing loose mix to 135°C for 4 hours. Mechanical performance tests on asphalt mixtures were the indirect tensile strength (ITS) and water sensitivity (ITSR), modulus, fatigue and the cyclic compression test. On the mastic the performance tests included fatigue and frequency at low temperature and complex modulus and phase angle at high temperature

- In "*WP2: Statistical analysis of long-term performance of SDA mixtures in Switzerland (km scale)*", the G+P database on the in-situ acoustic performance of SDA pavements in Switzerland was analyzed. Based on this extensive empirical data, the acoustic aging behavior of the in-situ measurements was first examined, and an aging model for various formulations (standard mixtures) was developed. Additionally, acoustically durable pavements were identified, and the corresponding formulations were analyzed. This allowed the most promising formulations from the field to be traced back to WP1, serving as a basis for the optimization steps.
- in "*WP3: Optimization and characterization of low noise pavements (µm-cm scale)"* the mastic and mixtures were modified and characterized; and the best mixtures were selected Benchmark samples of optimized SDA mixtures were produced. These laboratory-produced mixtures have to perform as required on the road and the target was to show that the imparted properties from the optimization processes listed above do not compromise their performance including durability and water sensitivity. Using tests that are routinely used in Switzerland and others that are not routinely used. As standard requirement, water sensitivity (ITSR) was investigated. As non-standard test, fatigue, complex modulus and Frequency and Temperature sweep test on the mastic, fracture resistance using the Semi-Circular Bend (SCB) test, rutting and cyclic compression test as well as particle loss using the micro-Deval were used
- in "*WP4: Large scale durability testing of optimized mixtures (m scale)*" were mechanically and acoustically examined on a m-scale. using the traffic simulator MMLS3. Selected solutions were constructed in the laboratory in the form of large test slabs (1.5m×0.5m) and tested until failure using the vehicle load simulator MMLS3, resulting in knowledge on pavement response from traffic loading. Using this type of simulator, monitoring of pavement performance under traffic load was investigated. The traffic simulation process accompanied various acoustically relevant measurements i.e., surface texture, sound absorption, as well as simulations to gather detailed insights in the traffic simulation process. As direct acoustic measurements during the traffic simulation is not possible due to the intrinsic sound generation of the MMLS3, for the purpose of acoustic simulations and performance predictions the an approach using the program SPERoN was selected and the detailed analysis of noise generation mechanisms were used. SPERoN allows for predictions of the acoustic performance if constructed on real road sections by contact force, airflow and sound propagation models, which are fed by surface characteristics data from laboratory measurements (texture, airflow resistance and sound absorption). The acoustic properties of aged mixtures was characterized by type and amount of filler and sand, durability of accessible voids as well as absorption durability (using impedance tube, ISO 10534-2) was performed on large slabs that represent the field situation. Mixture and surface characteristics (using a laser scanner) and how these change with ageing at different stages during the ageing experiments were measured and analyzed. Computed Tomography (CT) was used to characterize connected voids as well as surface characteristics. The compaction method used in the laboratory has a great influence on the shape of the pores as well as the texture. To ensure that the mixtures also have the required acoustical properties, the laboratory-compacted samples are analyzed regarding their acoustically effective void content using Acoustic Void Content Analysis AVCA, developed by G+P.
- Finally, "*WP5: Dissemination*" dealt with the publication of the results and findings.

The graphic overview of the activities are presented in Fig. 5.

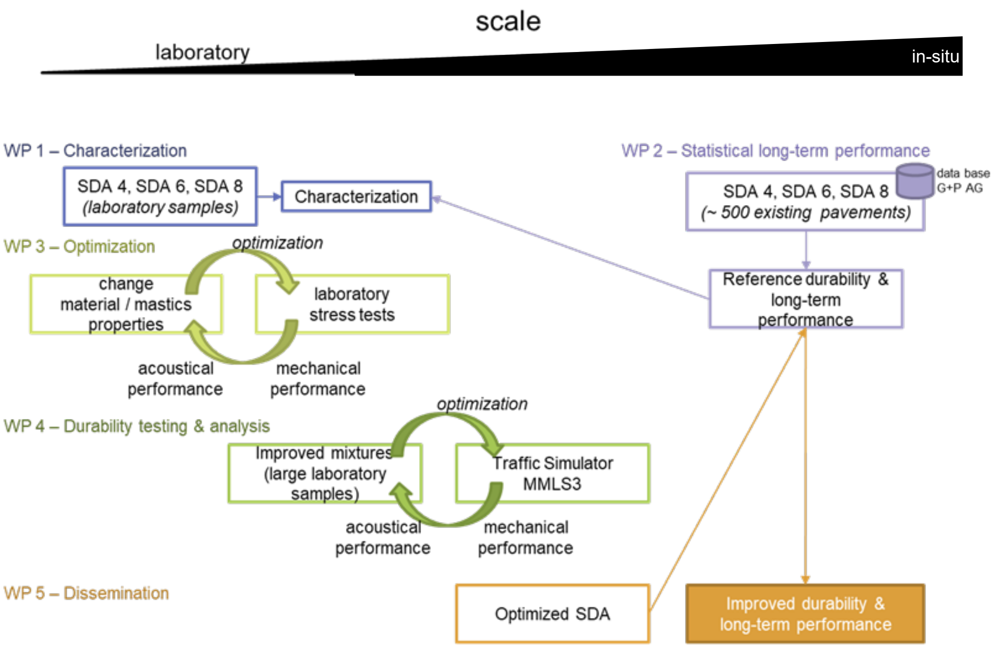

***Fig. 3** Schematic of the planned research*

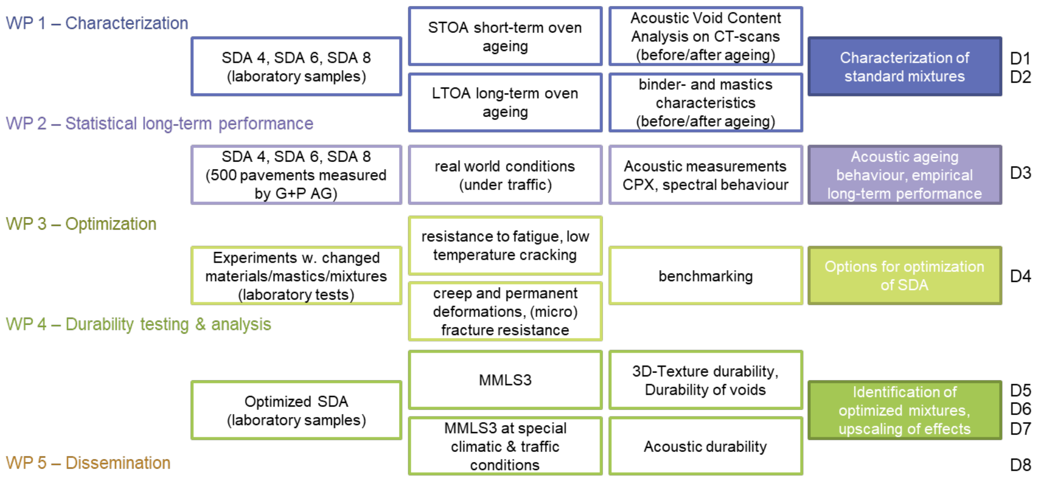

***Fig. 5** Overview of research plan*

Results

To date, acoustic measurements using Close-Proximity (CPX) noise (ISO 11819-2) are available for around 200 different SDA pavements. These measurements include not only acoustic data but also corresponding mixture information and drill core data, totaling approximately 1'000 combined data points. This data was collected in a database and was available for this project, allowing for the determination of acoustic aging based on the installed formulations. As a result of the data analysis, a void content of 15% was recommended for this project to maintain a balance between acoustic and mechanical durability. Additionally, the database analysis enabled the selection of pavement types and mixture formulations that had proven to be acoustically effective in practice. This allowed for the identification of specific mixture formulations for SDA 4, SDA 6, and SDA 8 that exhibit good acoustic properties. Fig. 12 shows a determined aging model of the acoustic effect of pavements based on the void content over the years. This was used as a basis for selecting pavement formulations. Subsequently, the mechanical and acoustic performances of the laboratory-aged materials (mastic and mixture) were determined and used as benchmarks (WP1).

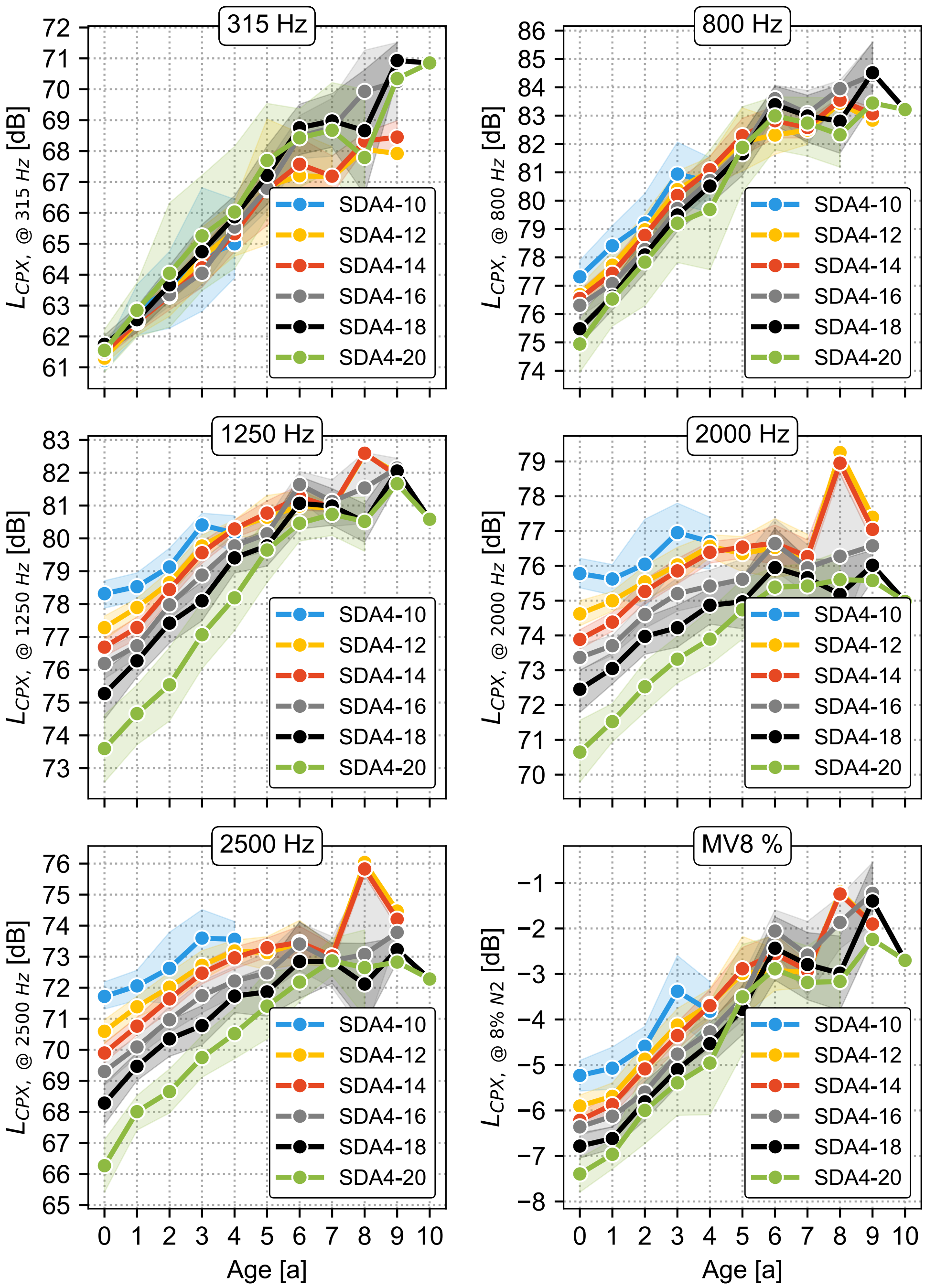

***Fig. 12** In-situ spectral ageing of CPX-Levels of different void content groups of SDA 4-mixtures. Differentiated per Marshall-Void content i.e SDA 4-10 corresponds to SDA 4 pavements with Marshall void content in the range of 8-12 Vol-%*

A multi-scale experimental method was utilized to investigate the performance of these mixtures more efficiently. First various binder, filler and additive combinations were investigated in the mastic scale (mm-scale) within WP1 (Benchmark) and WP3 (Modified). Fig. 35 shows an example of the complex modulus and phase angle of aged mastics using various filler combinations. It is clear that the combination of high modulus binder (HM) and

Zeobit filler improved the properties of the mastic at aged state especially above 30°C. For this scale, three options were identified for further investigation.

- **M1:** PmB 45/80-80HiMa + Zeobit
- **M2**: PmB 45/80-80HiMa + Limestone
- **M3:** PmB 45/80-80HiMa +Zeobit+ Hydrated lime

From the knowledge gained mixtures were fabricated for the cm-scale investigations within WP1 and WP3. Conventional and non-conventional experiments were performed namely, indirect tensile strength, cyclic compression, semi-circular bend, complex modulus and fatigue. Fig. 38 shows an example of the mechanical tests at the cm scale showing SDA 4 benchmark and three modified mixtures. Similarly, fatigue test, related to the expected mechanical performance of the materials over time, is presented in Fig. 52. The results show that the modified mixtures pass the water sensitivity requirement of 70%. From the cm-scale results mixtures were further selected for the m-scale laboratory investigations in WP4. Particle loss can be an important problem for these types of pavements. The modified -Micro-Deval test was performed on all mixtures, as shown in Fig. 53. The results indicate that the particle loss of the modified mixtures could not be improved.

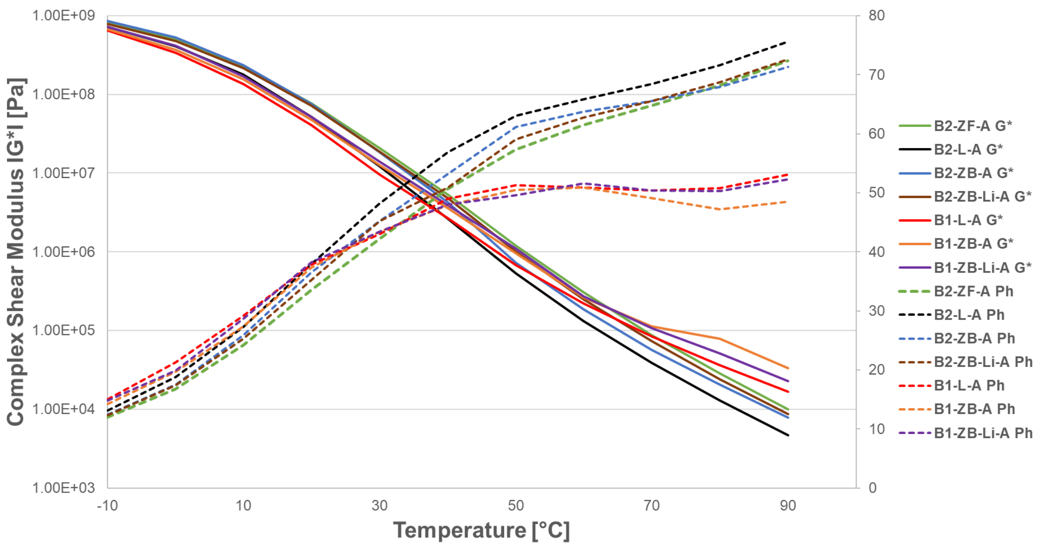

***Fig. 35** Example of the complex modulus (solid lines) and phase angle (dotted lines) of aged mastic using DSR*

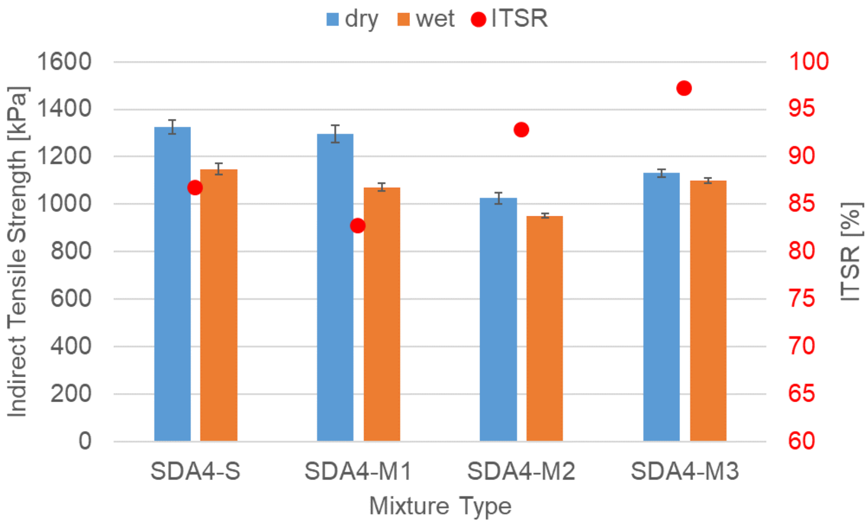

***Fig. 38** Example of indirect tensile strength and waste sensitivity results of benchmark and three modified SDA 4 mixtures*

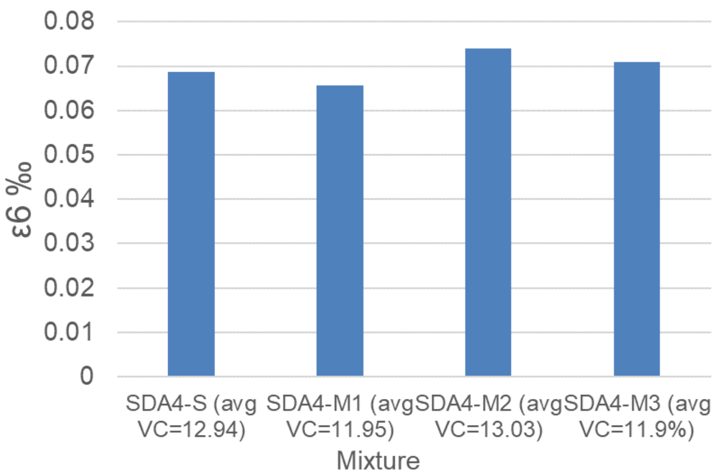

***Fig. 52** Fatigue performance of standard and modified mixtures SDA 4-S, SDA 4-M1, SDA 4-M2, SDA 4-M3*

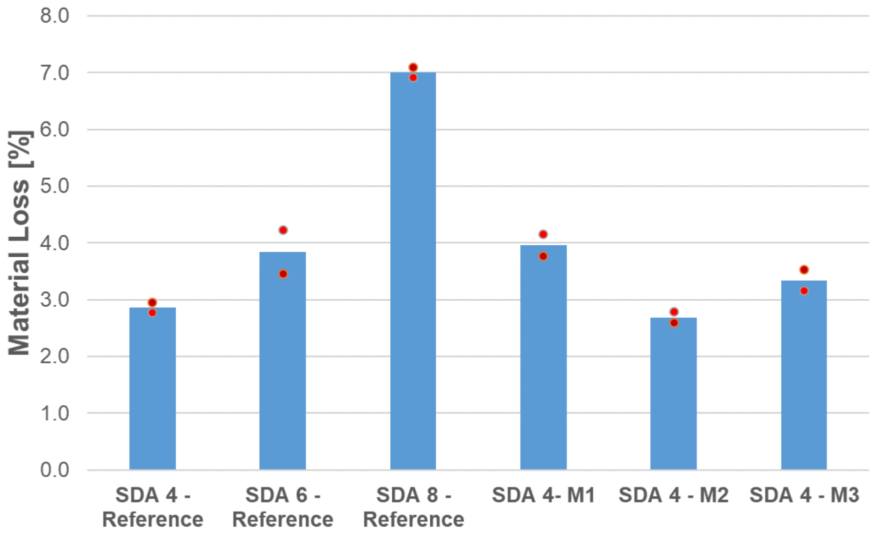

Fig. 53 *Particle loss according to the MDI test*

WP4 involved large-scale testing of the modifications identified in WP1/WP3 and the most promising modification (M3) compared to the reference. Test slabs of size (1.5 m × 0.5 m) were produced and subsequently tested with the MMLS3 traffic simulator. During the tests, ongoing acoustic and other measurements were conducted to investigate the behavior of the test plates. These tests included sound absorption, (3D) texture, and airflow resistance measurements. To simulate acoustic durability under simulated traffic load, the simulation program SPERoN was used. This allowed the measured results to be converted to an in-situ sound level.

Overall, it was demonstrated that the mechanical durability (here as rut depth) of the modified plates performed better than the reference measurements (S) (see Fig. 56).

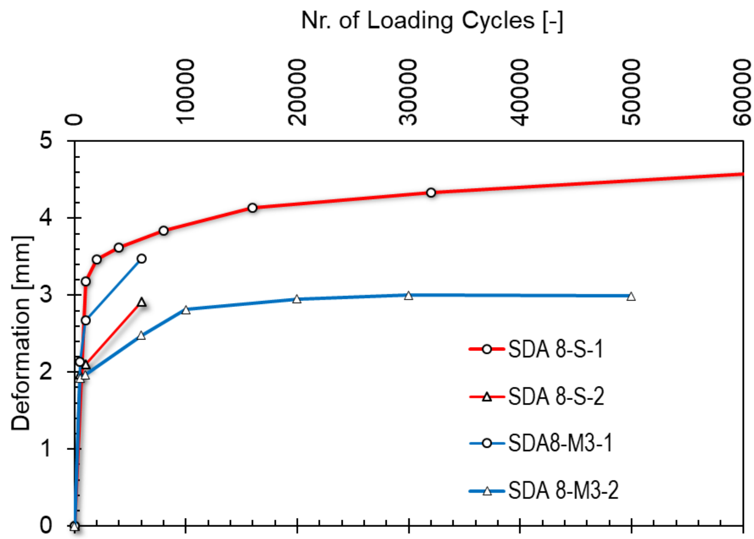

Fig. 56 *Development of rutting of two slabs of benchmark SDA 8-S and modified SDA 8-M3 using MMLS3*

As was also shown in the development of rut depth, slight improvements in acoustic durability were identified. Both for the SDA 4 and the SDA 8 sample plates with the modification M3, slightly more durable (stable) levels were recorded (after 6'000 passes of the MMLS3). This is illustrated in the following Fig. 70.

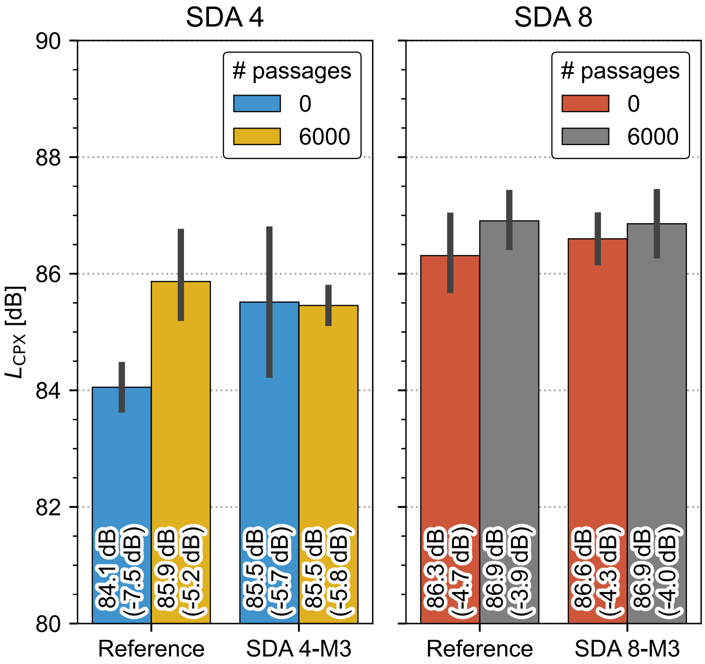

***Fig. 70** Results of the acoustic simulation for SDA 4 and SDA 8 for the reference and the optimized formulations (M3) before and after treatment in the MMLS3 traffic simulator*

Using computed tomography image series (CT) of extracted core samples from the reference and the modified slab M3 before and after testing with the MMLS3 traffic simulator, the accessibility of the pore structure was analyzed using the Acoustic Void Content Analysis (AVCA) method. The results confirmed that the pore connectivity with the M3 modification could generally be better maintained than with the reference. As an example, Fig. 62 illustrates this, showing that the pore accessibility for the reference SDA 8 at the aged measurement point (MP4) continuously decreases with increasing drill core depth. This is not the case for the modified slab M3. Consequently, the modification achieved stabilization of the pore structure.

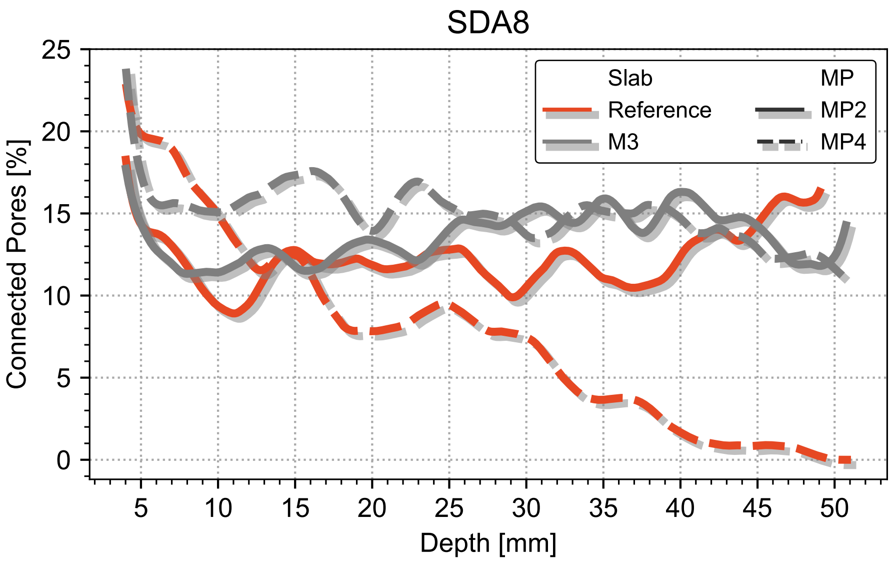

***Fig. 62** Connected pore network for the SDA 8-Slabs. Red: Reference Slab, gray: Optimized mixture (M3). Solid Lines: MP2: Wheelpath after MMLS (6'000 cycles) MP4: Outside wheelpath (dotted lines)*

Summary and Conclusions

A multi-scale approach was implemented to investigate mechanical and acoustic performance of SDA 4, SDA 6 and SDA 8 mixtures from mm to km scale. Tab. 18 shows a summary of the critical results. Benchmark mixtures were developed using the optimum acoustic in-situ performance of these mixtures using 200 test sections. As a first step, the mechanical performance of the benchmark mixtures were investigated. It was shown that the overall ranking of the benchmark mixtures was as follows: SDA 4>SDA 6>SDA 8. As a second step, combinations of binder and filler and additives were used to characterize the mastic. The best performing mastic was used thereafter in producing the modified mixtures. The SDA 4 mixtures were first modified and tested mechanically using a wide variety of tests in order to determine their performance. Thereafter, the optimized modification was applied to SDA 8 slabs. From the experimental results the following conclusions can be drawn:

- At the mastic scale, it was observed that the filler primarily had a stiffening effect with higher complex modulus and lower phase angle at higher temperatures above 30°C, with Zeobit filler having a stronger effect.
- At the mastic scale, highly modified binder with limestone and Zeobit filler as well as a combination of Zeobit filler and hydrated lime had the best results that were also similar.
- The optimized modification for the mixtures was a combination of highly modified binder, stiffening filler (Zeobit) and hydrated lime to improve water sensitivity.
- It should be noted that hydrated lime has a relatively high environmental footprint and this aspect should be considered when choosing the optimum materials.
- Laboratory scale mixture performance tests have shown that the modification improved the water sensitivity, fatigue- and cyclic compression resistance and had similar low temperature cracking results in comparison to the benchmark.
- The micro-Deval IMP test has shown higher particle loss for SDA 8 mixtures. The modified SDA 4 mixtures showed similar particle loss to the benchmark mixtures.
- The large scale MMLS tests showed that after 50'000 loading cycles, the modified M3 mixtures showed less rutting in comparison to the reference. This effect was greater for the SDA 8 mixtures. The modified mixtures had similar changes in surface texture and acoustic performance to the benchmark mixtures before and after the wheeltracking.

- Using the MMLS3 load simulator and measurements before and after exposure to loads, the acoustic modeling has shown that the modified mixture SDA 4 M3 and SDA 8-M3 noise levels improved between the unloaded measurement points and the loaded measurement points. This indicates that the modification maintained the structural integrity of the mixture after loading. This was confirmed by the CT scans of the loaded and unloaded samples showing that the void connectivity of the modified mixtures was larger contributing to better noise absorption.

Tab. 18 *Summary of results: arrows indicate results in comparison to SDA 4-S standard mixture; green arrow=improved performance; yellow arrow=similar performance; red arrow=worst performance. SCB and rutting results are only for the modified mixtures; yellow arrow shows similar results and green arrow shows better performance in comparison to the modified mixtures*

Mixture / Test	**ITSR**	**Fatigue**	**CCT**	**Rut***	**SCB***	**MicoDeval**	**MMLS3**		
							Def	**Noise Abs**	**Air**
Temp.	20°C	10°C 10Hz	50°C	60°C	0°C		40°C	40°C	40°C
SDA4-S	REF	REF	REF				REF	REF	
SDA6-S	→	↓	↓				→		
SDA8-S	↑	↓	↓				↓		
SDA4-M1	↓	→	↑	→	→	→			
SDA4-M2	↑	↑	↑	→	→	↑			
SDA4-M3	↑	↑	↑		→	→	↑	→	↑
SDA8-M3							↑	→	↑

Zusammenfassung

Einleitung

Semi-dichte Asphalte (SDA) sind bekannt für ihre Wirksamkeit bei der Reduktion des entstehenden Reifen-Fahrbahngeräuschs. Ihr Hauptmerkmal ist dabei ihre abgestufte Korngrössenverteilung im Mischgut. Trotz ihrer nachgewiesenen Wirksamkeit besteht ein dringender Bedarf, ihre mechanische und akustische Dauerhaftigkeit zu verbessern, um die Wirtschaftlichkeit über ihren kürzeren Lebenszyklus im Vergleich zu dichten Mischungen sicherzustellen. In der Schweiz dienen SDA-Beläge als etablierte Lärmminderungsmassnahmen. Dabei weisen SDA-Beläge, eine geringere Porosität als poröser Asphalt (PA) auf, und bieten ein vielversprechendes Gleichgewicht zwischen Lärmminderung und verbesserter mechanischer Haltbarkeit. Seiterledigt 2010 wurden in der Schweiz über 1'000 dieser lärmarmen Beläge gebaut, was die praktische Anwendung der SDA-Technologie widerspiegelt. Laufende Forschung und praktische Erfahrungen haben zu Fortschritten sowohl in der mechanischen als auch in der akustischen Leistung dieser Beläge geführt. Es bestehen jedoch weiterhin Fragen hinsichtlich der Dauerhaftigkeit dieser Beläge, die weitere Untersuchungen ihrer mechanischen und akustischen Eigenschaften erfordern.

Ziele

Eine kürzlich durchgeführtes D-A-CH -Forschungsprojekt hat speziell die Bedeutung der richtigen Auswahl der Menge und Art des Bindemittels für die akustische Dauerhaftigkeit der SDA-Beläge gezeigt [33]. Allerdings hat das D-A-CH-Projekt keine spezifischen Lösungen zur Erhöhung der Dauerhaftigkeit von SDA bereitgestellt. Das vorliegende Projekt wurde daher konzipiert, um diese Wissenslücke zu schliessen und konzentriert sich auf den schweizerischen Verkehr, die klimatischen und deren baulichen Bedingungen. Folglich ergaben sich für diese Forschungsarbeit die nachfolgenden Ziele:

- Die akustische und mechanische Dauerhaftigkeit der in der Schweiz hauptsächlich verwendeten SDAs, nämlich SDA 4, SDA 6 und SDA 8 zu verbessern. Dies soll durch die Optimierung und Anpassung der Mischgutrezepturen an die in der Schweiz vorherrschenden klimatischen- und Verkehrsbedingungen im National- und Hauptstrassennetz mittels eines multiskaligen Ansatzes erfolgen.
- Zwei prioritäre Forschungsschwerpunkte von ASTRA anzugehen: «*TRU 1 - Erhöhung der mechanischen Dauerhaftigkeit und Lärmreduktion von Belägen*» sowie «*TRU 3-Alterung von Bitumen: Mikrostruktur sowie chemische Zusammensetzung*».

Methodik

Zur Erreichung der Projektziele, wurde das vorliegende Projekt in unterschiedliche Arbeitspakte gemäss Fig. 3 gegliedert, wobei das Know-how und die Stärken der am Projekt beteiligten Partner, Empa, IMP und G+P, kombiniert wurden. Der erste Schritt bestand darin, die zu untersuchenden SDA-Rezepturen zu definieren um eine Referenz-Mischung als Benchmark zu setzen. Diese wurden anhand des bestehenden Wissenstands (best-practice) und anhand der akustischen Leistung von In-situ-Messungen der lärmarmen Belägen definiert. Die ermittelten vielversprechendsten Rezepturen wurden danach hinsichtlich ihrer mechanischen und akustischen Leistung in nicht gealtertem und gealtertem Zustand mittels eines multiskaligen Ansatzes untersucht. Anschliessend wurden systematische Optimierungen an Mastix Rezepturen (Füller+Bitumen+Additiv) durchgeführt. Die dabei am besten abschneidenden Kombinationen wurden dabei wieder der Mischgutrezeptur zurückgeführt und dadurch eine Optimierung zu erreichen. Diese optimierten Rezepturen (und auch die Referenz) wurden im Rahmen des Projektes auf mehreren Grössenskalen und auf unterschiedlichste Weise untersucht mit dem Ziel die akustische und mechanische Dauerhaftigkeit zu erhöhen. Dies erlaubte es das Wissen und die Erkenntnisse aus der In-situ-Langzeitleistung und der Laborleistung von lärmarmen Belägen zu kombinieren. Zu diesem Zweck wurden fünf Arbeitspakete (WP) konzipiert, um die Projektziele zu erreichen:

- Im Arbeitspaket „*WP1: Charakterisierung von nicht gealtertem und gealtertem SDA 4, SDA 6, SDA 8 (cm-Massstab)*“ wurden die mechanischen Eigenschaften von der Referenzmastix und dem (Referenz-) Mischgut untersucht. Die mechanische Leistung gealterter Materialien wurde ermittelt und als Benchmark verwendet. Die Alterung erfolgte durch kurzfristige Ofenalterung (STOA), bei der das lockere Gemisch für 4 Stunden bei 135°C erhitzt wird. Mechanische Leistungstests an Asphaltmischungen waren die indirekte Zugfestigkeit (ITS) und Wassereinwirkung (ITSR), Modul, Ermüdung und der zyklische Drucktest. Bei der Mastix wurden folgende Unterschung durchgeführt: Ermüdung und Frequenz bei niedriger Temperatur sowie komplexes Modul und Phasenwinkel bei hoher Temperatur.
- Im Arbeitspaket„*WP2: Statistische Analyse der Langzeitleistung von SDA-Mischungen in der Schweiz (km-Massstab)“* wurde die G+P-Datenbank zur In-situ-Akustikleistung von SDA-Belägen in der Schweiz analysiert. Auf Grundlage dieser umfangreichen empirischen Daten wurde als erstes das akusische Alterungsverhalten der In-situ Messungen untersucht und ein Alterungsmodell für verschiedene Rezepturen (Standardmischungen) erstellt. Ebenso wurden akustisch dauerhafte Fahrbahnen identifiziert und die entsprechenden Rezepturen analysiert. Dadurch liessen sich die vielversprechendsten Rezepturen aus dem Feld zurückführen in WP1, um als Grundlage für die Optimierungsschritte zu dienen.
- Im Arbeitspaket „*WP3: Optimierung und Charakterisierung von lärmarmen Belägen (µm-cm-Massstab)*“ wurden die Mastix und SDA-Rezepturen modifiziert gemäss den Spezifikationen aus WP1 & WP2 modifiziert und charakterisiert. Diese im Labor hergestellten Mischungen müssen auf der Strasse wie erforderlich funktionieren, und das Ziel war zu zeigen, dass die Eigenschaften, die aus den oben genannten Optimierungsprozessen resultieren, ihre Leistung einschliesslich Dauerhaftigkeit und Wassereinwirkung nicht beeinträchtigen. Als Standardanforderung wurde die Wassereinwirkung (ITSR) untersucht. Als nicht-standardmässiger Test wurden Ermüdung, komplexes Modul und Frequenz- und Temperatursweep-Test an der Mastik, Bruchfestigkeit mit dem Halbkreisbiege (SCB) Test, Spurrinnen und zyklischer Drucktest sowie Partikelverlust mit dem Mikro-Deval verwendet.
- Im Arbeitspaket „*WP4: Grossmassstäbliche Dauerhaftigkeitstests der optimierten Mischungen (m-Massstab)“* wurden die optimierten Rezepturen und die Referenz mechanisch und akustisch in der m-Skala mit dem Verkehrssimulator MMLS3 untersucht. Die Proben wurden als grosse Testplatten (1.5 m×0.5 m) hergestellt und mit dem Fahrzeuglastsimulator MMLS3 getestet. Dadurch liessen sich Ergebnisse über das Fahrbahnverhalten bei Verkehrsbelastung ableiten. Während des Versuchs wurden periodische Messungen, d.h. Oberflächentextur, Schallabsorption Luftströmungs-widerstand durchgeführt. Wegen der Schallerzeugung des MMLS3 wurden direkte akustische Messungen während der Verkehrssimulation nicht durchgeführt. Stattdessen wurde für die Vorhersage die Software SPERoN verwendet. SPERoN ermöglicht Vorhersagen der akustischen Leistung eines Testbelags. Das SPERoN -Modell basiert auf der Modellierung von Kontaktkraftkräften (Reifen-Fahrbahn) den durchgeführten Luftströmungs- und Schallabsorptions- und Oberflächentexturmessungen. Ebenso wurde die Zugänglichkeit der Hohlräume (Poren) auf den Testplatten vor- und nach der Verkehrssimulation mit dem Computertomographen (CT) untersucht. Dabei zeigte sich, dass die im Labor verwendete Verdichtungsmethode einen grossen Einfluss auf die Form der Poren sowie die Textur hat. Um sicherzustellen, dass die Mischungen auch die erforderlichen akustischen Eigenschaften haben, werden die im Labor verdichteten Proben hinsichtlich ihres akustisch wirksamen Hohlrauminhalts mit Hilfe der von G+P entwickelten Akustischen Hohlrauminhaltsanalyse AVCA analysiert.
- Schliesslich befasste sich „*WP5: Dissemination*“ mit der Veröffentlichung der Ergebnisse und Erkenntnisse.

Die grafische Übersicht über die Aktivitäten ist in Fig. 5 dargestellt.

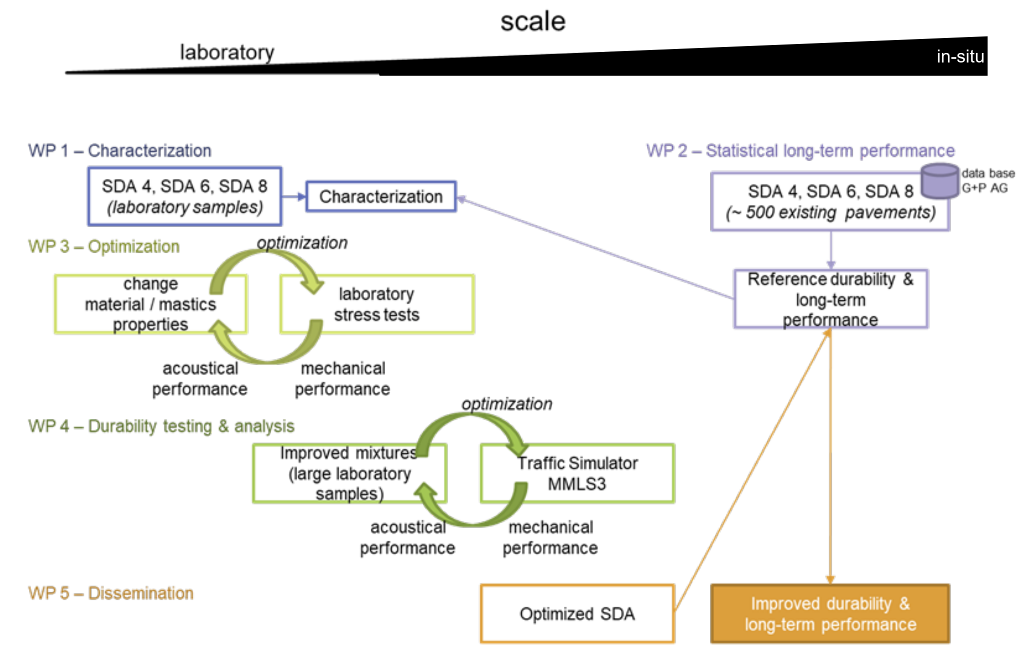

Fig. 3 *Schema der Untersuchunge*

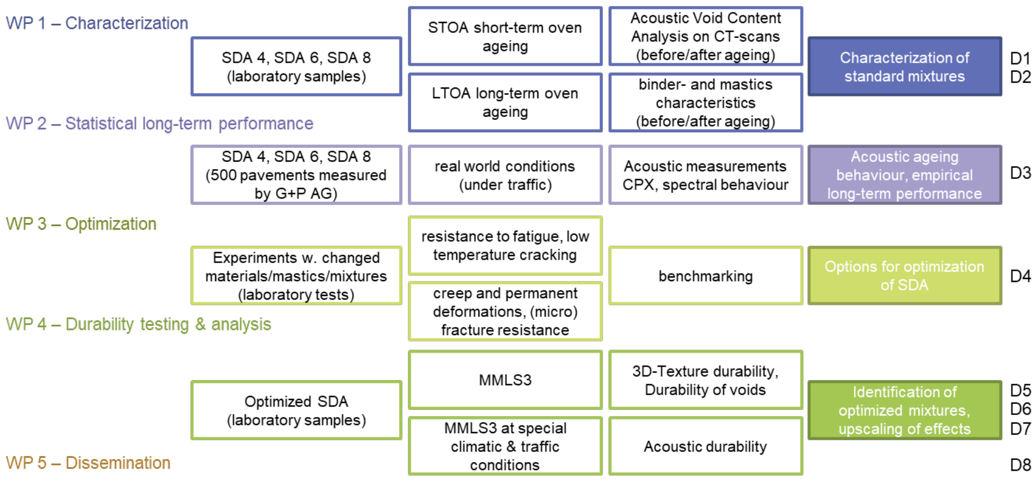

Fig. 5 *Übersicht des Untersuchungsplans*

Resultate

Bis heute liegen akustische Messungen mit Close-Proximity (CPX) Lärm (ISO 11819-2) an rund 200 verschiedenen SDA-Belägen vor, die neben den akustischen Messwerten ebenfalls dazugehörige Mischgutinformationen und Bohrkerndaten umfassen. Dies entspricht insgesamt ca. kombinierten 1'000 Datenpunkten. Diese Daten wurden in einer Datenbank gesammelt und standen innerhalb dieses Projektes zur Verfügung Dies liess es zu, die akustische Alterung in Abhängigkeit den verbauten Rezepturen zu ermitteln. Als Ergebnis der Datenanalyse wurde ein Hohlraumgehalt von 15% für dieses Projekt empfohlen, um ein Gleichgewicht zwischen akustischer und mechanischer Dauerhaftigkeit zu wahren. Ebenso ermöglichte die Analyse der Datenbank eine Auswahl an Belagstypen und Mischgutrezepturen zu treffen, die sich in der Praxis als akustisch wirksam erwiesen hatten. Dadurch konnten spezifische Mischungsrezepturen für SDA 4, SDA 6 und SDA 8 ermittelt werden, die gute akustische Eigenschaften aufweisen. Fig. 12 zeigt ein ermitteltes Alterungsmodell der akustischen Wirkung von Belägen in Funktion des Hohlraumgehalts über die Jahre. Dies wurde als Basis zur Auswahl der Belagsrezepturen verwendet. Anschliessend wurden die mechanischen und akustischen Leistungen der im Labor gealterten Materialien (Mastix und Mischung) ermittelt und als Benchmark verwendet (WP1).

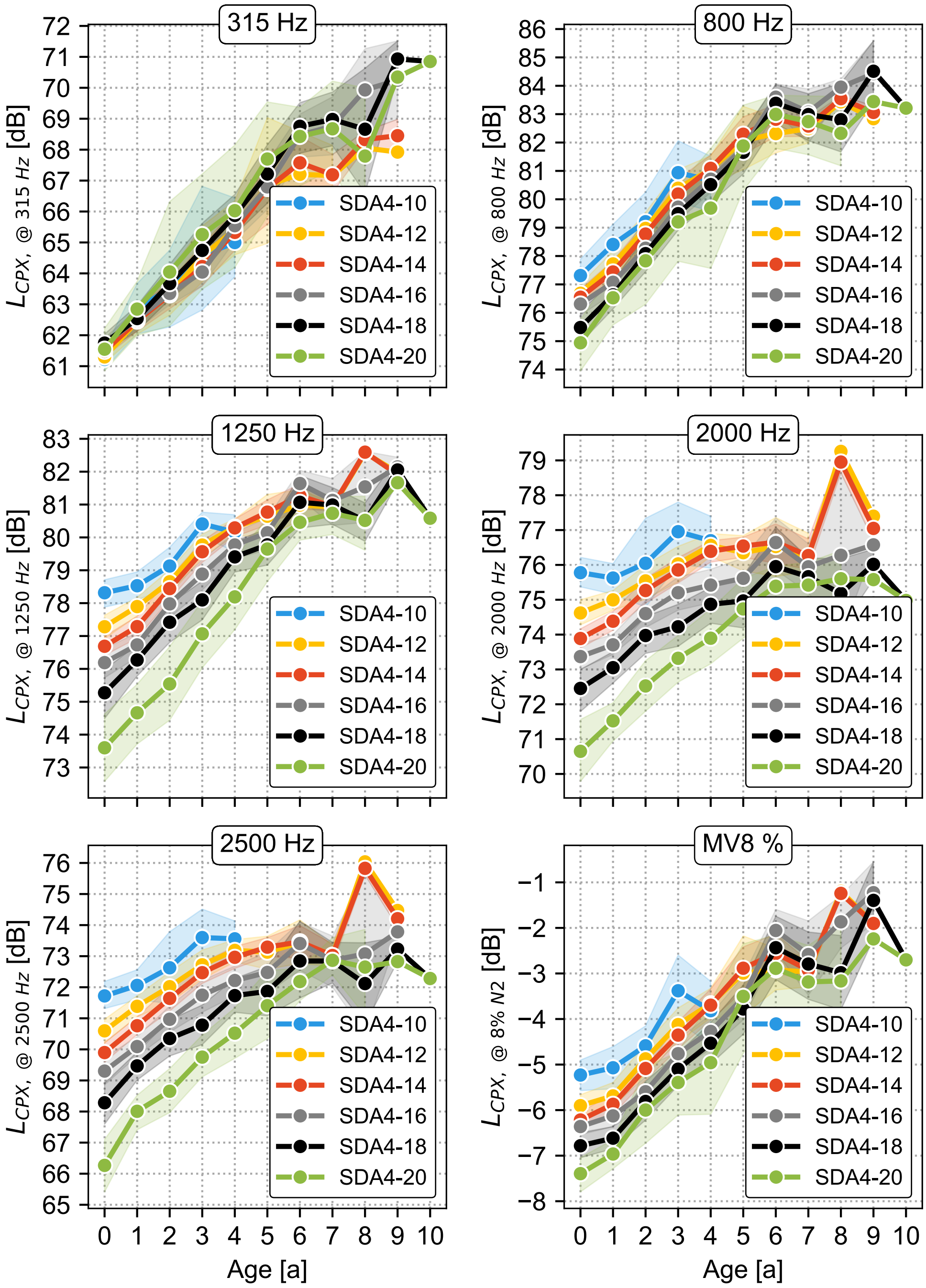

Fig. 12 *In-situ spektrale Alterung von CPX-Pegeln von verschiedenen Hohlraumgehalte SDA 4-Mischgütern. Dabei wurde anhand des Marshall-Hohlraumgehalts unterschieden. Z.B SDA 4-10 entspricht einem SDA 4 Belag mit einem Marshall-Hohlraumgehalt von 8-12 Vol-%*

Für die Analyse der Mischgutproben wurde ein multiskaliger experimenteller Ansatz verwendet. Damit mussten die (mechanischen) Eigenschaften der Proben bestimmt werden: Zunächst wurden verschiedene Bindemittel-, Füller- und Additivkombinationen im Mastix-Massstab (mm-Massstab) in WP1 (Benchmark) und WP3 (Modifiziert) untersucht. Fig. 35 zeigt ein Beispiel für die Resultate des komplexen Schermodus usund des

Phasenwinkels der gealtertern Mastix unter Verwendung unterschiedlicher Füllerkombinationen. Dabei zeigte sich, dass die Kombination aus Hochmodul-Bindemittel (HM) und Zeobit-Füller die Eigenschaften der Mastix im gealterten Zustand verbesserte. Dies ist insbesondere bei Temperaturen oberhalb von 30°C der Fall. Insgesamt resultierten aus diesem Arbeitspaket drei Optionen (vielversprechende Modifikationen) für weitere Untersuchungen (WP3/WP4):

- **M1:** PmB 45/80-80HiMa +Zeobit
- **M2**: PmB 45/80-80HiMa +Kalkstein
- **M3:** PmB 45/80-80HiMa +Zeobit+Kalkhydrat

Aufgrund der gewonnenen Erkenntnisse wurden in der Folge Mischungen für die cm-Massstab-Untersuchungen in WP1 und WP3 hergestellt. Konventionelle und nicht-konventionelle Experimente wurden durchgeführt, nämlich indirekte Zugfestigkeit, zyklische Kompression, halbkreisförmige Biegung, komplexer Modulus und Ermüdung. Fig. 38 zeigt ein Beispiel für die mechanischen Tests im cm-Massstab, die den SDA 4-Benchmark und drei modifizierte Mischungen zeigen. Ebenso wird der Ermüdungstest, der mit der erwarteten mechanischen Leistung der Materialien im Laufe der Zeit in Verbindung steht, in Fig. 52 dargestellt. Die Ergebnisse zeigen, dass die modifizierten Mischungen die Anforderung an die Wasserempfindlichkeit von 70% erfüllen. Basierend auf den Ergebnissen im cm-Massstab wurden Mischungen für die m-Massstab-Laboruntersuchungen in WP4 weiter ausgewählt. Partikelverlust kann für diese Art von Fahrbahnen ein wichtiges Problem darstellen. Der modifizierte Micro-Deval-Test wurde an allen Mischungen durchgeführt, wie in Fig. 53 gezeigt. Die Ergebnisse deuten darauf hin, dass der Partikelverlust der modifizierten Mischungen nicht verbessert werden konnte.

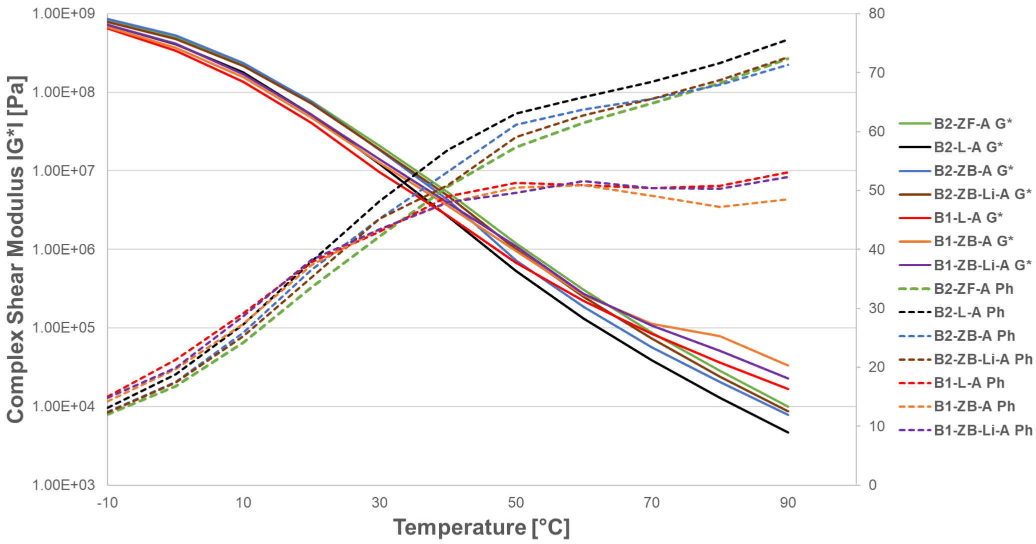

***Fig. 35** Beispiel des Komplexen Schermoduls (ausgezogene Linien) und des Phasenwinkels (dotted lines) der gealterten Masitix mit dem DSR-Verfahren*

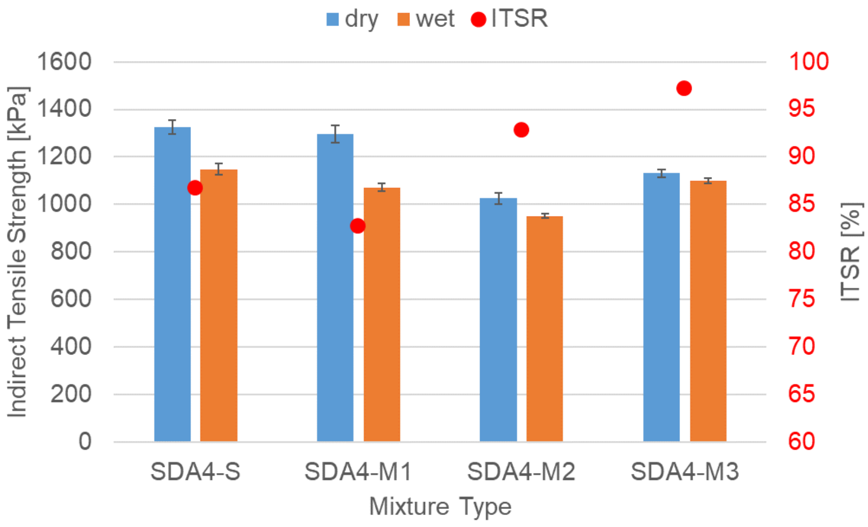

***Fig. 38** Beispiel des Resultats des indirect tensile strength und Wasserempfindlichkeit ds Benchmarks (SDA-S) und von drei optimierten Mischunngen SDA 4*

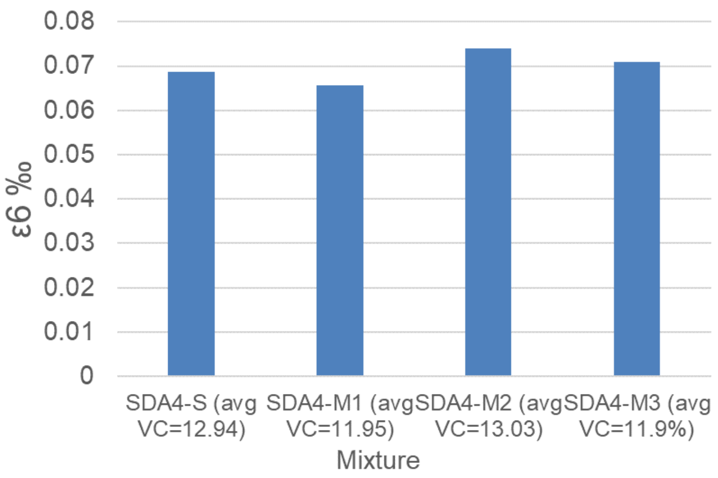

***Fig. 52** Test der Ermüdung des Benchmarks (SDA4-S) und von drei modifizierten SDA 4-Mischgüter: SDA 4-S, SDA 4-M1, SDA 4-M2, SDA 4-M3*

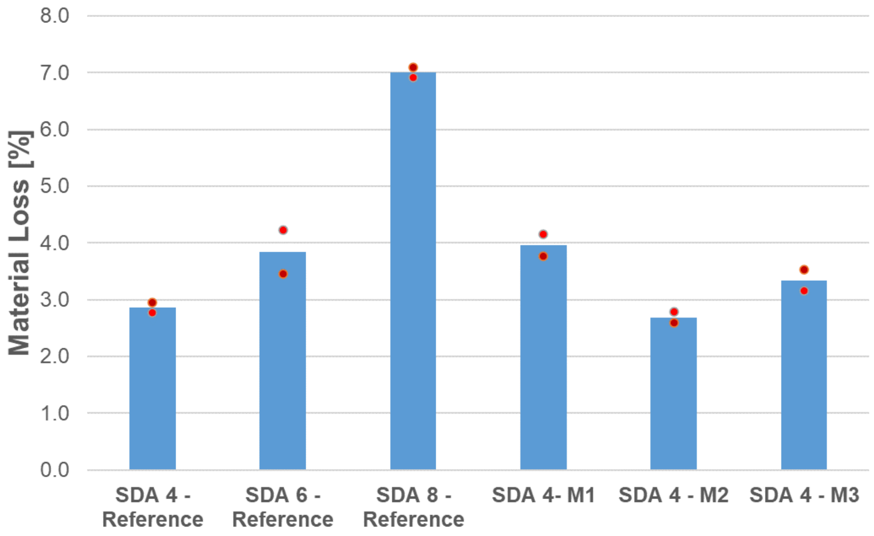

Fig. 53: *Ergebnisse des Micro-Deval-Tests*

Das WP4 umfasste die grossskalige Prüfung der in WP1/WP3 ermittelten und der am vielversprechendsten Modifikation (M3) und der Referenz. Dabei wurden Platten in der Grösse (1.5 m × 0.5 m) hergestellt und anschliessend mit dem MMLS3-Verkehrssimulator getestet. Während der Tests wurden laufend akustische und weitere Messungen durchgeführt, um das Verhalten der Testplatten zu untersuchen. Diese umfassten Schallabsorptions-, (3D-) Textur- und Luftströmungswiderstandsmessungen. Um die akustische Dauerhaftigkeit unter der simulierten Verkehrslast zu simulieren, wurde das Simulationsprogramm SPERoN verwendet. Damit konnten die gemessenen Messresultate zu einem In-situ – Schallpegel umgewandelt werden.

Insgesamt konnte gezeigt werden, dass die mechanische Dauerhauftigkeit (hier als Spurrinnentiefe) bei den modifizierten Platten besser abgeschnitten haben, als die Referenzmessungen (S) (Vgl. Fig. 56).

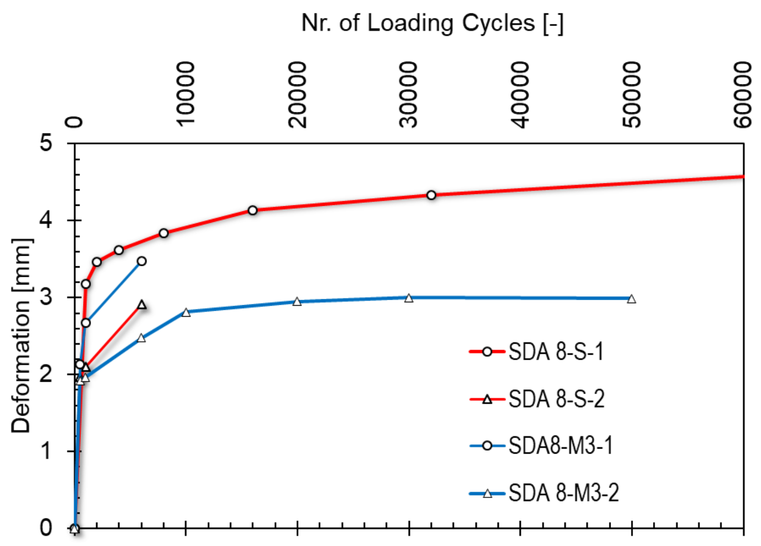

Fig. 56: Development of rutting of two slabs of benchmark SDA 8-S and modified SDA 8-M3 using MMLS3

Wie sich auch in der Entwicklung der Spurrinnentiefe gezeigt hat, konnten auch Kleine Verbesserungen in Bezug auf die Dauerhaftigkeit der Akustik ermittelt werden. So konnten sowohl für die SDA 4, wie auch für die SDA 8 – Probeplatten mit der Modifikation M3 leicht dauerhaftere (stabilere) Pegel verzeichnet werden (Nach 6'000 Überrollungen des MMLS3). Dies ist in der folgenden Fig. 70 dargestellt.

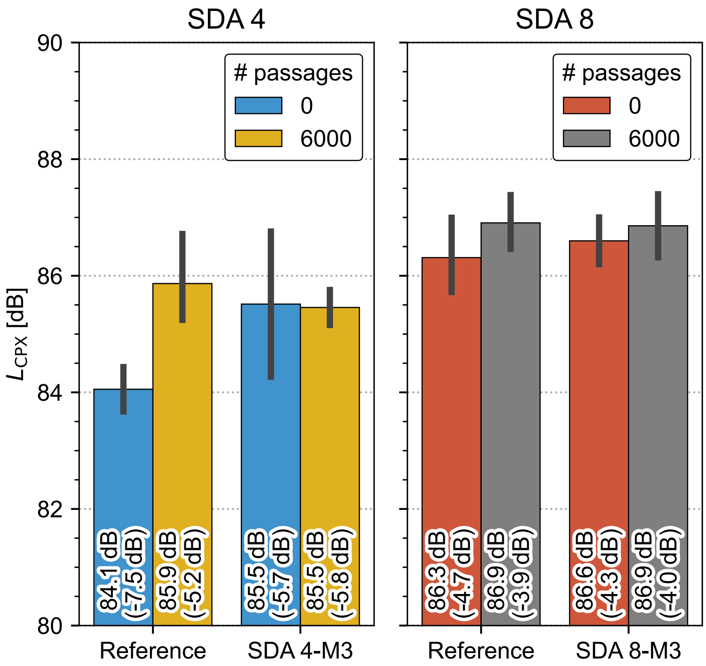

Fig. 70 *Resultate der akustischen Simulation für SDA 4 and SDA 8 für die Referenz und die optimierten Rezepturen (M3) vor und nach der Behandlung im MMLS3 Verkehrssimulator*

Mittels der Computertomographie-Bildserien (CT) von gezogenen Bohrkernen der Referenz- und der modifizierten Platte M3 vor und nach dem Testen durch den MMLS3-Verkehrssiumlator wurde die Zugänglichkeit des Porengefüges analysiert mit dem Verfahren AVCA (Acoustic Void Content Analysis) durchgeführt. Hierbei bestätigten sich die Resultate, dass die Verbindung der Poren mit der Modifikation M3 in der Tendenz besser aufrechterhalten werden konnten, als bei der Referenz. Als Beispiel sei hierfür die Fig. 62 dargestellt, bei welcher die Zugänglichkeit des Hohlraums für die Referenz des SDA 8 am gealterten Messpunkt (MP4) über die Tiefe kontierlich abnimmt. Dies ist bei der modifizierten Rezeptur M3 nicht der Fall. Folglich konnte mit der Modifikation eine Stabilisierung der Hohlraumstruktur erreicht werden.

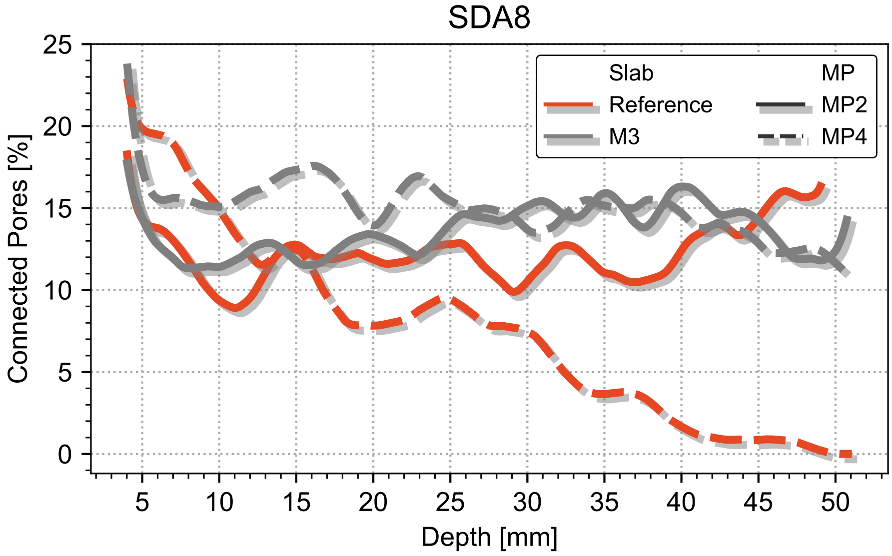

***Fig. 62:** Verbundenes Porennetzwerk für die SDA 8-Platten. Rot: Referenzplatte, Grau: Optimierte Mischung (M3). Durchgezogene Linien: MP2: Reifenspur nach MMLS (6'000 Zyklen), MP4: Ausserhalb der Reifenspur (gestrichelte Linien)*

Zusammenfassung & Empfehlungen

In diesem Projekt wurden SDA-Beläge auf mehreren Ebenen (Grössenmässig unterschiedliche Skalen) untersucht. Damit wurde die mechanische und akustische Leistung von SDA 4, SDA 6 und SDA 8 Belägen vom mm- bis zum km-Massstab untersucht. Die folgende Tab. 18 zeigt eine Zusammenfassung der Ergebnisse. Die Referenz-Mischgüter wurden durch die Analyse der akustischen Leistung der In-Situ-Messungen ermittelt. Dabei wurde aus dem Datensatz, bestehend aus 200 verschiedenen Belägen die akustisch vielversprechendsten Mischungen ermittelt. Danach wurde im ersten Schritt die mechanische Leistung dieser Referenz (Benchmark)-Mischungen untersucht. Es zeigte sich, dass das Gesamtranking der Referenz-Mischungen wie folgt war: SDA 4 > SDA 6 > SDA 8. Im zweiten Schritt wurden verschiedene Kombinationen von Bindemittel, Füllern und Additiven verwendet, um die Mastix zu charakterisieren. Die am besten abschneidende Mastix wurde anschliessend zur Herstellung der modifizierten Mischungen verwendet. Die SDA 4-Mischungen wurden zuerst modifiziert und mechanisch mit einer Vielzahl von Tests getestet, um ihre Leistung zu bestimmen. Danach wurde die optimierte Modifikation auf SDA 8-Platten angewendet. Aus den durchgeführten Untersuchungen können folgende Schlussfolgerungen gezogen werden:

- Im Mastix-Massstab zeigte sich, dass der Füller hauptsächlich eine versteifende Wirkung hatte. Dies vor Allem mit einem höheren komplexen Modul und einem niedrigeren Phasenwinkel bei höheren Temperaturen über 30°C, wobei der Zeobit-Füller eine stärkere Wirkung zeigte.
- Im Mastix-Massstab zeigten stark modifizierte Bindemittel mit Kalkstein und Zeobit-Füller sowie eine Kombination aus Zeobit-Füllstoff und Kalkhydrat die besten Ergebnisse. Wobei die Unterschiede zwischen den beiden relative klein waren.
- Die optimierte Modifikation für die Mischungen war eine Kombination aus stark modifiziertem Bindemittel, steifendem Füllstoff (Zeobit) und Kalkhydrat zur Verbesserung der Wasserempfindlichkeit.
- Es sollte beachtet werden, dass Kalkhydrat einen relativ hohen ökologischen Fussabdruck hat und dieser Aspekt bei der Auswahl der optimalen Materialien berücksichtigt werden sollte.
- Labortests zur Leistung der Mischungen haben gezeigt, dass die Modifikation die Wasserempfindlichkeit, Ermüdungs- und zyklische Druckfestigkeit verbesserte und ähnliche Ergebnisse bei niedrigen Temperaturen im Vergleich zum Benchmark zeigte.

- Der Mikro-Deval IMP-Test zeigte bei den modifizierten SDA 8-Mischungen einen höheren Partikelverlust als bei der Referenz. Die modifizierten SDA 4-Mischungen zeigten einen ähnlichen Partikelverlust wie die Referenz.
- Die MMLS-Versuche zeigten, dass nach 50'000 Belastungszyklen die modifizierten M3-Mischungen im Vergleich zur Referenz weniger Spurrinnenbildung aufwiesen. Dieser Effekt war bei den SDA 8-Mischungen starker als bei den SDA 4-Belägen. Die modifizierten Mischungen hatten ähnliche Veränderungen in der Oberflächentextur und der akustischen Leistung wie die Benchmark-Mischungen vor und nach dem Radspurtest.
- Mit dem MMLS3-Lastsimulators zeigte sich hinsichtlich der akustischen Modellierung eine Verbesserung der Stabilität zwischen den befahrenen und unbefahrenen Abschnitten bei den modifizierten Proben SDA 4 M3 und SDA 8-M3. Dies deutet darauf hin, dass die Modifikation die strukturelle Integrität der Mischung nach der Belastung erhalten hat. Dies wurde durch die CT-Scans der belasteten und unbelasteten Messpunkten bestätigt. Dabei konnte gezeigt werden, dass der zugängliche Hohlraum der modifizierten Proben höher war und somit insgesamt zu einer besseren Schallabsorption beitrug.

***Tab. 18** Summary of results: arrows indicate results in comparison to SDA 4-S standard mixture; green arrow=improved performance; yellow arrow=similar performance; red arrow=worst performance. SCB and rutting results are only for the modified mixtures; yellow arrow shows similar results and green arrow shows better performance in comparison to the modified mixtures*

Mixture / Test	**ITSR**	**Fatigue**	**CCT**	**Rut***	**SCB***	**MicoDeval**	**MMLS3**		
							Def	**Noise Abs**	**Air**
Temp.	20°C	10°C 10Hz	50°C	60°C	0°C		40°C	40°C	40°C
SDA4-S	REF	REF	REF				REF	REF	
SDA6-S	→	↓	↓				→		
SDA8-S	↑	↓	↓				↓		
SDA4-M1	↓	→	↑	→	→	→			
SDA4-M2	↑	↑	↑	→	→	↑			
SDA4-M3	↑	↑	↑		→	→	↑	→	↑
SDA8-M3							↑	→	↑

Résumé

Introduction
Les enrobés semi-denses (SDA) sont connus pour leur efficacité dans la réduction du bruit de roulement des pneus. Leur caractéristique principale est leur répartition granulométrique échelonnée dans l'enrobé. Malgré leur efficacité prouvée, il est urgent d'améliorer leur durabilité mécanique et acoustique afin d'assurer leur rentabilité sur leur cycle de vie plus court que celui des enrobés denses. En Suisse, les revêtements SDA sont des mesures de réduction du bruit bien établies. Les revêtements SDA présentent une porosité inférieure à celle des Betons bitumineux drainants (PA) et offrent un équilibre prometteur entre la réduction du bruit et l'amélioration de la durabilité mécanique. Depuis 2010, plus de 1'000 de ces revêtements peu bruyants ont été construits en Suisse, ce qui reflète l'application pratique de la technologie SDA. Les recherches en cours et l'expérience pratique ont permis de progresser tant sur le plan des performances mécaniques que sur celui des performances acoustiques de ces revêtements. Toutefois, des questions subsistent quant à la durabilité de ces revêtements, ce qui nécessite des études supplémentaires sur leurs propriétés mécaniques et acoustiques.

Objectifs
Une récente recherche scientifique menée dans le cadre de l'initiative D-A-CH a spécifiquement montré l'importance d'une sélection correcte de la quantité et du type de liant pour la durabilité acoustique du matériau [33]. Cependant, le projet D-A-CH n'a pas fourni de solutions spécifiques pour augmenter la durabilité des SDA. Ce projet a donc été conçu pour combler cette lacune dans les connaissances, en se concentrant sur les conditions de circulation, de climat et de construction en Suisse. Dans cette optique, les objectifs spécifiques de ce travail étaient les suivants:

- Améliorer la durabilité acoustique et mécanique des principaux SDA utilisés en Suisse, à savoir le SDA 4, le SDA 6 et le SDA 8, en optimisant et en adaptant les mélanges aux différentes conditions de circulation et de climat présentes sur le réseau routier national et principal suisse à l'aide d'une approche multi-échelle.
- Répondre à deux axes de recherche prioritaires d'ASTRA "TRU 1 - Erhöhung der mechanischen Dauerhaftigkeit und Lärmreduktion von Belägen" ainsi que "TRU 3- Alterung von Bitumen: Mikrostruktur sowie chemische Zusammensetzung".

Méthodologie
Afin d'atteindre le résultat souhaité, le travail a été organisé comme indiqué dans la Fig. 3, en combinant le savoir-faire et les forces des partenaires impliqués dans le projet: Empa, IMP et G+P. La première étape a consisté à définir les mélanges à étudier, qui ont été sélectionnés sur la base de l'état actuel des performances in situ des chaussées à faible bruit, car ils sont connus pour leurs bonnes performances en Suisse. Ces mélanges ont été testés pour leurs performances mécaniques et acoustiques à l'état non vieilli et vieilli en utilisant une approche multi-échelle. Ensuite, un protocole d'optimisation systématique a été appliqué à ces mélanges. Les mélanges les plus performants ont été sélectionnés et les paramètres d'optimisation ont été identifiés. Le projet a pu combiner de manière unique les connaissances sur les performances à long terme in situ et les performances en laboratoire des chaussées à faible bruit. Ces mélanges ainsi que le mastic correspondant (filler+bitume+additif) ont été testés pour leurs performances mécaniques et acoustiques, partiellement à l'état non vieilli et vieilli, en utilisant une approche multi-échelle (du mm au km). Un protocole d'optimisation systématique a ensuite été appliqué à ces mastics et les résultats prometteurs ont été appliqués à l'échelle du mélange. Les mélanges les plus performants ont été sélectionnés et les paramètres d'optimisation ont été identifiés. Ces paramètres ont été appliqués aux dalles à l'échelle m afin de déterminer les performances mécaniques et acoustiques. Le projet proposé pourrait combiner de manière unique les connaissances sur les performances à long terme in situ et les performances en laboratoire

des chaussées à faible bruit. À cette fin, cinq groupes de travail (WP) ont été conçus pour atteindre les objectifs du projet.

- Dans le "WP1: Caractérisation de SDA 4, SDA 6, SDA 8 (échelle cm) non vieillis et vieillis", les propriétés mécaniques des mastics et des mélanges de référence ont été examinées. Les performances mécaniques des matériaux vieillis ont été déterminées et utilisées comme référence. Le vieillissement a été effectué avec un vieillissement à court terme en étuve (STOA), qui reproduit en laboratoire le vieillissement que le mélange subit pendant la production, en exposant le mélange en vrac à 135°C pendant 4 heures. Les essais de performance mécanique sur les enrobés bitumineux ont porté sur la résistance à la traction indirecte (ITS) et la sensibilité à l'eau (ITSR), le module, la fatigue et l'essai de compression cyclique. Sur le mastic, les essais de performance comprenaient la fatigue et la fréquence à basse température et le module complexe et l'angle de phase à haute température.
- Dans le lot de travaux "WP2: Analyse statistique des performances à long terme des mélanges SDA en Suisse (échelle km)", la base de données G+P sur les performances acoustiques in situ des revêtements SDA en Suisse a été analysée. Sur la base de ces nombreuses données empiriques, le comportement de vieillissement acoustique des mesures in-situ a d'abord été étudié et un modèle de vieillissement a été établi pour différentes formules (mélanges standard). De même, des chaussées acoustiquement durables ont été identifiées et les formules correspondantes analysées. Les formulations les plus prometteuses ont ainsi pu être ramenées du terrain au WP1 afin de servir de base aux étapes d'optimisation.
- Dans le package de travail "WP3: Optimisation et caractérisation des revêtements à faible émission sonore (échelle µm-cm)", les formulations de mastic et de SDA ont été modifiées et caractérisées selon les spécifications du WP1 & WP2. Ces mélanges préparés en laboratoire doivent fonctionner sur la route comme requis, et l'objectif était de montrer que les propriétés résultant des processus d'optimisation mentionnés ci-dessus n'affectent pas leurs performances, y compris la durabilité et l'exposition à l'eau. L'exposition à l'eau (ITSR) a été étudiée en tant qu'exigence standard. Comme test non standard, nous avons utilisé la fatigue, le module complexe et le test de balayage de fréquence et de température sur le mastic, la résistance à la rupture avec le test de flexion semi-circulaire (SCB), l'orniérage et le test de pression cyclique ainsi que la perte de particules avec le micro-Deval.
- dans "WP4 : Large scale durability testing of optimized mixtures (m scale)" ont été examinées mécaniquement et acoustiquement à l'échelle m. à l'aide du simulateur de trafic MMLS3. Les solutions sélectionnées ont été construites en laboratoire sous la forme de grandes dalles d'essai (1,5m×0,5m) et testées jusqu'à la rupture à l'aide du simulateur de charge de véhicule MMLS3, ce qui a permis d'acquérir des connaissances sur la réponse de la chaussée à la charge du trafic. Ce type de simulateur a permis d'étudier la surveillance des performances de la chaussée sous l'effet des charges de trafic. Le processus de simulation du trafic s'est accompagné de diverses mesures acoustiques pertinentes (texture de la surface, absorption acoustique), ainsi que de simulations visant à recueillir des informations détaillées sur le processus de simulation du trafic. Comme il n'est pas possible d'effectuer des mesures acoustiques directes pendant la simulation du trafic en raison de la production intrinsèque de bruit du MMLS3, une approche utilisant le programme SPERoN a été choisie pour les simulations acoustiques et les prévisions de performance, et l'analyse détaillée des mécanismes de production de bruit a été utilisée. SPERoN permet de prédire les performances acoustiques d'une construction sur des tronçons routiers réels grâce à des modèles de force de contact, d'écoulement de l'air et de propagation du son, qui sont alimentés par des données sur les caractéristiques de la surface provenant de mesures en laboratoire (texture, résistance à l'écoulement de l'air et absorption du son). Les propriétés acoustiques des mélanges vieillis ont été caractérisées par le type et la quantité de filler et de sable, la durabilité des vides accessibles ainsi que la durabilité de l'absorption (à l'aide d'un tube d'impédance, ISO 10534-2) ont été réalisées sur de grandes dalles qui représentent la situation sur le terrain. Les caractéristiques du mélange et de la surface (à l'aide d'un scanner laser) et leur évolution avec le vieillissement à différents stades des expériences de vieillissement ont été mesurées et analysées. La tomographie assistée par ordinateur

(TAO) a été utilisée pour caractériser les vides connectés ainsi que les caractéristiques de surface. La méthode de compactage utilisée en laboratoire a une grande influence sur la forme des pores et la texture. Pour s'assurer que les mélanges présentent également les propriétés acoustiques requises, les échantillons compactés en laboratoire sont analysés quant à leur teneur en vides effective sur le plan acoustique à l'aide de l'Acoustic Void Content Analysis AVCA (analyse de la teneur en vides acoustiques), développée par G+P.

- - Enfin, le "WP5: Diffusion" a traité de la publication des résultats et des conclusions.

L'aperçu graphique des activités est présenté à la Fig. 5.

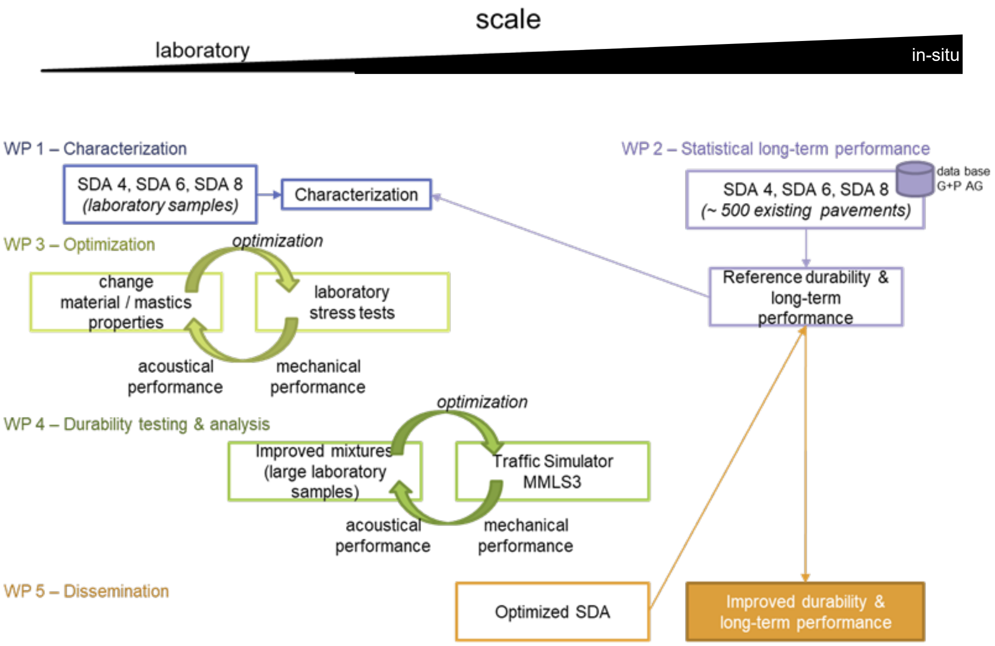

Fig. 3 *Schéma de la recherche prévue*

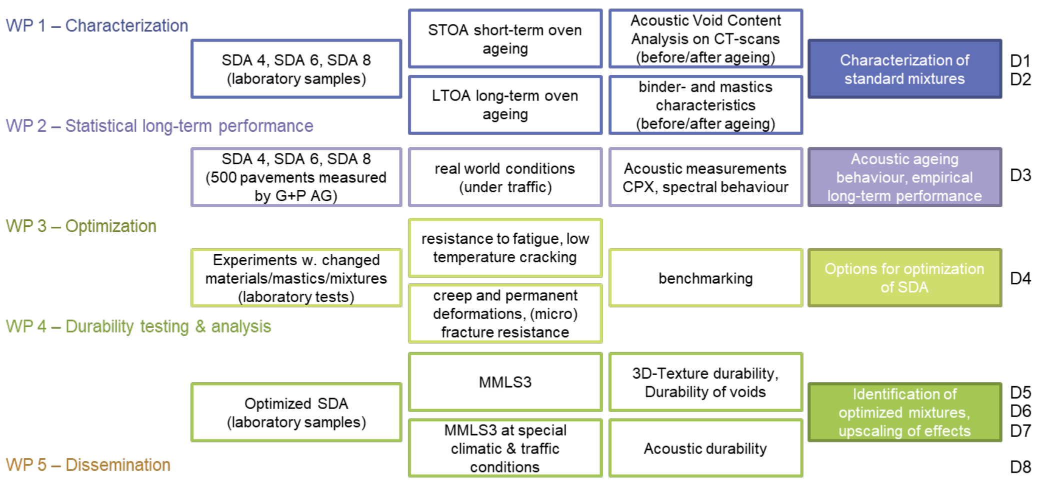

Fig. 5 *Aperçu du plan de recherche*

Résultats

À ce jour, des mesures acoustiques utilisant le bruit de proximité (CPX) (ISO 11819-2) sont disponibles pour environ 200 chaussées SDA différentes. Ces mesures comprennent non seulement des données acoustiques, mais aussi des informations sur le mélange correspondant et des données sur les carottes de forage, soit un total d'environ 1'000 points de données combinés. Ces données ont été rassemblées dans une base de données et étaient disponibles pour ce projet, ce qui a permis de déterminer le vieillissement acoustique en fonction des formulations installées. L'analyse des données a permis de recommander une teneur en vides de 15 % pour ce projet afin de maintenir un équilibre entre la durabilité acoustique et mécanique. En outre, l'analyse de la base de données a permis de sélectionner des types de chaussées et des formulations de mélanges dont l'efficacité acoustique a été démontrée dans la pratique. Cela a permis d'identifier des formulations de mélanges spécifiques pour SDA 4, SDA 6 et SDA 8 qui présentent de bonnes propriétés acoustiques. La Fig. 12 montre un modèle de vieillissement déterminé de l'effet acoustique des chaussées basé sur la teneur en vides au fil des ans. Ce modèle a servi de base à la sélection des formulations de chaussée. Par la suite, les performances mécaniques et acoustiques des matériaux vieillis en laboratoire (mastic et mélange) ont été déterminées et utilisées comme références (WP1).

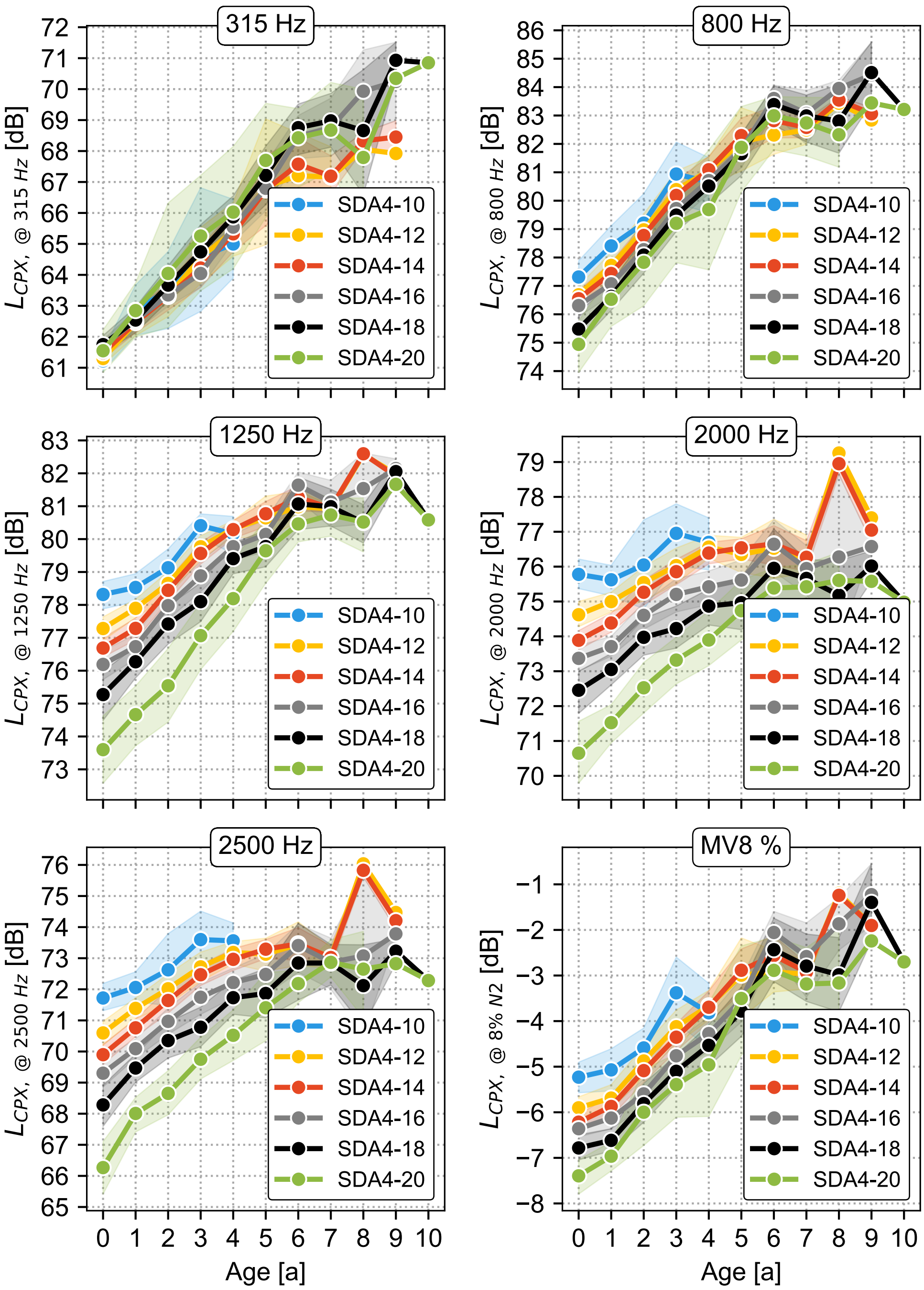

***Fig. 12** Vieillissement spectral in situ des niveaux CPX de différents groupes de teneur en vides des mélanges SDA 4. Différenciés par la teneur en vides Marshall, c'est-à-dire que SDA 4-10 correspond aux chaussées SDA 4 avec une teneur en vides Marshall de l'ordre de 8-12 Vol-%*

Une méthode expérimentale multi-échelle a été utilisée pour étudier plus efficacement les performances de ces mélanges. Tout d'abord, diverses combinaisons de liants, de charges et d'additifs ont été étudiées à l'échelle du mastic (échelle du mm) dans le cadre du WP1 (Benchmark) et du WP3 (Modified). La Fig. 35 montre un exemple du module complexe et de l'angle de phase de mastics vieillis utilisant diverses combinaisons de charges. Il est clair que la combinaison d'un liant à haut module (HM) et d'une charge Zeobit améliore les propriétés du mastic à l'état vieilli, en particulier au-dessus de 30°C. Pour cette échelle, trois options ont été identifiées pour une étude plus approfondie.

- **M1**: PmB 45/80-80-80HiMa +Zeobit
- **M2**: PmB 45/80-80-80HiMa + Calcaire
- **M3**: PmB 45/80-80-80HiMa +Zeobit+ Chaux hydratée

Sur la base des connaissances acquises, des mélanges ont été fabriqués pour les études à l'échelle centimétrique dans le cadre des WP1 et WP3. Des expériences conventionnelles et non conventionnelles ont été réalisées, à savoir la résistance à la traction indirecte, la compression cyclique, la flexion semi-circulaire, le module complexe et la fatigue. La Fig. 38 montre un exemple d'essais mécaniques à l'échelle cm montrant la référence SDA 4 et trois mélanges modifiés. De même, l'essai de fatigue, lié à la performance mécanique attendue des matériaux dans le temps, est présenté à la Fig. 52. Les résultats montrent que les mélanges modifiés satisfont à l'exigence de sensibilité à l'eau de 70 %. A partir des résultats obtenus à l'échelle cm, les mélanges ont été sélectionnés pour les essais en laboratoire à l'échelle m dans le WP4. La perte de particules peut être un problème important pour ces types de chaussées. Le test Micro-Deval modifié a été effectué sur tous les mélanges, comme le montre la Fig. 53. Les résultats indiquent que la perte de particules des mélanges modifiés n'a pas pu être améliorée.

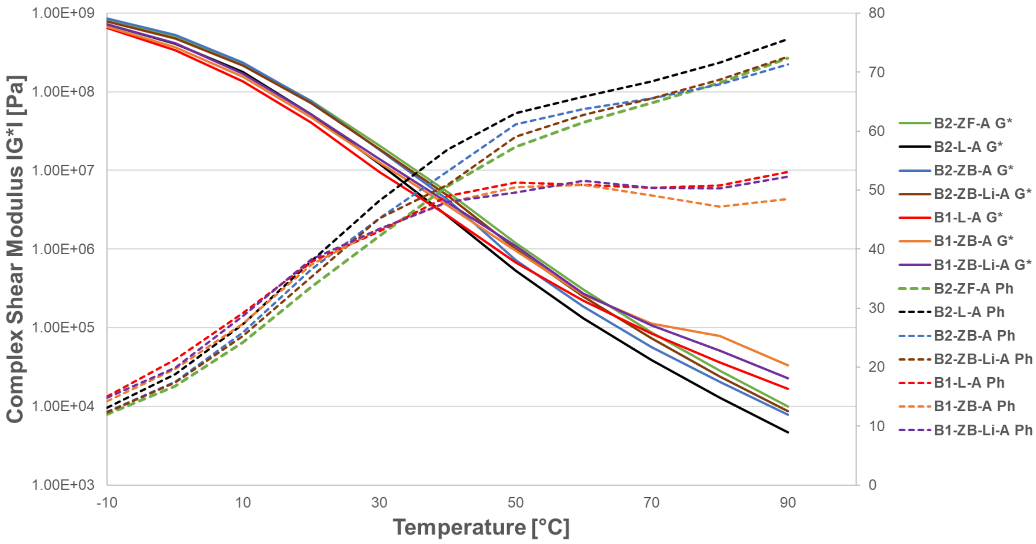

Fig. 35 *Exemple du module complexe (lignes pleines) et de l'angle de phase (lignes pointillées) du mastic vieilli à l'aide du DSR*

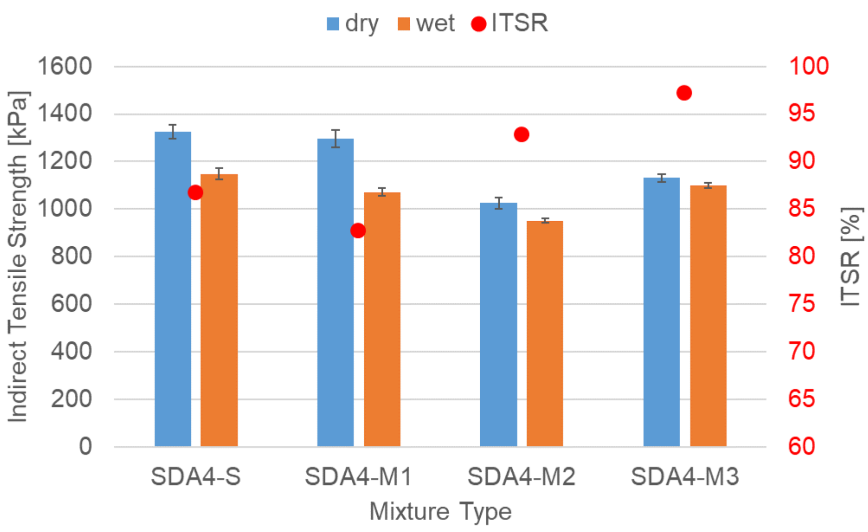

Fig. 38 *Exemple de résistance à la traction indirecte et de sensibilité aux déchets pour des mélanges de référence et trois mélanges SDA 4 modifiés*

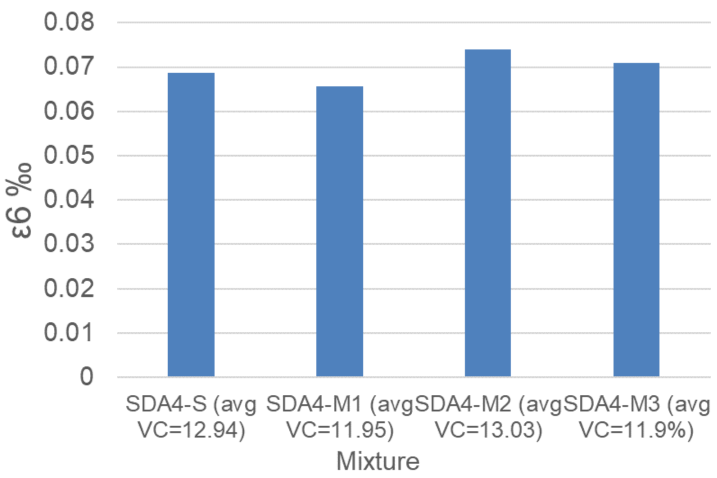

Fig. 52 *Performance à la fatigue des mélanges standards et modifiés SDA 4-S, SDA 4-M1, SDA 4-M2, SDA 4-M3*

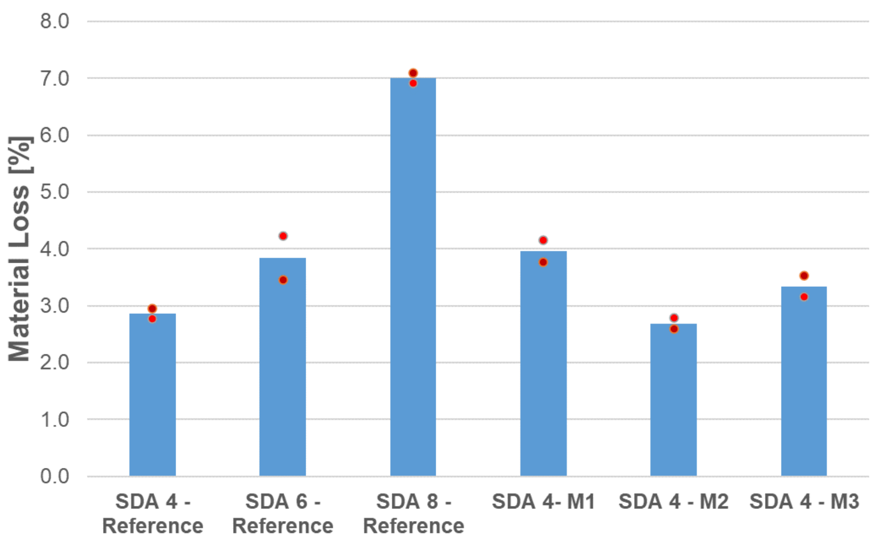

Fig. 53 *Perte de particules selon le test MDI*

Le WP4 a consisté à tester à grande échelle les modifications identifiées dans les WP1/WP3 et la modification la plus prometteuse (M3) par rapport à la référence. Des plaques d'essai de taille (1,5 m × 0,5 m) ont été produites et ensuite testées avec le simulateur de trafic MMLS3. Pendant les essais, des mesures acoustiques et autres ont été effectuées pour étudier le comportement des plaques d'essai. Ces tests comprenaient des mesures d'absorption acoustique, de texture (3D) et de résistance à l'écoulement de l'air. Le programme de simulation SPERoN a été utilisé pour simuler la durabilité acoustique sous une charge de trafic simulée. Cela a permis de convertir les résultats mesurés en un niveau sonore in situ.

Dans l'ensemble, il a été démontré que la durabilité mécanique (ici la profondeur de l'ornière) des plaques modifiées était meilleure que les mesures de référence (S). (Voir Fig. 56).

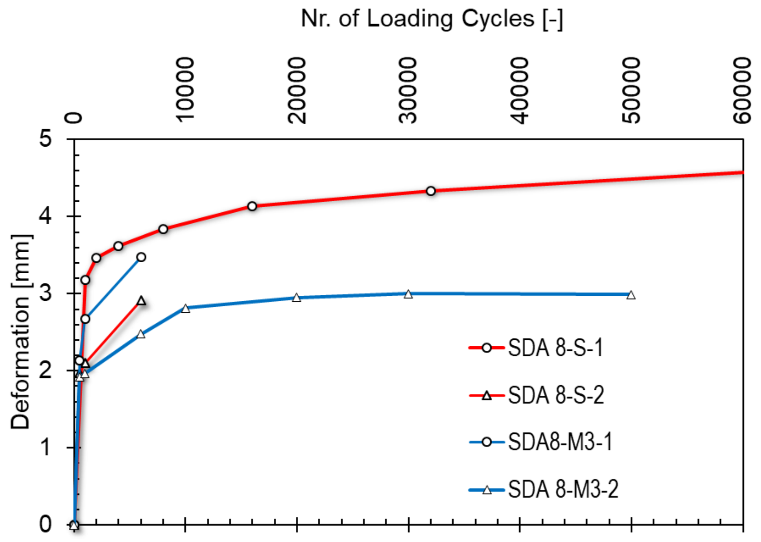

Fig. 56 *Développement de l'orniérage de deux dalles de référence SDA 8-S et SDA 8-M3 modifiée à l'aide de MMLS3*

Comme l'a également montré l'évolution de la profondeur des ornières, de légères améliorations de la durabilité acoustique ont été constatées. Pour les plaques échantillons SDA 4 et SDA 8 avec la modification M3, des niveaux légèrement plus durables (stables) ont été enregistrés (après 6'000 passages du MMLS3). Ceci est illustré dans la Fig. 70 suivante.

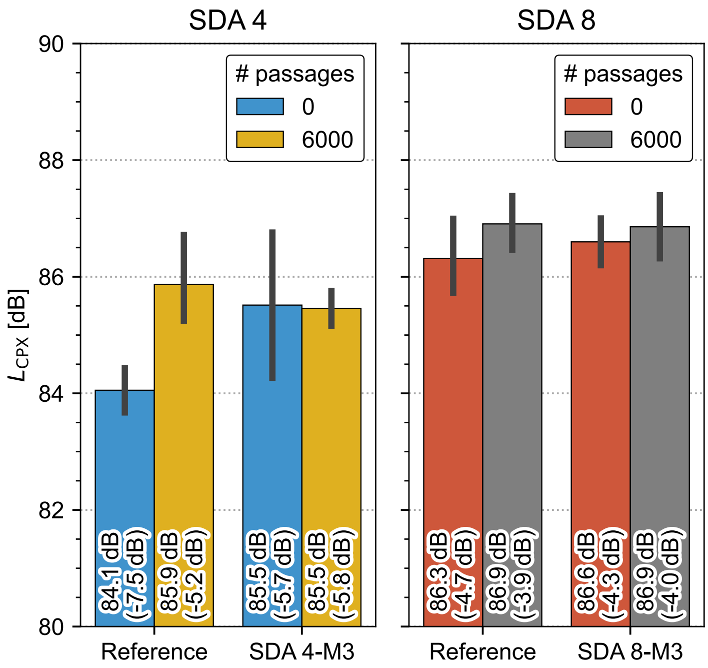

***Fig. 70** Résultats de la simulation acoustique pour SDA 4 et SDA 8 pour les formulations de référence et optimisée (M3) avant et après traitement dans le simulateur de trafic MMLS3*

L'accessibilité de la structure des pores a été analysée à l'aide de la méthode AVCA (Acoustic Void Content Analysis) en utilisant des séries d'images de tomographie assistée par ordinateur (CT) de carottes extraites de la dalle de référence et de la dalle modifiée M3 avant et après les essais avec le simulateur de trafic MMLS3. Les résultats ont confirmé que la connectivité des pores avec la modification M3 pouvait généralement être mieux maintenue qu'avec la référence. A titre d'exemple, la Fig. 62 montre que l'accessibilité des pores pour la référence SDA 8 au point de mesure vieilli (MP4) diminue continuellement avec l'augmentation de la profondeur de la carotte de forage. Ce n'est pas le cas pour la dalle modifiée M3. Par conséquent, la modification a permis de stabiliser la structure des pores.

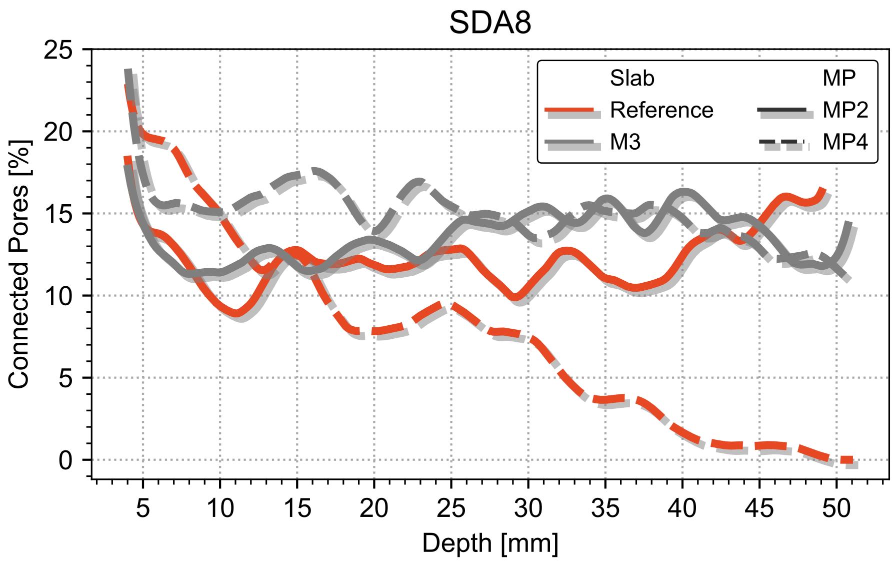

***Fig. 62** Réseau de pores connectés pour les SDA 8-Slabs. Rouge: Dalle de référence, gris: Mélange optimisé (M3). Lignes pleines: MP2, trajectoire après MMLS3 (6'000 cycles) et MP4, trajectoire extérieure (lignes pointillées)*

Résumé et conclusions

Une approche multi-échelle a été mise en œuvre pour étudier les performances mécaniques et acoustiques des mélanges SDA 4, SDA 6 et SDA 8, de l'échelle du millimètre à celle du kilomètre. Le Tab. 18 présente un résumé des résultats critiques. Des mélanges de référence ont été développés en utilisant les performances acoustiques optimales in situ de ces mélanges à l'aide de 200 sections d'essai. Dans un premier temps, les performances mécaniques des mélanges de référence ont été étudiées. Il a été démontré que le classement général des mélanges de référence était le suivant: SDA 4>SDA 6>SDA 8. Dans un deuxième temps, des combinaisons de liant, de charge et d'additifs ont été utilisées pour caractériser le mastic. Le mastic le plus performant a ensuite été utilisé pour produire les mélanges modifiés. Les mélanges SDA 4 ont d'abord été modifiés et testés mécaniquement à l'aide d'une grande variété d'essais afin de déterminer leur performance. Ensuite, la modification optimisée a été appliquée aux dalles SDA 8. Les résultats expérimentaux ont permis de tirer les conclusions suivantes:

- À l'échelle du mastic, il a été observé que la charge avait principalement un effet raidisseur avec un module complexe plus élevé et un angle de phase plus faible à des températures supérieures à 30°C, la charge Zeobit ayant un effet plus important.
- À l'échelle du mastic, le liant hautement modifié avec du calcaire et de la charge Zeobit ainsi qu'une combinaison de charge Zeobit et de chaux hydratée ont obtenu les meilleurs résultats, qui étaient également similaires.
- La modification optimisée pour les mélanges était une combinaison de liant hautement modifié, de charge raidissante (Zeobit) et de chaux hydratée pour améliorer la sensibilité à l'eau.
- Il convient de noter que la chaux hydratée a une empreinte environnementale relativement élevée et que cet aspect doit être pris en compte lors du choix des matériaux optimaux.
- Les essais de performance des mélanges à l'échelle du laboratoire ont montré que la modification améliorait la sensibilité à l'eau, la résistance à la fatigue et à la compression cyclique et présentait des résultats similaires à la fissuration à basse température par rapport à la référence.
- L'essai IMP micro-Deval a montré une perte de particules plus importante pour les mélanges SDA 8. Les mélanges SDA 4 modifiés ont montré une perte de particules similaire à celle des mélanges de référence.

- Les essais MMLS à grande échelle ont montré qu'après 50'000 cycles de chargement, les mélanges M3 modifiés présentaient moins d'orniérage que les mélanges de référence. Cet effet était plus important pour les mélanges SDA 8. Les mélanges modifiés présentaient des changements similaires en termes de texture de surface et de performance acoustique par rapport aux mélanges de référence avant et après le passage des roues.
- En utilisant le simulateur de charge MMLS3 et les mesures avant et après l'exposition aux charges, la modélisation acoustique a montré que les niveaux de bruit des mélanges modifiés SDA 4 M3 et SDA 8-M3 se sont améliorés entre les points de mesure sans charge et les points de mesure avec charge. Cela indique que la modification a maintenu l'intégrité structurelle du mélange après le chargement. Cela a été confirmé par les tomodensitogrammes des échantillons chargés et non chargés, qui ont montré que la connectivité des vides des mélanges modifiés était plus importante, ce qui a contribué à une meilleure absorption du bruit.

Tab. 18 *Summary of results: arrows indicate results in comparison to SDA 4-S standard mixture; green arrow=improved performance; yellow arrow=similar performance; red arrow=worst performance. SCB and rutting results are only for the modified mixtures; yellow arrow shows similar results and green arrow shows better performance in comparison to the modified mixtures*

Mixture / Test	**ITSR**	**Fatigue**	**CCT**	**Rut***	**SCB***	**MicoDeval**	**MMLS3**		
							Def	**Noise Abs**	**Air**
Temp.	20°C	10°C 10Hz	50°C	60°C	0°C		40°C	40°C	40°C
SDA4-S	REF	REF	REF				REF	REF	
SDA6-S	→	↓	↓				→		
SDA8-S	↑	↓	↓				↓		
SDA4-M1	↓	→	↑	→	→	→			
SDA4-M2	↑	↑	↑	→	→	↑			
SDA4-M3	↑	↑	↑		→	→	↑	→	↑
SDA8-M3							↑	→	↑

1 Introduction

Already in the early 2000s, reports [30] and [20] showed the relationship between void content and noise generation on the one hand and void content and service life on the other.

It was already recognized at the time that although a high void content leads to more favorable acoustic behavior, it reduces the service life of the road surface (see Fig. 1). As a compromise, a range of void contents was proposed at which both good acoustic behavior and a long service life could be expected. This range was called "semi-dense asphalt" for the first time. Since then, this term has become established and is now defined in a Swiss Standard VSS 40 436 [19].

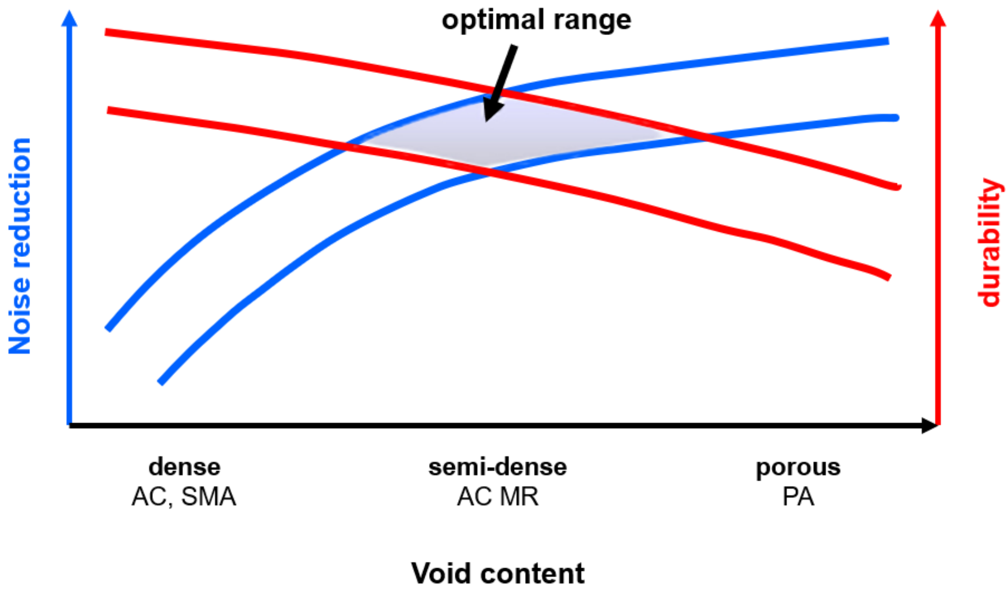

Fig. 1 *Schematic representation of the influence of void content on noise reduction (blue curve) and on the technical service life (red curve) of an asphalt pavement. The intersection of the two curves results in an optimum void content, called semi-dense-asphalt [20]*

Semi Dense Asphalt (SDA) pavements are gap graded mixtures and have been one of the most effective noise abatement measures. However, there is an urgent need to optimize their mechanical and acoustic durability in order to make such solutions cost effective during their life cycle which is considerably shorter than dense mixtures. In Switzerland, SDA pavements are an established and effective noise abatement measure at the source. The SDA mixtures have lower porosity than porous asphalt (PA) and theoretically combine the reduced noise properties with better mechanical durability in comparison to PA. Since 2010, over 1'000 low-noise pavements were constructed in Switzerland [77]. Thanks to the research efforts in recent years and many practical experiences, the asphalt mixtures have been improved mechanically as well as acoustically to a certain extent [27], [42]. Nevertheless, questions remain about the durability of these pavements both mechanically and acoustically. The recently completed D-A-CH project ADURA Akustische Dauerhaftigkeit lärmmindernder dichter oder semi-dichter Asphaltdeckschichten [33] shows that the acoustic durability of SDA can be influenced by the amount and choice of binder. The project, however, does not provide specific solutions for increasing the durability of SDA. Since the lifecycle cost analysis of SDA are largely influenced by their service life, improving the acoustic and mechanical durability of SDA remains a key priority in order to holistically assess the effectiveness of this pavement as a noise abatement measure.

The project has the following specific objectives:

1. Improving the acoustic and mechanical durability of SDA 4, SDA 6 and SDA 8 by optimizing and adapting the mixtures to different traffic and climatic conditions present on the Swiss national and main road network using a multi-scale approach
2. The project addresses two priority research focuses of ASTRA «TRU 1 - Erhöhung der mechanischen Dauerhaftigkeit und Lärmreduktion von Belägen» as well as «TRU 3- Alterung von Bitumen: Mikrostruktur sowie chemische Zusammensetzung».

2 State of the Art

A recent report by the World Health Organization (WHO) indicates that in the EU, traffic noise is the second largest environmental problem affecting health after air pollution [34]. In Switzerland, every seventh person is exposed to excessive road traffic noise [27]. The Federal Council therefore released an action plan in 2017 to combat excessive road traffic noise more forcibly and effectively than before by taking measures at the source which is the road/tire interaction [82]. Possible measures are primarily speed reductions, traffic diversion and low-noise pavements. Two factors influence the noise generation of vehicles: engine noise and tire/road contact noise. As tire/road noise dominates at speeds of around 20 km/h and above [25], low-noise pavements have become an effective and widely used noise abatement measure in Switzerland.

Comparative burden studies suggest that, after particulate matter, noise is the second major cause of Disability Adjusted Life Years (DALYs) lost [35]. This new health evidence highlights the urgency of adopting more stringent noise standards and implementing noise reduction technologies. One way to mitigate the exposure of residents to noise is to take advantage of the existing public spaces and transform the available surfaces of pavements into elements that foster comfort and health for urban residents. To this end, an effective noise abatement method has been the use of semi dense asphalt (SDA) pavements. Long-term in-situ measurements of SDA pavements by G+P have shown that the acoustic performance of such pavements, although high after construction, can significantly diminish after several years [42]. Therefore, there is an urgent need to develop know-how on how to improve the acoustic and mechanical durability of such pavements.

Various parameters such as surface texture, porosity, interconnected voids, and aggregate size of pavements contribute to the noise reduction character of a pavement. For example porous asphalt or open-graded asphalt can reduce the noise significantly, especially in the first years [39] [79].This is possible because of the high porosity (around 25%) compared to conventional dense asphalt (4%) which enables the air to flow readily through the pavement, thus absorbing the noise [79]. Full-scale testing at a test track demonstrated that increased pavement surface porosity decreases noise levels almost at any frequency [52]. It is important, however, to balance porosity with mechanical durability of the pavement, because open-graded mixtures generally have a shorter lifetime compared to dense-graded pavements. For dense graded mixtures, sur-face texture is the main parameter regarding the low noise character. Low texture will reduce noise levels at lower frequencies (below 1600 Hz) [52] [56]. Reduction of surface texture, however, comes at the cost of lowered tire friction, thus one must find an optimum balance between noise and driving safety [52]. Fig. 2 shows effects related to vehicle and surroundings during driving, such as noise, rolling resistance, and tire wear, plotted against texture wavelength. It can be seen from this illustration that lower macro-texture has positive effects on road noise and the opposite effect on rolling resistance, which is a safety consideration. Apart from pavement noise reduction based on different mixture porosity (volumetric) level, in parallel, the use of alternative materials could be a viable approach to achieve such measures. Introduction of rubber in mixtures, including ground tires, can also contribute towards reduction of traffic noise by as much as 2dB [54].This is due to the sound transmission attenuation properties of rubber. Development of low noise pavements specifically for the urban environment considering the frequencies and loading of such pavements due to traffic is lacking. In Switzerland the SDA have shown promising [27] as discussed above.

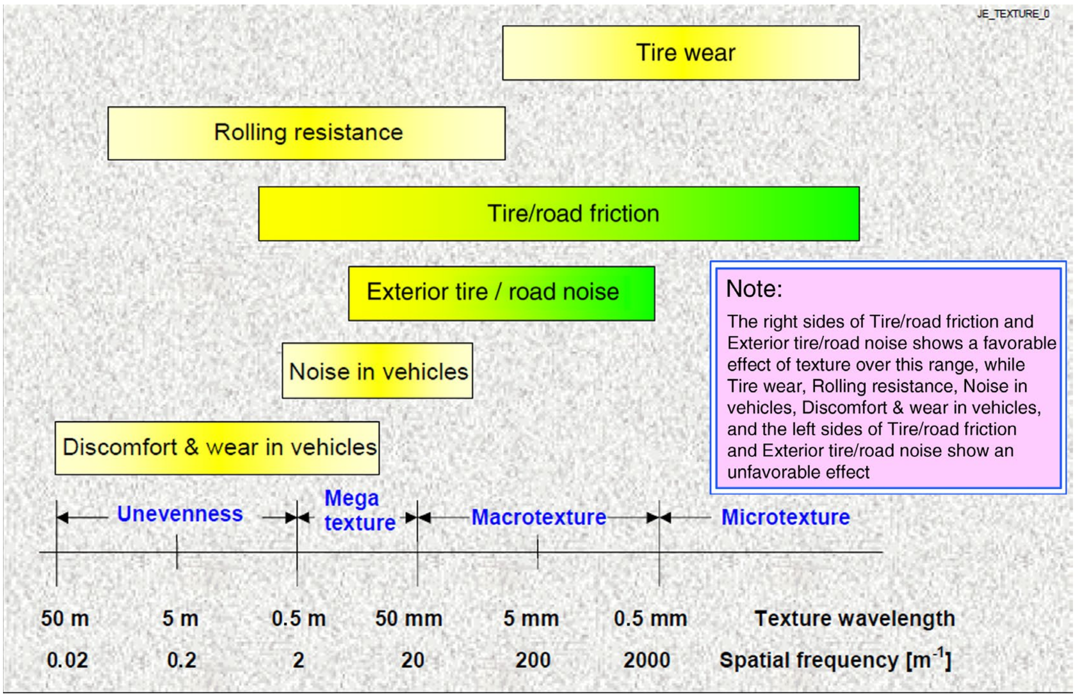

Fig. 2 *Illustration of texture wavelengths, anticipated effects showing that noise is affected by macro-texture [81] EN 12473-1*

In 2010, the federal government launched a research package in which SDA in urban areas were extensively tested on 15 test tracks with substantial traffic volumes with regard to their noise reduction properties [21] [29]. In addition, a Swiss standard was developed (SN 40 436 [19]), which should allow any construction company to produce and construct noise-reducing SDA mixtures. The findings on the acoustic effect and the structural requirements of these test pavements were recorded in the final report of the accompanying long-term monitoring [24]. The asphalt mixtures have also been tested by various cantons with further implementation on high traffic volume roads. The availability of additional test results under full traffic load allowed for new conclusions to be drawn about the most important parameters for the successful implementation of SDA. In a new study commissioned by the federal government and the Canton of Aargau, as the most important parameters materials, mixture and construction parameters were identified by statistical analysis of a sample of approximately 150 SDA pavements [42]. The results of this study allowed for a further increase in noise reduction and durability of SDA. These results are currently being incorporated into the upper gradation curves for the existing standard of SDA4 and SDA8 [32]. Furthermore, this prior study on SDA revealed that the filler and sand content are the most decisive factors regarding long-term acoustic performance as well as the presence of surface-connected, and hence acoustically active, voids in the pavement [42] [32]. Moreover, this study presented interdependent maxima for these two factors with the aim to ensure that voids in the pavement are connected to the surface. This existing knowledge about de-signing mixtures with acoustically effective void structures will be used as input for the current project.

Recently, Empa has led a national project funded by the Swiss National Science Foundation (SNSF) addressing the application of low noise pavements in the urban environment using urban waste materials. An integral part of this ongoing project is the investigation and characterization of various low noise pavement in Canton Zurich for their acoustic and mechanical properties. The knowledge generated by this completed project (Urban mining for low noise urban roads and optimized design of street canyons) flowed directly into the proposed project.

Simultaneously, G+P has been working on the D-A-CH project ADURA that investigated the processes of acoustic ageing of low-noise pavements. The project shows that the acoustic durability of SDA can be influenced by the choice of binder. The project, however, does not provide specific solutions for increasing the durability of SDA. The potential stemming from the optimization of binder and mastics properties is pointed out by various researchers [33]. The results from the project ADURA and the knowledge gained will be also used in the current proposed project.

3 Methodology

The project aimed to improve mechanical and acoustic durability of various low noise pavements. As outlined in Fig. 3, based on the current state of in-situ performance of low noise pavements, three well performing mixture types are selected: SDA 4, SDA 6 and SDA 8. These mixtures were tested for their mechanical and acoustic performance in non-aged and aged states using a multi-scale approach. Thereafter a systematic optimization protocol was applied to these mixtures. Thereby, the best performing mixtures were selected and optimization parameters identified. The project could uniquely combine knowledge from in-situ long term performance and laboratory performance of low noise pavements.

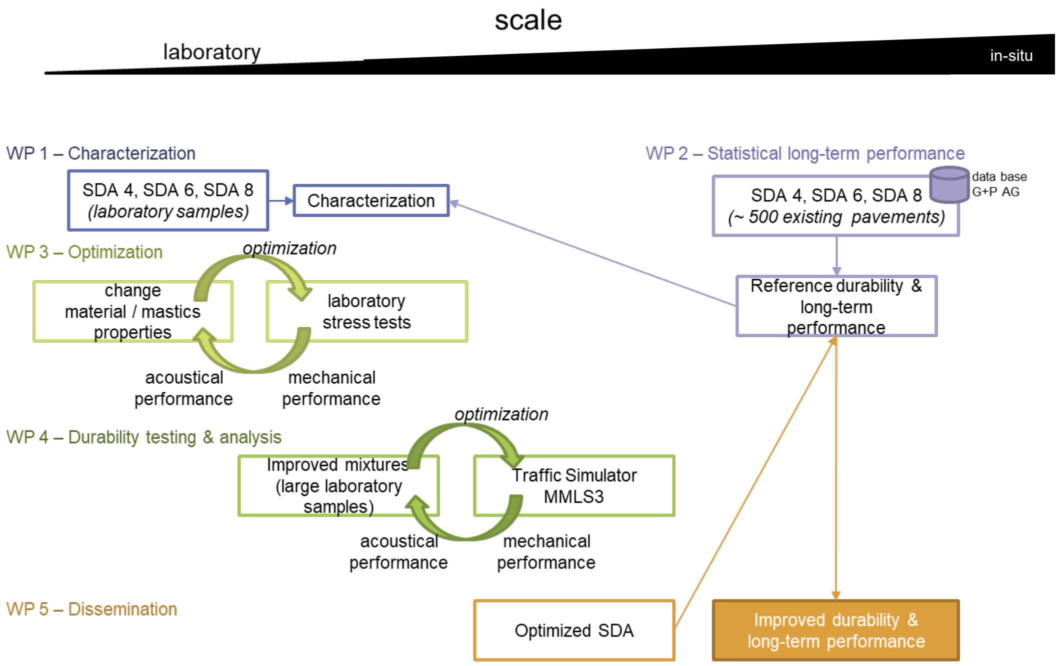

Fig. 3 *Schematic of the planned research*

3.1 Availability of the required data

As discussed in WP2 in detail in section 5, G+P has created a unique, large database on in-situ acoustic performance of low noise pavements in Switzerland. This data was available to the project for evaluating in-situ ageing properties of all low noise pavement types used in Switzerland. This available knowledge, was analyzed within the project (WP2) and allowed to select pavements for further investigation and optimization that have proven in-situ acoustic performance. Moreover, it allows for the upscaling of results obtained from the optimization cycles through laboratory testing. Fig. 4 shows the distribution of the pavement locations in Switzerland, where G+P has long-term in-situ acoustic measurements.

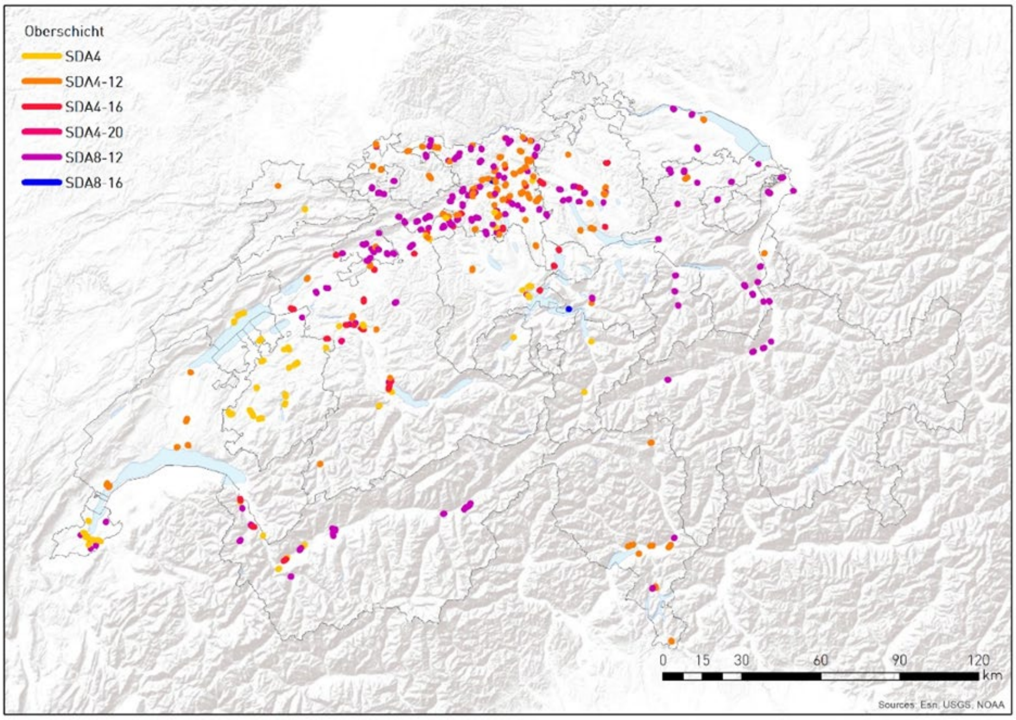

Fig. 4 *Distribution of test track locations and SDA pavement types with long-term acoustic measurements in Switzerland*

3.2 Research plan

3.2.1 Work Program

The pavement structure consists of aggregates, bitumen and pores. Each of these parameters (aggregates, bitumen and pores) can be controlled in order to achieve optimum acoustic properties. At the same time road structures need to withstand heavy traffic and environmental loads. In order to reach the goals of the project five work packages (WP) were identified as shown in Fig. 5 and discussed in detail below. In WP1, reference mixture properties were determined. WP2 delivered the field data results to be used as input for optimization performed in WP3. WP4 investigated the up-scaled properties and the gained knowledge is disseminated in WP5.

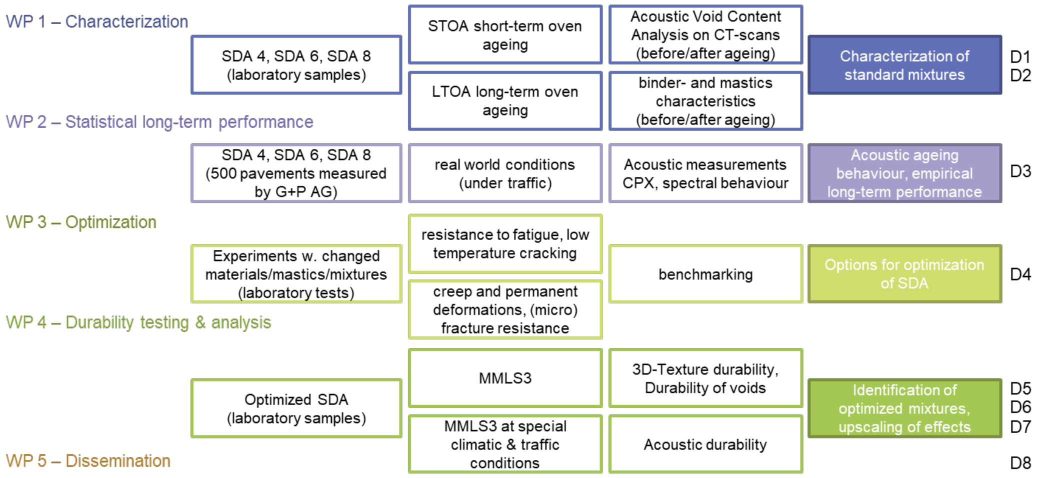

Fig. 5 *Overview of research plan*

3.2.2 WP1: Characterization of unaged and aged SDA 4, SDA 6, SDA 8 (cm scale)

In this WP, asphalt mastic was modified using alternative binder and fillers. Following the findings at the mastic scale, SDA 4 mixtures were produced in the lab with the best performing modifications. Mechanical performance of aged materials were determined and used as a benchmark. Aging was performed as follows: short-term oven aging (STOA). STOA replicates the aging that the mixture experiences during production. This is simulated in the laboratory by exposing loose mix to 135°C for four hours. Mechanical performance tests on asphalt mixtures were the indirect tensile strength (ITS) and water sensitivity (ITSR), modulus, fatigue and the cyclic compression test. On mastic the performance tests included fatigue and frequency at low temperature and complex modulus and phase angle at high temperature.

Deliverables:

- D1: Standard (benchmark) mechanical properties of aged laboratory samples

3.2.3 WP2: Statistical analysis of long-term performance of SDA mixtures in Switzerland (km scale)

G+P has a substantial database on the in-situ acoustic performance of SDA mixtures in Switzerland. To date, acoustic measurements using Close-Proximity (CPX) noise (ISO 11819-2) on around 1'000 different SDA pavements are available that include yearly measurements to assess the ageing effect.. Based on this large amount of empirical data, firstly, reference acoustic ageing behavior for standard SDA mixtures in loss of dB(A)/year are determined and used as input and as reference for the optimized lab mixtures. Secondly, a model for the acoustic ageing of SDA mixtures was created accounting for the different acoustic ageing phenomena (e.g. texture induced, compaction through traffic, ingress of dirt). A first model generally describing the acoustic ageing behavior of SDA 8 and SDA 4 was established in the scope of the D-A-CH project ADURA. Based on this model, more refined models differentiating the different aging processes was developed in this project. To achieve this, G+P's database with CPX measurements was joined with a database with detailed measurements of surface characteristics and detailed information on the mixture and the constructed layer. Tire-road-interaction modelling was used to estimate their contribution to overall acoustic ageing. The model for acoustic ageing of SDA was an essential component for upscaling the acoustic performance from the laboratory to real field situations. Thirdly, acoustically durable pavements were identified and the corresponding mixture were analyzed.

Deliverables:

- D2: long-term acoustic performance and acoustic ageing model of existing SDA mixtures and identification of most durable solutions.

3.2.4 WP3: Optimization and characterization of low noise pavements (μm-cm scale)

A prior study on SDA revealed that the filler, sand and binder content are the most decisive factors regarding long-term acoustic performance as well as the presence of surface connected, and hence acoustically active, voids in the pavement [12]. Moreover, this study presented interdependent maxima for these two factors with the aim to ensure that voids in the pavement are connected to the surface. This existing knowledge about designing mixtures with acoustically effective void structures was used as a starting point in the optimization process.

The aim of this part of the project was to develop improved mixtures with regard to acoustic and mechanical long-term performance. Acoustic properties were tested in WP4 on larger slabs that represent the in-situ performance closer. In this WP, relevant properties with direct effect on acoustic properties was optimized: mixture and mastic and material parameters such as high softening point binder additives and filler characteristics will be explored.

Benchmark samples of optimized SDA mixtures were produced. These laboratory-produced mixtures have to perform as required on the road and the target was to show that the imparted properties from the optimization processes listed above do not compromise their performance including durability and water sensitivity. Using tests that are routinely used in Switzerland and others that are not routinely used. As standard requirement, water sensitivity (ITSR) was investigated. As non-standard test, fatigue, complex modulus and Frequency and Temperature sweep test on the mastic, fracture resistance using the Semi-Circular Bend (SCB) test [80], rutting and cyclic compression test as well as particle loss using the micro-Deval were used.

Deliverables:

- D3 Mechanical properties: Meso-scale microstructural and mechanical properties of the mastic and mixture.

3.2.5 WP4: Large scale durability testing of optimized mixtures (m scale)

In this work package the modified SDA 4 mixtures were tested using the traffic simulator MMLS3. Selected solutions were constructed in the laboratory in the form of large test slabs (3m×1m) and tested until failure using the vehicle load simulator MMLS3, resulting in knowledge on pavement response from traffic loading. Using this type of simulator, monitoring of pavement performance under traffic load was investigated.

According to the number of load applications required to reach failure of the slab, a ranking containing the most mechanically durable materials was obtained. The model mobile load simulator MMLS3 is a laboratory sized accelerated pavement testing (APT) machine for studying scaled pavement distress under repetitive rolling tires. The MMLS3 is a movable and flexible traffic simulator that applies a downscaled load with four single pneumatic tires. They are smaller than standard truck tires, having a diameter of 0.3 m and a width of 0.11 m. The machine is 2.4m long by 0.6m wide and 1.2m high. Each tire loads the pavement width over a path length of 1 m with a load up to 2.1kN, induced through a spring suspension system. At a maximum speed of 9 km/h, the MMLS3 allows approximately 7200 load applications per hour, corresponding to nearly a 2 Hz loading frequency rate.

The traffic simulation process accompanied various acoustically relevant measurements i.e., surface texture, sound absorption, as well as simulations to gather detailed insights in the traffic simulation process. As direct acoustic measurements during the traffic simulation is not possible due to the intrinsic sound generation of the MMLS3, for the purpose of acoustic simulations and performance predictions the same approach as in [4] was chosen: the program SPERoN [28] and the detailed analysis of noise generation mechanisms [41] will be used. SPERoN allows for predictions of the acoustic performance if constructed on real road sections by contact force, airflow and sound propagation models, which are fed by surface characteristics data from laboratory measurements (texture, airflow resistance and sound absorption). Experiences [22] show that the model works particularly well for acoustical benchmarking of different mixtures of the same pavement design.

The acoustic properties of aged mixtures was characterized by type and amount of filler and sand, durability of accessible voids as well as absorption durability (using impedance tube, ISO 10534-2) was performed on large slabs that represent the field situation.

Mixture and surface characteristics (using a laser scanner) and how these change with ageing at different stages during the ageing experiments were measured and analyzed. Computed Tomography (CT) was used to characterize connected voids as well as surface characteristics. The compaction method used in the laboratory has a great influence on the shape of the pores [36] as well as the texture [22].

To ensure that the mixtures also have the required acoustical properties, the laboratory-compacted samples are analyzed regarding their acoustically effective void content using Acoustic Void Content Analysis AVCA, developed by G+P [73]. The standard mixtures produced in WP 1 served as a reference. AVCA calculates and characterizes connected voids to the surface (separating blocked pores by dirt), by applying a machine learning image classification algorithm on the CT-image series and a subsequent pathway analysis.

Deliverables:

- D4 Acoustic properties: Surface texture, porosity, absorption, SPERoN – Simulations (before and after exposure to the traffic simulator).
- D5: Upscaled mechanical performance.
- D6: Upscaled acoustic performance (including influence on standard acoustical ageing curve).
- D7: Benchmark acoustic properties of aged and unaged mixtures: Filler and sand, durability of accessible voids, absorption durability

3.2.6 WP5: Dissemination

The results of this project will be disseminated at national and international conferences, industry publication as well as scientific publications.

Deliverables

- D8: Dissemination

4 Materials

The aggregates were sandstone from Massongex, Switzerland (FAMSA), complying with the performance requirements for SDA by Swiss standards (VSS 40 436 [16]). In addition certain modifications were done as listed in Tab. 1, Tab. 2 and Tab. 3.

Tab. 1 *Materials used in the project*

Type of Material	Category	Description
Aggregates	Famsa 0.1/2, 2/4, 4/6, 6/8	
Filler	I	Weak filler (lower bound of standard) Kalkstein (Limestone)
Filler	II	Filler with a strong stiffening effect (upper bound of standard) Zeofill
Filler	III	Filler with a very strong stiffening effect (special type) Zeobit
Binder PmB	Type E	PmB 45/80-65(CH-E)
	HiMa	Highly polymer modified asphalt (PmB 45/80-80)
Additives	Calcium hydroxide	Improve aging and water sensitivity

4.1 Bitumen properties

Two types of bitumen were used in this project. Bitumen 2 is the standard PmB used for SDA mixtures in Switzerland and Bitumen 1 is highly polymer modified. The material properties provided by the supplier (Grisard) are listed in Tab. 2 as well as penetration and softening point values determined for the batch received in the lab shown in parentheses. Type 1 (PmB 45/80-80 HiMa) and 2 bitumen (PmB 45/80-65 (CH-E)) are identified as appropriate for surface courses such as SMA, PA, AC MR, SDA providing resistance to rutting and temperature variations. Type 1 is a highly modified blend and it is also identified as appropriate for recycling asphalt. High polymer content guarantees a high elastic recovery also when high amounts of recycling is used.

Tab. 2 *Bitumen properties provided by the supplier and measured in the lab in parentheses*

Designation	Standard	1	2
	EN14023:2010	PmB 45/80-80HiMa	PmB 45/80-65 (CH-E)
Penetration 25°C (1/10mm) Min/max	EN 1426	45/80 (53)	45/80(66)
Softening Point (°C	EN 1427	80 (92.5)	65 (84)
Elastic recovery 25°C (%)	EN 13398	80	80
Plasticity range (°C)	EN 14023	80	80
Mass loss (%)	EN 12607-1	0.5	0.5
Remaining Penetration (%)	EN 1426	60	60
Increase softening point (°C)	EN 1427	8	8
Elastic recovery 25°C (%)	EN 13398	60	60

4.2 Additives

Calcium hydroxide was used as an additive. According to the current knowledge this additive enhances the water sensitivity of the mixtures. The results of the research by

Gorkem and Sengoz indicated that the addition 1%, 1.5%, and 2% of hydrated lime by mass of aggregates and polymer modification increased the resistance of asphalt mixtures to the detrimental effect of water. Moreover, it was found out that samples prepared with SBS PmB exhibited more resistance to water damage compared to samples prepared with EVA PmB [46]. However, it should be noted that hydrated lime has a relatively high environmental footprint and this aspect should be considered when choosing the optimum materials.

4.3 Mixture designations

In WP2, benchmark mixtures were chosen based on the in situ acoustic performance of SDA mixtures. As described in detail in chapter 5, although the mixtures fulfilled the aggregate gradation defined in the standard, there were mixtures that had much better acoustic performance. Using this information, three benchmark mixtures were produced as part of the work program of WP1 and WP4 and three modified mixtures were produced as part of the work program of WP3 and WP4. The designation of mixtures and materials used is shown in Tab. 3.

***Tab. 3** Mixture designation: S stands for standard and is not related to the classification of the mix according to traffic load N, L, S, H*

Designation	Description
SDA 4-S	Benchmark SDA 4 mixture with PmB45/80-65E and Zeofill filler
SDA 6-S	Benchmark SDA 6 mixture with PmB45/80-65E and Zeofill filler
SDA 8-S	Benchmark SDA 8 mixture with PmB45/80-65E and Zeofill filler
SDA 4-M1	Modified SDA 4 mixture with highly modified bitumen Zeobit filler
SDA 4-M2	Modified SDA 4 mixture with highly modified bitumen limestone filler
SDA 4-M3	Modified SDA 4 mixture with highly modified bitumen Zeobit filler and calcium hydroxide (hydrated lime) as additive
SDA 8-M3	Modified SDA 8 mixture with highly modified bitumen Zeobit filler and calcium hydroxide (hydrated lime) as additive

5 Statistical analysis of long-term performance of SDA mixtures (km scale)

As a starting point for the project, the most promising mix designs should be used for further optimization of the SDA technology. Thus, a statistical analysis of the in-situ constructed pavements is performed to identify the most promising solutions. The focus of the analysis is laid out in giving i) a good acoustical initial performance of the pavement and ii) a most durable solution (in terms of acoustic performance).

5.1 Data description

Data regarding acoustic performance of SDA 4 and SDA 8 pavements comprises 2500 CPX measurements for over 500 SDA sections collected since 2012. 200 SDA sections including the construction data as well as acoustic performance are available. 1327 drill cores taken after construction were analyzed from 775 different mixtures. Fig. 6 and Fig. 7 show the location of all test sections [32].

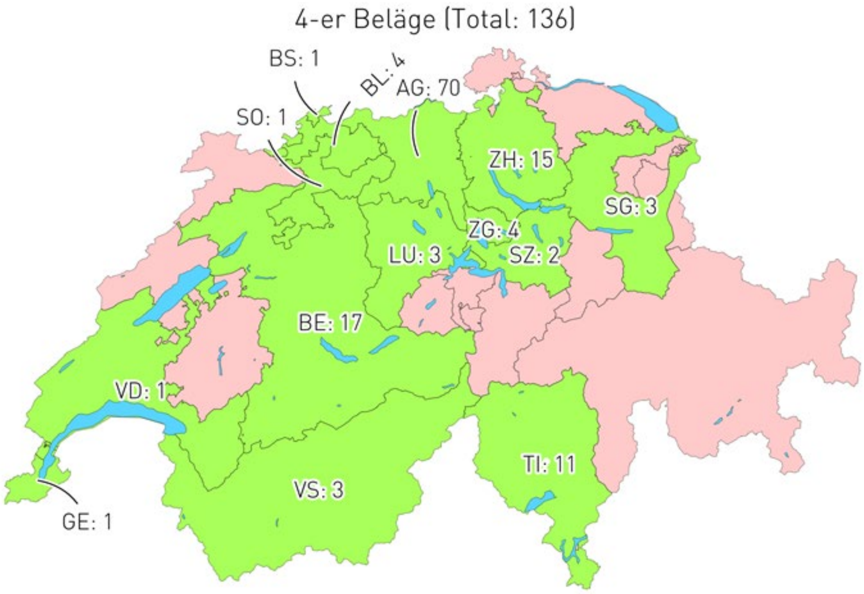

Fig. 6 *Location and number of the SDA 4 test sections in this study by canton*

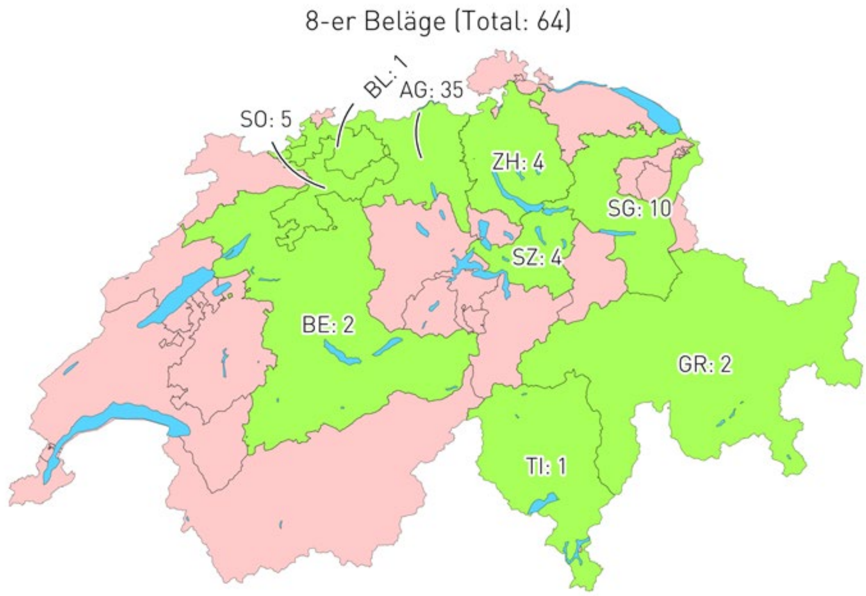

Fig. 7 *Location and number of the SDA 8 test sections in this study by canton*

5.2 Mixture design and initial acoustic performance

This data allows for connecting the acoustic performance of such mixtures with their aggregate gradation after their service years. Fig. 8 shows the relation between gradation and acoustic performance for the SDA 4 and SDA 8 mixtures, with warmer colors indicating better acoustic performance. Here all the mixtures as presented in Fig. 7 are characterized with respect to their (initial) acoustic performance. This data allows for the estimation an optimal recipe from an acoustic point of view. The goal was to reduce the voids content as much as possible to improve mechanical performance but to have acoustically active pores; that is pores that are connected to the surface. Fig. 8 further demonstrates that although all the mixtures examined fall within the requirements of the old standard (VSS 40 436:2019 [16], black dashed lines), they can have very different acoustic performance. Furthermore, it is apparent that getting closer to the lower part of the curve can be acoustically beneficial. The new standard (VSS 40 436:2022 [19]) therefore partially addresses this issue and has lowered the finer part of the maximum sieve curve.

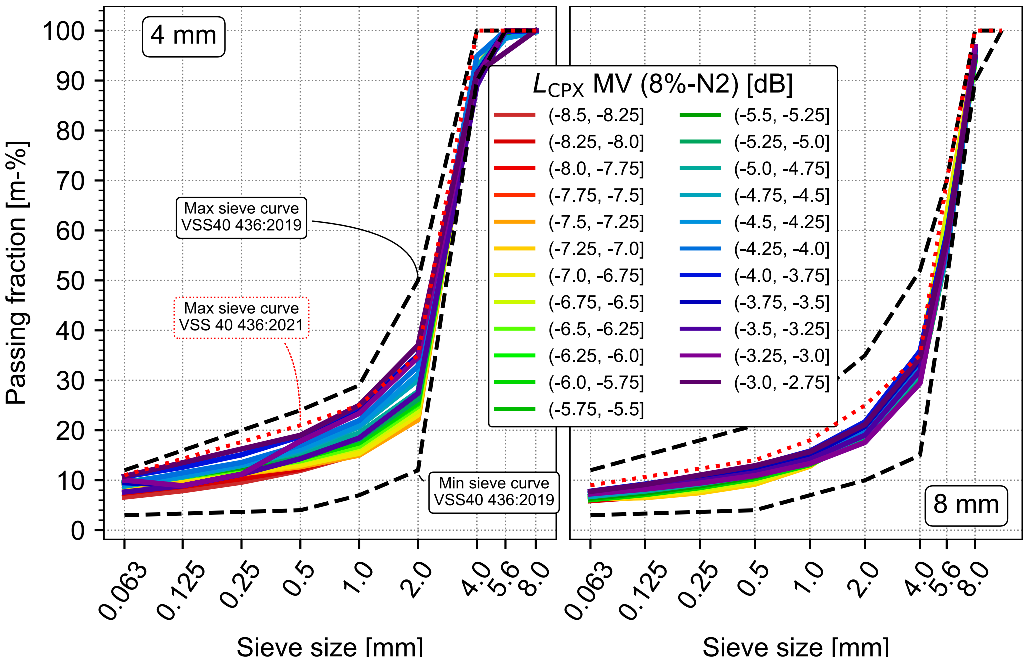

Fig. 8 *In-situ (initial) acoustic performance of SDA 4 and SDA 8 mixtures. Black indicates the upper and lower bounds as defined by the SN VSS 40 436:2019, whereas the red dotted lines indicate the upper bounds of the current valid standard VSS 40 436:2022 [19]*

The gradation curve thus has a major impact on the initial acoustic performance. But the gradation curve also has an impact on the resulting Marshall void content in the mixture. Fig. 9 depicts the influence of the Marshall voids for SDA 4 and SDA 8 in relation to the acoustic factor, defined with the data available at the time that it was developed. This acoustic factor was defined in [42] and is basically a ratio of the filler and sand content in the mixture. The acoustic factor is defined as follows for SDA 4 (Equation (1) with the constraints (2)):

$$AF_{SDA4} = 2 \cdot Sieb_{0.063mm} + Sieb_{2.0mm} \tag{1}$$

while $Sieb_{0.063mm} < 10.7\ \%$ and $Sieb_{2.0mm} < 28.1\ \%$ and $AF_{SDA4} < 41.1$ (2)

For SDA 8, the ratio of filler and sand is defined as given in Equation (3).

$$AF_{SDA8} = Sieb_{0.063mm} + Sieb_{2.0mm} \tag{3}$$

while $Sieb_{0.063mm} < 8.7\ \%$ and $Sieb_{2.0mm} < 24.2\ \%$ and $AF_{SDA8} < 30.5$ (4)

Thus, the acoustic factor is a measure of the distribution of grain sizes in the mixture design. As can be shown in Fig. 9, the acoustic factor is highly correlated the Marshall voids measured using the geometric method. From Fig. 9 it is also apparent that for SDA 4 mixtures with low void content (say below 14 Vol-%) have difficulties fulfilling the acoustic factor criterion.

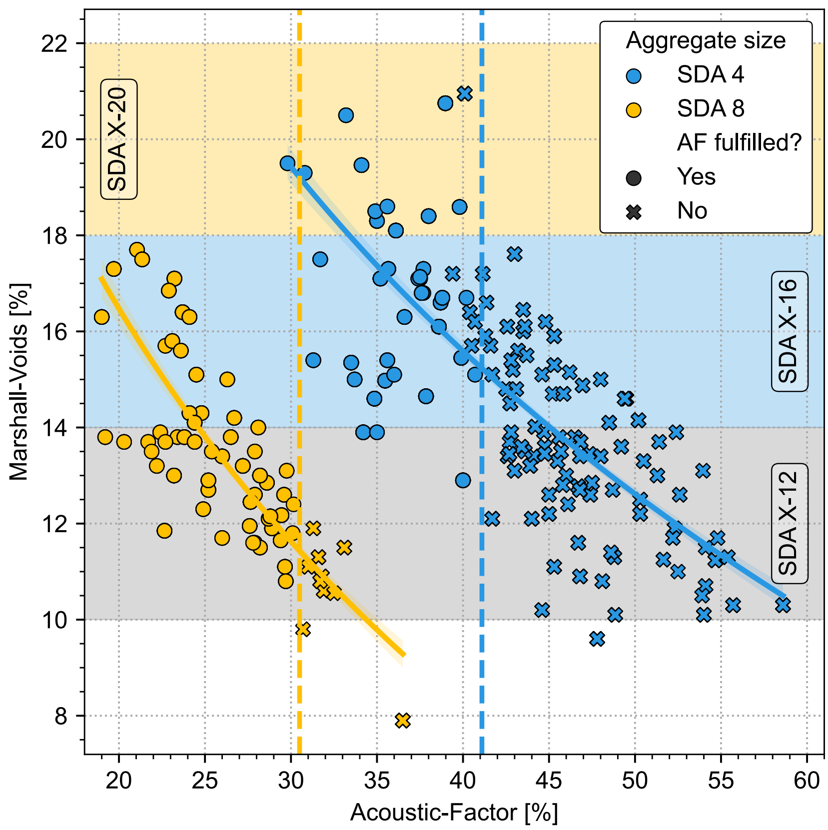

***Fig. 9** Dependence of the Acoustic-Factor and their Marshall voids for SDA 4 and SDA 8*

Increased void content in the mixture is beneficial up to a certain extent regarding the initial noise reduction potential of the road surfaces as the sound absorption and airflow is reduced. Fig. 10 shows the relationship between voids in the mixture and acoustic performance, showing that once the voids reach 18 Vol-% and better, the acoustic performance is considerably higher. However the repeatability of these results is not guaranteed, as higher air voids can also decrease the mechanical durability, a voids content of 15 Vol-% was recommended for this project in order to strike a balance between acoustic and mechanical performance [32].

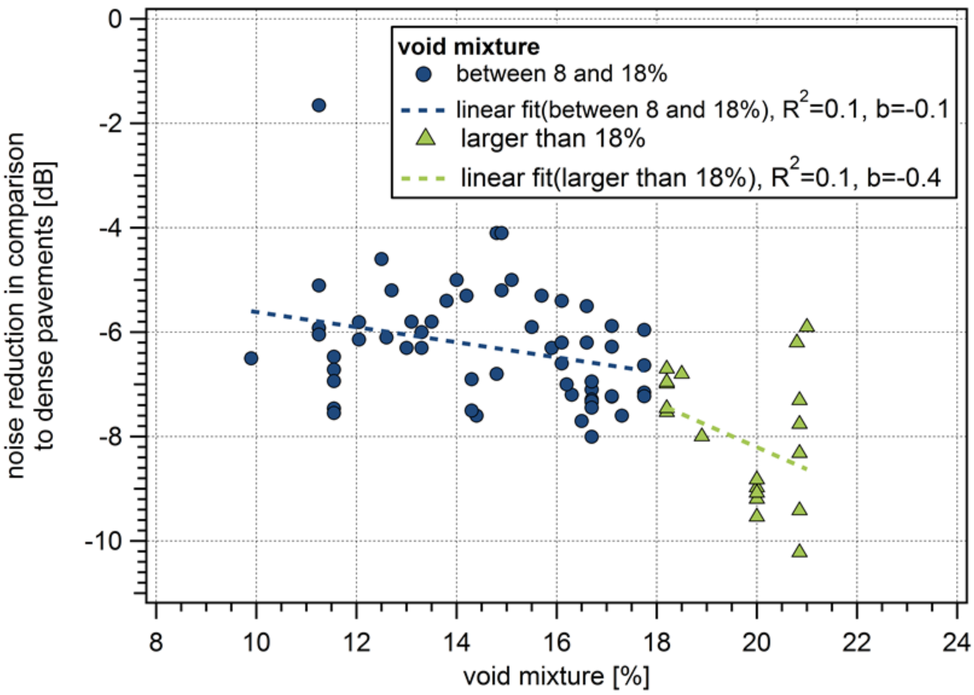

Fig. 10 *Noise reduction as a function of the voids in the mixture*

A closer look at the data indicates that 50% of the observed variation is due to the filler and sand content.

5.3 Long-term statistical acoustic performance

The acoustic performance of low noise pavements over time depends on various influencing factors. Especially in the case of porous mixtures like SDA, where the accessibility of the pores is crucial for the acoustic performance, the detrimental effects during the service life such as exposure to traffic and the environmental conditions such as exposure to temperature changes and precipitation on the pavements are decisive.

5.3.1 Total level

Using in-situ measured data a model was developed as shown in Fig. 11. The figure shows a model of the evolution of the acoustic performance of SDA 4 with 12 Vol-% (range of 10-14 Vol-%) and 16 Vol-% (range of 14-18 Vol-%) void content and SDA 8 with 12 Vol-% (range of 10-14 Vol-%) void content, mixtures over an 11 year period. As can be seen from the data in general SDA 4 pavements (blue and yellow lines) have a higher noise reduction in comparison to SDA 8 pavements (red line) even when the void contents are in the same range (12 Vol-%), because of a lower level for microtexture (ref our literature review). It should be noted that a noise reduction of -1 dB, -3 dB and -6 dB are equivalent to a traffic noise reduction of 20%, 50% and 75% respectively. The reduction can also be interpreted as a noise reduction potential in comparison with an AC 11 mixture after 2 to 5 years of service.

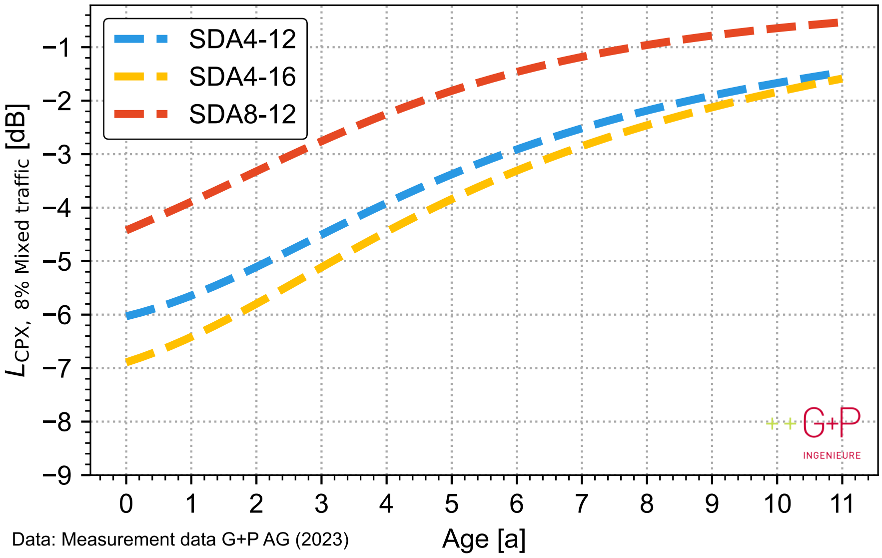

Fig. 11 *Statistical model of the acoustic performance of SDA 4 and SDA 8 mixtures with regard to pavement age*

It is clear from Fig. 11 that different acoustic ageing properties result depending on the void content of the SDA 4. SDA 4-12 mixtures tend to start at around – 6 dB while SDA 4-16 mixtures (with Marshal void content from 14-18 Vol-%) start around -7 dB. This difference is being reduced over a decade of service to around -2 dB. But over the whole life cycle, a potential benefit from the noise reduction is apparent. Tab. 4 summarizes the various parameters that affect the acoustic performance of road materials, highlighting the complexity of their influence on overall performance

Tab. 4 *Influence of various parameters on the acoustic performance of mixtures MPK = Marshall samples, BK= field samples; more * indicates higher degree of significance*

Mixture parameter	**Material Parameters**	**Construction parameter**
Voids filled with binder *	Water sensitivity	Voids content (BK)**
Binder content	Binder type	Max density (BK)
Marshal Flow*	Filler type	Layer thickness*
Void content (MPK)*	Aggregate origin	Compaction degree
Bulk density (MPK)**		Humidity
Max density (mixture)		Wind speed*
Sieve 0.063 mm (Filler)***		Air temperature*
Sieve 0.5 mm		Slope
Sieve 2 mm (Sand)***		Construction company
Sieve 4 mm		
Sieve 8 mm		
Mix Temperature*		
Travel time**		
Mischgutzentrale		

5.3.2 Spectral acoustical ageing SDA 4

From the model presented in Fig. 11, we have learned that increasing the Marshall void content leads to initially better acoustic performance, though the acoustic ageing is somewhat elevated compared to lower Marshall void mixtures. The spectral characteristics of the noise signal is a further important measure, which can be used as indicator for different acoustic ageing processes. For instance, the frequency level of 315 Hz is mostly associated with elevated tyre vibration stemming from rougher surfaces. Whilst higher frequency bands are associated with intact pore structure and accessible air voids leading to sound absorption and the air trapped between the tyre and pavement being reduced.

In order to illustrate the acoustic ageing behavior of different frequency bands, Fig. 12 shows the results for different SDA 4 variants. In this case, the SDA 4 is differentiated according to their Marshall void content. Each entry corresponds to a span of 4 Vol-%. i.e. SDA 4-10 corresponds to Marshall voids between 8 and 12 Vol-%, which is not allowed in the standard, but is still present enough in the field data.

From Fig. 12, different acoustical ageing patters can be recognized. First of all, elevated Marshall void contents seem to be very beneficial for sound absorption characteristics, as indicated by the good initial noise levels of these mixtures in the mid to high frequency range. These good initial acoustic properties, on the other hand, deteriorate more quickly than in mixtures with a low Marshall void content.

On the other hand, regarding the low frequency range, no direct influence of the void content is detectable until about 5-6 year. All the mixtures tend to age in a very linear pattern with respect to the first year. Only in the last years of the data series, slightly elevated values for higher Marshall-Void-mixtures is observable. This is certainly due to the somewhat lower stability of the pavement. Because with higher voids content, and with degradation of the road surface, these kinds of mixtures tend to have a coarser surface, leading to elevated sound emission in the low frequency range.

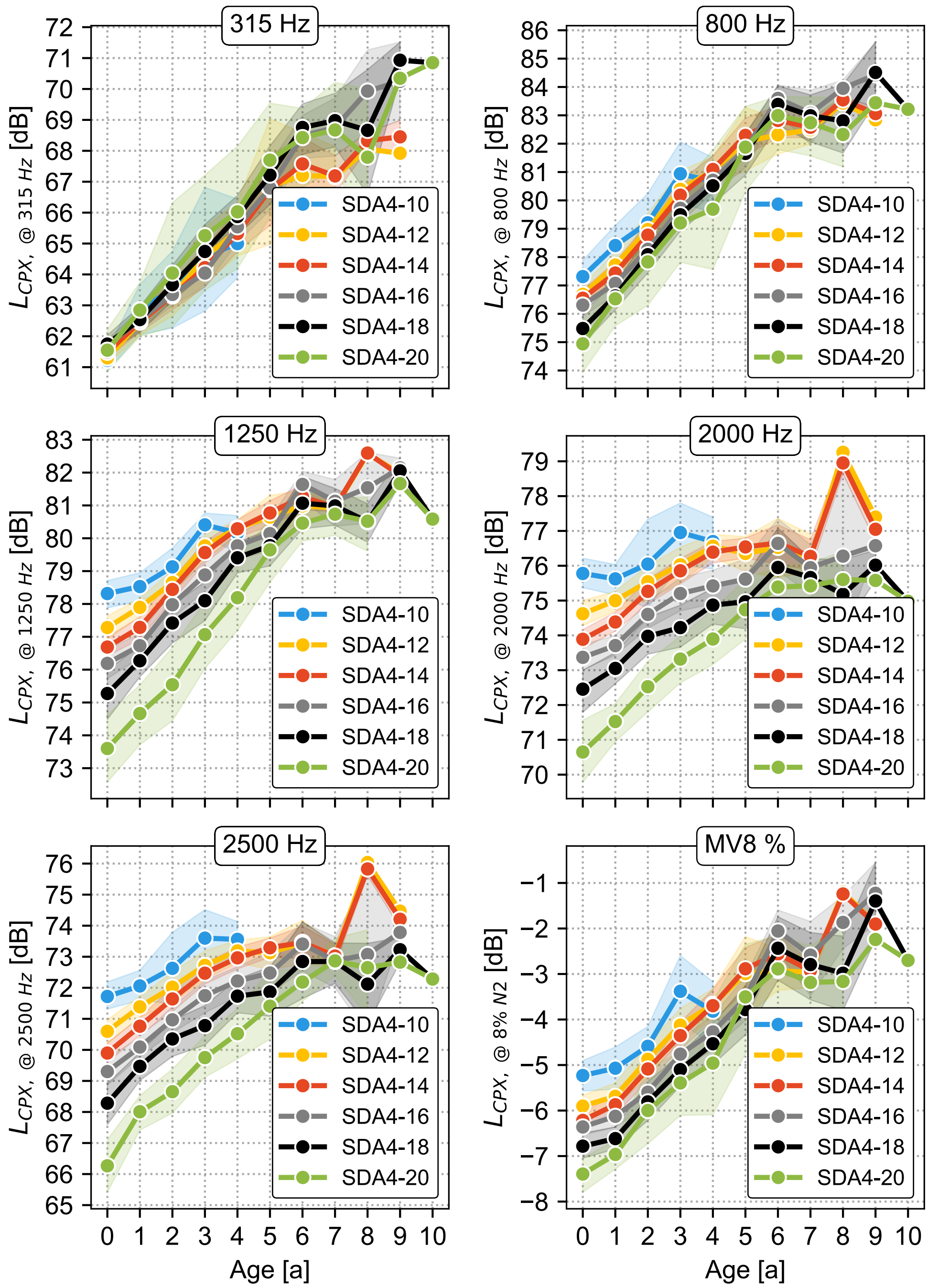

Fig. 12 *In-situ spectral ageing of CPX-Levels of different void content groups of SDA 4-mixtures. Differentiated per Marshall-Void content i.e SDA 4-10 corresponds to SDA 4 pavements with Marshall void content in the range of 8-12 Vol-%*

5.3.3 Spectral acoustical ageing SDA 8

Similar to the previous chapter, the spectral ageing of SDA 8 surfaces is shown below in Fig. 13 as a function of their void content. It should be noted that the data basis for SDA 8 surfaces is considerably smaller. However, the results from SDA 4 can also be reproduced with the SDA 8 pavements: the higher the void content, the better the long term acoustic performance.

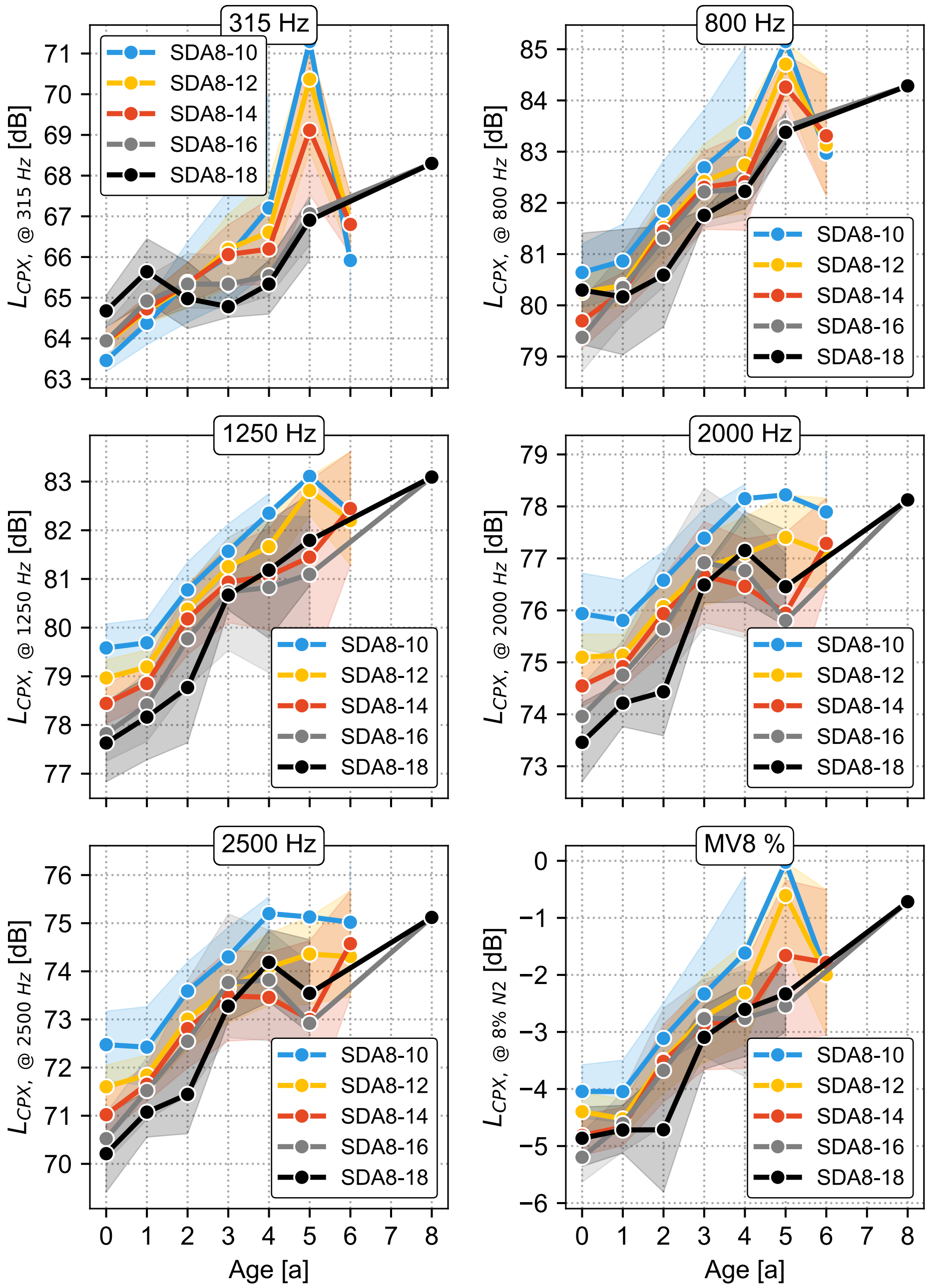

Fig. 13 *Spectral ageing of CPX-Levels of different variants of SDA 8-mixtures. Differentiated per Marshall-Void content i.e SDA 8-10 corresponds to SDA 8 pavements with Marshall void content in the range of 8-12 Vol-%*

5.4 Proposed mixtures

As a result of the statistical analysis the following mixtures are recommended for initial trials as shown in Tab. 5. The proposed mixture was checked for plausibility on the basis of experience in asphalt production and it was found that the proposals corresponded well with previous experience.

***Tab. 5** Recommended mixtures for SDA 4, SDA 8 and SDA 6 for the initial trials*

Parameter	**SDA 4**		**SDA 8**		**SDA 6**
	VSS 40 436:2021	**Optimum**	**VSS 40 436:2021**	**Optimum**	**Optimum**
Designation	SDA 4	SDA 4-opt	SDA 8	SDA 8-opt	SDA 6-opt
Marshall-Voids Vol-%	10..22 %	15.0 %	10..18 %	15 %	~15%
Sieve 0.063 mm M-%	3..12 %	9.0%	3..9 %	6.7 %	8.8%
Sieve 0.5 mm M-%	4..24 %	14.5%	4..14 %		14.7%
Sieve 1 mm M-%	7..29 %	17.5%	7..18 %		17.9%
Sieve 2 mm M-%	12..35 %	24.5%	10..25 %	19.5%	27.1%
Sieve 4 mm M-%	90..100 %	97.0%	15..35 %	33.0%	77.1%
Sieve 5.6 mm M-%	100 %	100%	50..70 %		100%
Sieve 8.0 mm M-%	100 %	100.0%	90..100 %		100%
Akustic-Factor	-	42	-	26.2	?
BK-HR Vol-%	10..20%	15%	12..18 %	15 %	15 %
Comp Deg	>=97%	100.00%	>=97%	100 %	100%
Bitmen content M-%	>= 6.0 %	6.0%	>= 5.8 %	6.00 %	5.7%

BK-HR= Drill core void content

6 Mix Design

The mix designs of the SDA 4 and SDA 8 benchmark mixtures were developed based on the empirical gradation limits established in VSS 40 436 [19]. Considering the in-situ acoustical results, this gradation range allowed a high number of outcomes in terms of noise generation as described in the previous section. Therefore, the gradations were further adjusted, with the goal of attaining a Marshall air voids (EN 12697-30) content as close to 15 Vol-% as possible. The SDA 6 was approximated based on the limited empirical data from the SDA 6 as well as from some of the other mixtures. Zeofill was chosen as the first filler for the benchmark trials.

6.1 Gradations and Marshall air voids

The actual gradations on the mixtures were based on the gradations of the individual fractions (Filler, 0/2, 2/4, 4/6, 6/8 mm) in the sieved material, so the optimum gradations were approximations based on the sieve analysis according to EN 933-1. The gradations for the fractions used in the benchmark mixtures are shown in Tab. 6.

Tab. 6 *Gradation for aggregated fractions used in benchmark mixtures*

Sieve (mm)	Fractions M-%				
	6/8	4/6	2/4	0/2	Zeofill
11.2	100	100	100	100	100
8.0	97.8	100	100	100	100
5.6	22.7	96.8	100	100	100
4.0	0.4	7.1	93.3	100	100
2.8	0.4	3.8	50.7	99.3	100
2.0	0.3	0.5	8.1	98.6	100
1.4	0.3	0.5	4.5	79.7	100
1.0	0.3	0.4	0.8	60.8	100
0.500	0.2	0.3	0.6	34.0	100
0.250	0.2	0.3	0.5	21.5	100
0.125	0.2	0.3	0.5	11.9	89
0.063	0.1	0.2	0.4	4.7	73

The gradations were calculated by minimizing the difference between the theoretical and real sieve curves while changing the proportion of the different fractions. The bitumen content was kept just above the minimum of 6 M-% due to evidence that higher bitumen content being trending inversely with acoustic performance. While the real (recovered) curves were close to the theoretical ones, this created a challenge in SDA 8, where the theoretical curve prescribed a certain quantity of aggregates above 8 mm, but the 6/8 fraction was more closely sieved to below 8 mm. The trial benchmark mix designs and their fractions are shown in Tab. 7. After the first trials did not attain a close enough air void content, the next were subject to extraction and recovery (EN 12697-1) to verify that the gradations and the bitumen content were consistent. It should be noted that the bitumen content recovered is generally lower than the prescribed bitumen content due to losses during the mixing process.

Tab. 7 *Benchmark mix designs based on fractions, Mashall voids and recovered binder; F/B= filler binder ratio*

Mixture	Trial #	Fractions M-%						F/B	Marshall	Recov. binder
		6./8	4./6	2./4	0/2	Zeofill	Binder		voids Vol-%	M-%
SDA 4	1	0	0	74.9	6.6	12.4	6.02	2.07	13.3	
	2	0	0	76	7.2	10.8	6.02	1.79	16.3	5.69
	3	0	0	75.4	6.9	11.6	6.02	1.93	16.3	5.37
SDA 6	1	0	19.3	53.5	8.5	12.6	6.02	2.1	12.7	-
	2	0	21	55.6	6.2	11.2	6.02	1.85	14.9	5.81
SDA 8	1	51.7	11.7	12.7	8.5	9.4	6.02	1.57	10.4	-
	2	55.5	13.2	13.2	3.3	8.9	6.02	1.48	18.1	5.26
	3	51.7	14.1	14.1	5.2	8.9	6.02	1.48	15.8	5.31

The initial mixture for the SDA 4 resulted in Vol-13.3% Marshall voids, but slightly increasing the proportion of the 2/4 mm fraction resulted in an increase in the Marshall voids to 16.3 Vol-%, which was deemed to be close enough to the target value. The comparative gradations for the design and recovered mixtures are shown in, Fig. 14 where it can be seen they are close together, but with the recovered gradations somewhat finer below 2 mm, likely from some fracturing of the aggregates during mixing in the drum.

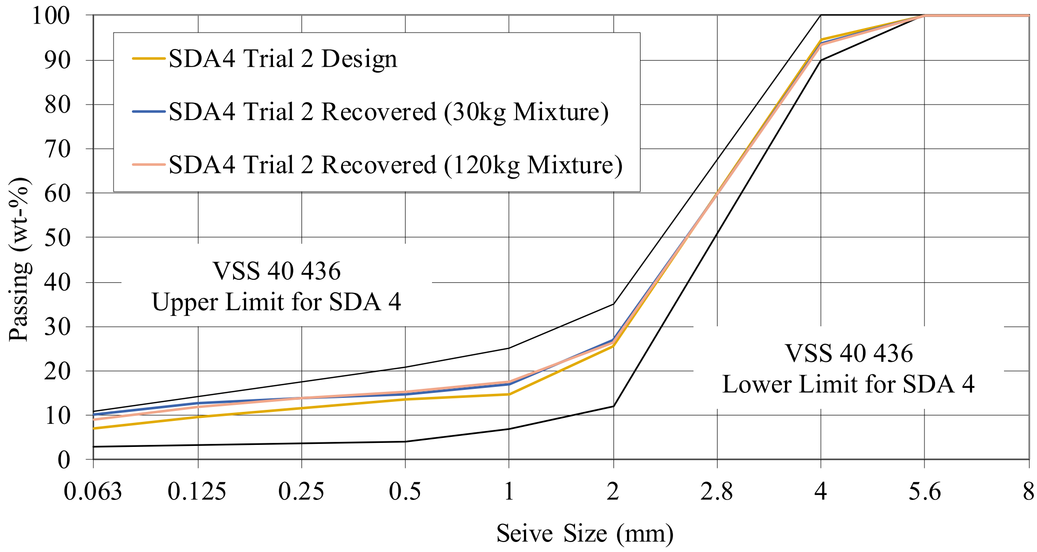

Fig. 14 *Gradations according to VSS 40 436 for SDA 4 Trial 2*

The first trial for SDA 6 only achieved 12.7 Vol-% in Marshall voids, but increasing the proportion of the 4/6 and 2/4 mm fractions resulted in the Marshall voids attaining 14.9 Vol-%. The gradation for the Trial 2 mixture is shown in Fig. 15.

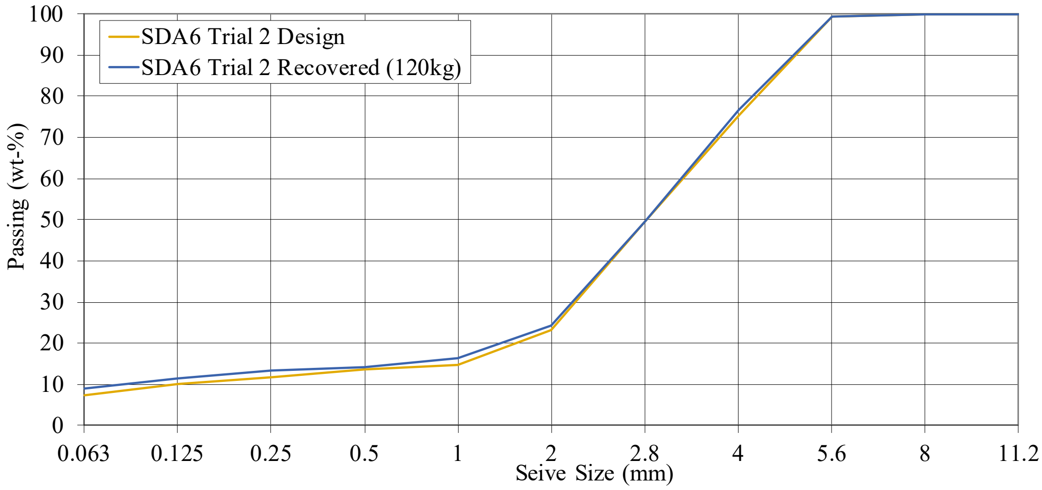

Fig. 15 *Gradations according to VSS 40 436 for SDA 6 Trial 2*

The first trial for SDA 8 also required adjustment as the Marshall voids were only at 10.4 Vol-%. However, the increase in the 6/8 mm fraction and decrease in the 0/2 mm fraction for the 2nd trial was an overcompensation and resulted in 18.1 Vol-%. The overall refinement in the third trial achieved 15.8 Vol-%, with the gradations shown in Fig. 16.

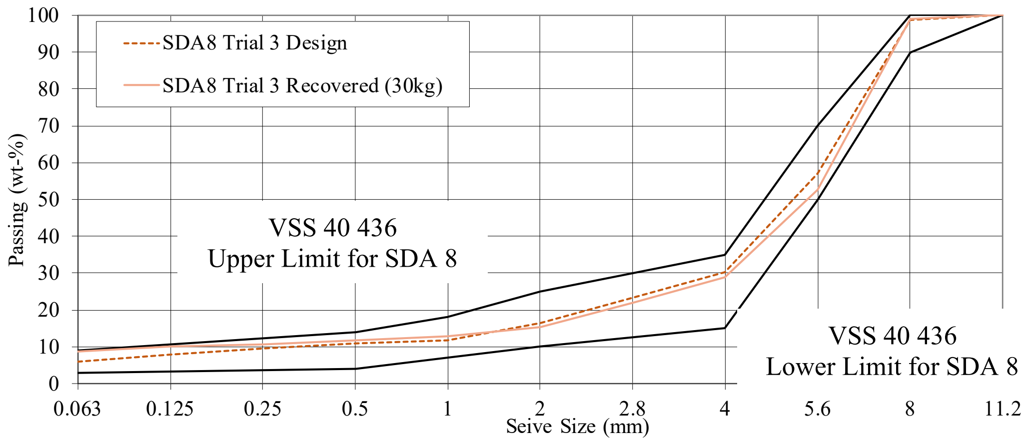

Fig. 16 *Gradations according to VSS 40 436 for SDA 8 Trial 3*

6.2 Height tolerance of Marshall samples

One issue encountered with the Marshall tests was the effect of the sample sized on the result. The EN 12697-30 prescribes the samples of 101.6±0.1 mm diameter and 63.5±2.5 mm in height. The tolerance on the diameter is very low because it is controlled by the confines of the steel mold and will translate to the sample as long as it is not extracted from the mold too early (while it is hot and could potentially settle). On the other hand, the height is controlled by the person carrying out the test. This is done based on an initial estimated mass of sample based on the maximum relative density of the mixture (EN 12697-5), which would result in a mass to target a diameter of 101.6 mm and a height of 63.5 mm. The sample mass may be increased or reduced based on the result from 50 blows from the Marshall hammer.

When considering dense asphalt, where the target porosity is around 3 - 4 %, the Marshall method, first developed in 1939, can be sufficient as a height different of ±2.5 mm in a sample is not so crucial. However, when this method is applied to asphalt with higher porosity such as SDA, this tolerance can be more critical. For example, if we calculate a sample mass of 1.083 kg for a sample with the height of 63.5 mm and 15 Vol-% voids, this could mean a mass range of 1.041-1.125 within the height range of 61 – 66 mm. The difference in the compaction mass will affect the amount of energy input into the sample as a fraction of the sample mass, with a lower mass receiving more compaction energy. If we take the sample mass as constant, the void content range would be 11.5-18.2 Vol-% although this range would not be seen in practice due to the sample with more voids being compacted more and vice-versa.

This was an issue encountered during our Marshall tests as shown in Fig. 17. Part of our issue with attaining the desired voids content was sample heights being outside of the standard range of 61 – 66 mm. This was solved by preparing the samples within this range, but especially trying to attain a sample height as close to 63.5 mm as possible. Based on this experience, it would be advisable to lower the Marshall Sample height limits to ± 1 mm. This is not only a “laboratory issue” as all SDA mixtures in the field are designed using these same standards.

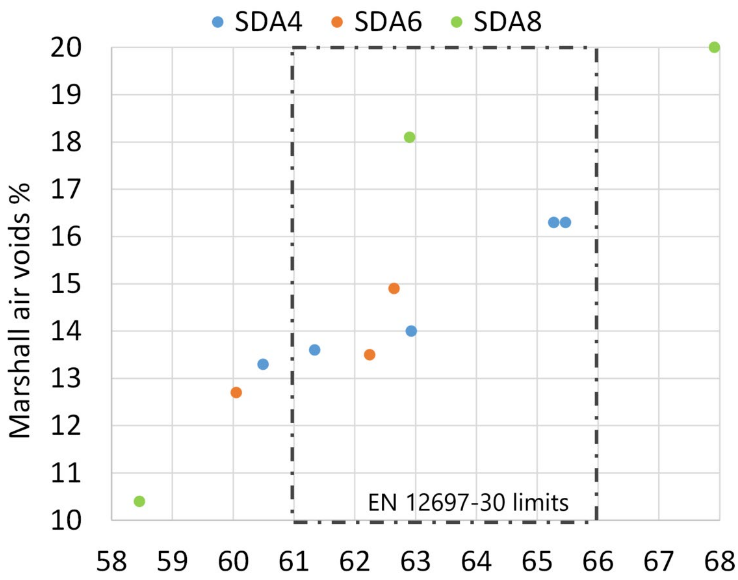

Fig. 17 *Marshall air voids results compared to the average heights of the samples*

6.3 Final Mixture information

Fig. 18 shows the gradation of the final benchmark SDA 4-S, SDA 6-S, SDA 8-S mixtures and Fig. 19 shows the gradation of the modified SDA 4-M1, SDA 4-M2, SDA 4-M3 mixtures in comparison to the benchmark SDA 4-S. Tab. 8 shows the properties of the resulting

Tab. 8 *Mixture information*

Sieve	**Mixture Designation**					
[mm]	**SDA 4-S**	**SDA 6-S**	**SDA 8-S**	**SDA 4-M1**	**SDA 4-M2**	**SDA 4-M3**
63.0	100.0	100.0	100.0	100.0	100.0	100.0
45.0	100.0	100.0	100.0	100.0	100.0	100.0
31.5	100.0	100.0	100.0	100.0	100.0	100.0
22.4	100.0	100.0	100.0	100.0	100.0	100.0
16.0	100.0	100.0	100.0	100.0	100.0	100.0
11.2	100.0	100.0	100.0	100.0	100.0	100.0
8.0	100.0	100.0	98.9	100.0	99.9	100.0
5.6	100.0	99.4	52.7	99.9	99.9	99.9
4.0	93.5	76.6	29.0	95.3	94.5	94.2
2.8	59.8	49.4	21.9	64.6	63.8	60.9
2.0	26.5	24.4	15.3	28.6	28.0	27.7
1.4	19.5	18.2	12.9	19.9	19.0	19.1
1.0	17.7	16.5	11.8	17.5	17.0	16.9
0.500	15.2	14.3	10.6	15.1	14.4	14.1
0.250	13.9	13.2	10.0	13.9	13.2	13.2
0.125	11.9	11.5	8.8	12.9	12.2	12.2
0.063	9.1	9.1	7.0	9.7	8.8	9.1
Binder content (M-%)	5.4	5.8	5.3	6.2	5.8	6.0
Max density (tonne/m^3)	2.5	2.5	2.5	2.5	2.5	2.4
Bulk density (tonne/m^3)	2.1	2.1	2.1	2.1	2.1	2.1
Voids content (Vol-%)	16.3	14.9	15.8	14.7	15.5	13.2
VFB (Vol-%)		44.4	40.4	46.1	43.2	48.3
VMA (Vol-%)		26.8	26.5	27.2	27.2	
Richness modulus		3.6	3.5	3.8	3.6	3.7

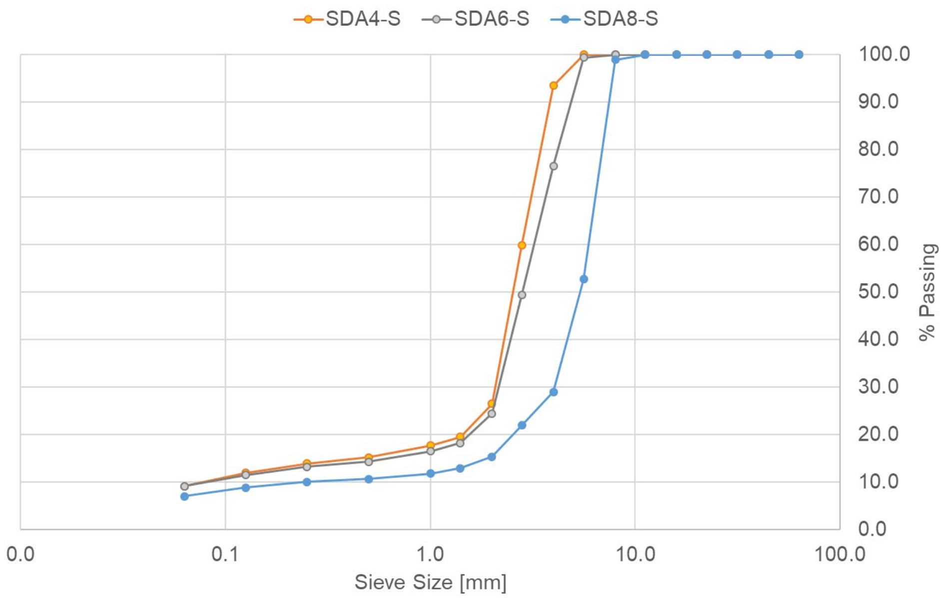

***Fig. 18** Gradation of the final benchmark mixtures*

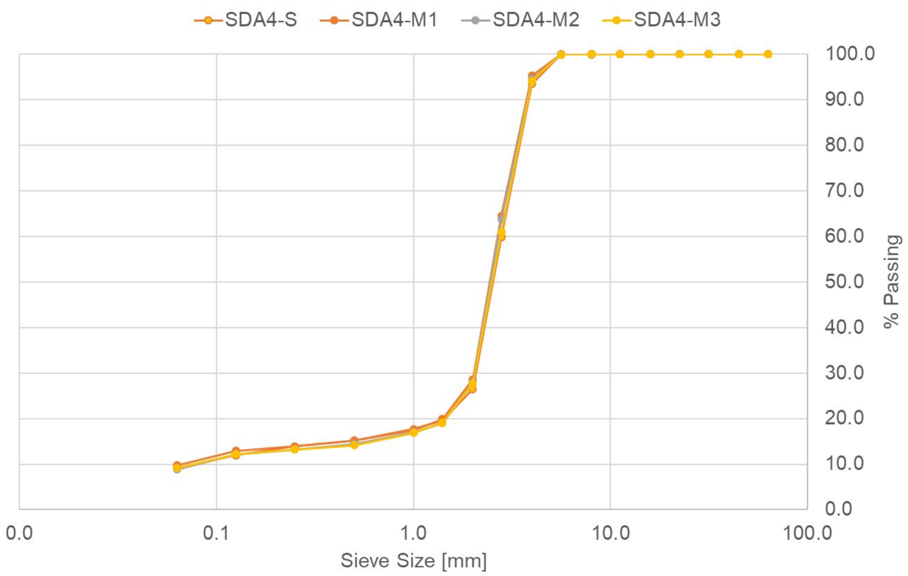

***Fig. 19** Gradation of the SDA 4 modified mixtures in comparison to the benchmark mixture*

7 Experimental Methods

A multi-scale experimental method was utilized to investigate the performance of these mixtures more efficiently. First various binder, filler and additives were investigated in the mastic scale (mm-scale). From the knowledge gained mixtures were fabricated for the cm-scale investigations. From the cm-scale results mixtures were further selected for the m-scale laboratory investigations.

7.1 Tests on filler

The properties of the filler were evaluated using the Rigden voids content method [70]. The filler property found to be most simply related to the stiffening effect is the value of the fractional volume voids in the tightly-compacted dry filler. Void content is dependent of particle shape, particle size distribution and particle surface structure.

$$\%RV = \frac{V_{fb} - V_{fs}}{V_{fb}} \tag{5}$$

where,

$\%RV$ is the percent of Rigden voids

V_{fb} is the bulk volume of compacted filler

V_{fs} is the volume of filler

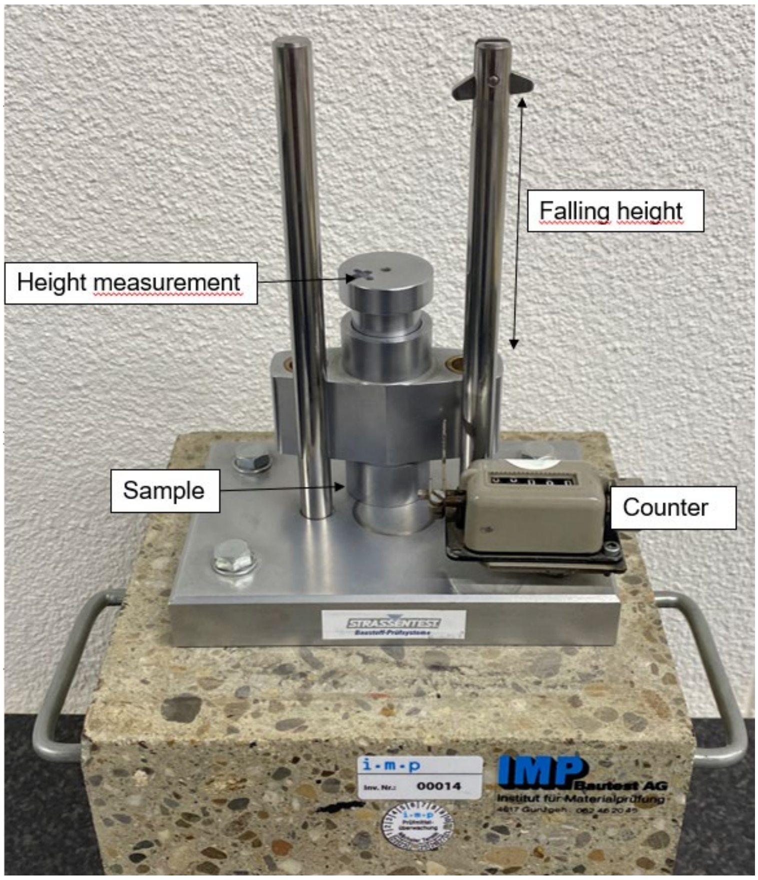

Fig. 20 *Rigden voids content apparatus*

The experimental set up is shown in Fig. 20. For the test, 10 g of filler are filled into the cylinder and are compacted by letting the whole cylinder/sample holder fall from a given height 100 times and then measuring the compacted height of the sample.

Tab. 9 *Rigden Voids*

Type of Material	Category		Result [Vol.-%]
Filler	I	Kalkstein (Limestone)	31
Filler	II	Zeofill	34
Filler	III	Zeobit	44

The results were as expected. Zeobit has a highly stiffening effect compared to limestone, while Zeofill lies in between.

7.2 Tests on mastic

First tests were performed to determine a reasonable ratio for the filler and bitumen as well as determining the aging procedure.

To produce a mastic mixture, the received fillers were sieved down to 0.125 mm and dried for two days in the oven. Firstly, the base bitumen was heated to reach a molten state at 145°C. Thereafter, the different fillers and additives, also at 145°C, were gradually introduced into the binder using a low-speed mixer at 145°C. Next the blend was heated to 180°C and homogenized again, before the samples were molded into the sample holders for the DSR measurements and the containers for the ageing.

7.2.1 Mastic aging

The mastic was aged using the PAV (pressure ageing vessel) method (SN 670 558/EN 14769 [12]). 50g of mastic per container was prepared and put into the vessel for 20 hours at 100°C and 21 bar pressure. Afterwards the samples were homogenized and allowed to cool. The procedure was repeated for the second ageing step (2PAV). At this point samples were also prepared for the rheometer that were measured after one ageing step. After the second ageing step, the containers were again combined, homogenized, and allowed to cool. As preparation for the DSR measurements the sample was again heated to 180°C and homogenized before it was poured into the prepared molds for the DSR.

The normally performed Rolling Thin Film Oven Test (RTFOT) (SN EN 12607-1) short term ageing was not performed, as this is not possible with a mastic mixture. However, as the aim was to see whether the different fillers influence the ageing effect of the mixture the short time ageing is not relevant.

7.2.2 Dynamic shear rheometer (DSR)

This European standard (EN 14770, [13]) specifies a method to measure the rheological properties of bituminous binders using a dynamic shear rheometer (DSR). The procedure involves determining the complex shear modulus and phase angle of binders over a range of test frequencies and test temperatures when tested in oscillatory shear. From the test, the norm of the complex shear modulus, $|G^*|$, and its phase angle, δ, at a given temperature and frequency can be calculated. Frequency sweep tests were carried out from 0.01 to 100 rad/s over a temperature range of -10°C-40°C in 10°C steps. In addition, a temperature sweep from 30°C - 90°C with a frequency of 1.59 Hz was performed with an increment of 10°C. Before the frequency sweep tests, strain amplitude sweep tests were conducted to identify the linear viscoelastic (LVE) range of different binders and thus to guarantee that the frequency sweep tests were undertaken within the binder's LVE region of response. The low temperature range was performed with a plate-plate geometry of 8 mm diameter and a gap width of 2 mm, while the higher temperatures were measured with the 25 mm plate-plate geometry with a gap width of 1 mm. The results of the overlap of the two geometries agreed and were confirmed within expected uncertainties. Furthermore, at least two measurements with the same geometry had to be within 5% to be accepted as reasonable.

7.3 Tests on Mixtures

7.3.1 Mixture preparation and compaction

The aggregates and bitumen were heated to the mixing temperature of 170°C in the oven. The compaction was done at 155°C using the Marshall compaction with 50 blows per side or a gyratory compactor to the required height. The samples that were produced for water sensitivity tests were under compacted to 50 gyrations as required by the standard.

7.3.2 Mixture aging

Once the mixture was prepared it was spread to a thickness of 3 – 4 cm on a metal sheet and placed in the oven at 155°C for two hours (Fig. 21). This aging procedure replicates the state of the mixture after manufacturing in the asphalt mixing plant and until it is laid. The mixing plants in Switzerland are normally close to the job sites.

Fig. 21 *Short term oven aging on mixture left and compacted and cut samples, right*

7.3.3 Indirect tensile strength

For each asphalt mixture, a set of cylindrical specimens was compacted in the laboratory to obtain the target air voids content given in Tab. 7. According to EN 12697-12 [3], specimens were divided into two equally sized subsets, named “dry” and “wet”. The dry subset was stored at room temperature (20°C - 25 °C) while the other subset was saturated and conditioned in water at 40°C for a period of 72 h. After conditioning, the indirect tensile strength (ITS) of each of the two subsets was determined (EN 12697-23).

ITS tests were conducted at 25°C with a displacement rate of (50 ± 2) mm/min. ITS was calculated from the peak load diametrically applied to the cylindrical specimen using the following equation:

$$ITS = \frac{2 \cdot P}{\pi \cdot d \cdot h} \qquad (6)$$

where *P* is the peak load [N]; *d* and *h* are the diameter and the height of the specimen [mm], respectively. At least three replicates were tested for each mixture type and average values were considered in the analysis.

7.3.4 Water sensitivity

The moisture sensitivity of asphalt mixtures was then determined in terms of ITS ratio (ITSR) as follows:

$$ITSR\ (\%) = \frac{ITS_{wet}}{ITS_{dry}} \cdot 100\ [\%] \quad (7)$$

where ITS_{wet} is the average ITS of the wet group [kPa] and ITS_{dry} is the average ITS of the dry group [kPa].

7.3.5 French rutting test

The rutting test was conducted to determine the susceptibility of bituminous materials to deform under load at elevated temperatures. Two replicate asphalt mixture slabs with dimensions 500 mm (length) x 180 mm (width) x 50 mm (thickness) were prepared using a laboratory slab compactor. The test was conducted either in air at 60°C, as per EN 12697-22 [5], Procedure B. According to this method, a pneumatic wheel loaded to 700 ± 10 N travels a total distance of 230 ± 10 mm at a frequency of 26.5 ± 1 cycles per minute while the resulting surface rut depth is measured after a selected number of passes.

Fig. 22 *French rutting test set up*

7.3.6 Cyclic compression test

The cyclic compression test was used to investigate the creep performance of the mixtures as per the European Standards EN 12697-25 [8] method A2. The test offers a method to evaluate the performance against permanent deformation of asphalt mixtures at high temperature (50°C). The duration of the haversine loading cycle was 1.7 s with a rest period of 1.5 s. The 100 mm diameter and 60 mm height specimens were conditioned in the climatic chamber at the test temperature of 50°C for at least 4 h before the tests. The top and bottom surfaces of the test specimens were polished to achieve even and plane parallel faces that is perpendicular to the cylinder axis. The specimen is placed between two plane parallel loading plates, and the compressive stress is distributed evenly through a plate over the top of the sample, with upper and lower stresses of 0.35 MPa and 0.025 MPa, respectively. Two sets of specimens were used for each test. The creep curve shows the cumulative axial strain, in %, of the test specimen as a function of the number of loading cycles. Three stages can be generally identified in the creep curve. In stage 1 or the initial part the slope of the curve decreases with the number of loading cycles; in stage 2 which is the middle part of the creep the slope of the curve is constant and can be expressed by the creep rate, f_c. The exact turning point of the creep curve lies within this stage; in stage 3, the last part of the curve, the slope increases with increasing number of loading cycles. Depending on the testing conditions and on the mixture, one or more stages may be absent. The cumulative axial permanent strain ϵ_n, from the creep curve expressed in percent (%), as a function of the number of load applications can be calculated using Eq. (8). The test is ended when 10'000 cycles are reached or the cumulative axial strain ϵ_n has reached 40 %.

$$\epsilon_n = \frac{u_n}{t_i}.100 \tag{8}$$

where,

ϵ_n is the cumulative axial strain of the test specimen after n loading cycles, in percent (%)
u_n is the cumulative permanent deformation of the test specimen after n loading cycles
t_i is the initial thickness of the test specimen in mm

7.3.7 Semi-circular bend test

One of the testing methods commonly used to assess fracture of asphalt pavement is the semi-circular bending (SCB) test. This test was originally developed for determining the fracture resistance and it has been reported as a simple but useful testing method for mixture design and quality control of asphalt mixtures [55].

The SCB test was performed using 100 mm diameter specimens with a 3.5 by 10 mm notch. The test was performed at 0°C in accordance with the European standard EN 12697-44 [10]. Two replicates of specimens were required but four were tested using SCB test. During the test, specimens were loaded with a loading strip moving at a rate of 5 mm/min. The schematic in Fig. 23 shows the preparation of the specimens and the dimensions for the specimen.

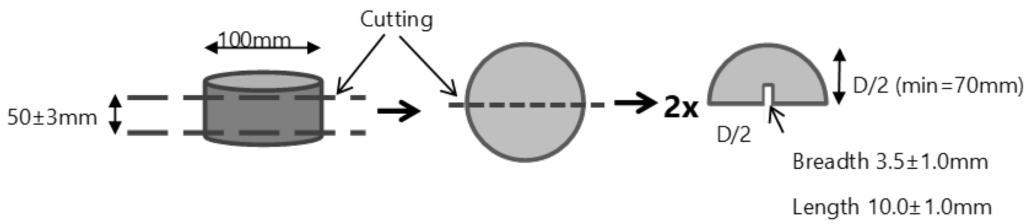

***Fig. 23** Semicircular bend test sample preparation*

7.3.8 Stiffness modulus

The stiffness modulus was determined using the Cyclic Indirect Tensile Test (CIT-CY) according to the European standard EN 12697-26 [9]. The tests were performed on compacted bituminous mixtures under sinusoidal loading. The procedure is used to rank bituminous mixtures on the basis of complex modulus and it is used as a guide to rank the relative performance of the pavement and for obtaining data for estimating the structural behavior in the road according to specifications for bituminous mixtures.

Cylindrical samples were compacted using the gyratory compactor to target voids, and cut to 100mm diameter and 40 mm height. The test is performed in the linear range of the material, under repeated loads. The linear range was determined using pre-tests at the different frequencies and temperatures. The tests were conducted at frequencies of 0.1, 1, 10 Hz and temperatures of 10, 15 and 20°C. The amplitudes of the stress and strain are measured, together with the phase difference between stress and strain.

Fig. 24 shows the experimental setup of the cylindrical specimen for the CIT-CY test. According to the standards 4 samples are needed for the modulus tests.

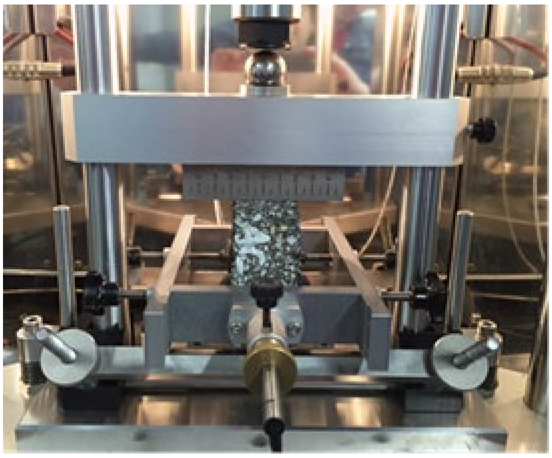

Fig. 24 *Experimental set up for the stiffness modulus and fatigue tests*

7.3.9 Fatigue

The concept of fatigue life is based on the idea that most materials undergo a gradual deterioration under repeated stresses that are much smaller than the ultimate strength of the material. Therefore, knowledge of fatigue behavior of asphalt concrete materials is imperative for material evaluation. The fatigue tests were performed as per EN 12697-24 [7]. The specimen is loaded sinusoidally at the imposed displacement amplitude until it reaches a certain failure criterion. The goal is to measure the number of cycles Ni at failure in a Wöhler type of diagram. At least 9 specimens are tested for the IT-CY fatigue test. The strain ε_i is selected so that either the values are approximately regularly spaced on a logarithmic scale; or there are at least 3 levels of deformation, with a sufficient number of specimens at each level.

On the basis of the results, different fatigue life values, N_i are determined for different maximum applied initial strain ε_i. A linear regression is plotted between the decimal logarithms of N_i and the decimal logarithms of ε_i as follows:

$$\boldsymbol{log\ (N) = a + (1/b) \cdot log\ (\varepsilon)} \tag{9}$$

where $\boldsymbol{\varepsilon}$ is the strain; a is the ordinate of the fatigue line; $1/b$ is the slope of the fatigue line. R^2 is the linear correlation coefficient [$log(N_i)$, $log(\varepsilon_i)$].

A high R^2 value is an indication of the goodness of the fatigue curve. In this study, all fatigue lines have been calculated using decimal logarithm (log) as in equation (10). The initial complex stiffness modulus E^*_{100} (or $S_{mix,0}$ as defined by the standard) is measured after 100 load applications. The conventional criteria of failure (constant displacement amplitude) defined in the standard as fatigue life is the number of load applications, $N_{f/50}$, at which point the complex stiffness modulus has decreased to half its initial value (Fig. 25). ε_6 is used as a measure of fatigue and is the strain at one million cycles.

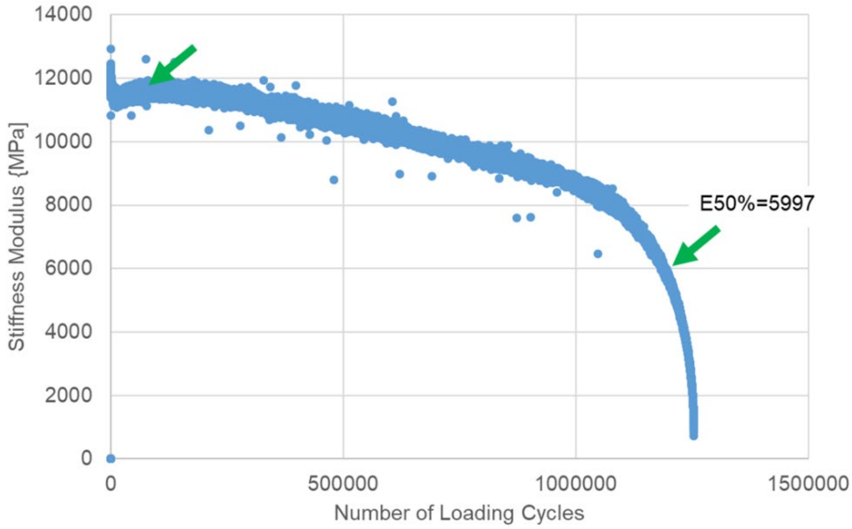

***Fig. 25** Example of a fatigue behavior and failure criteria for an asphalt sample*

7.3.10 Micro Deval IMP (MDI)

In order to characterize the particle loss from the mixture the MDI (Micro Deval IMP) test was used. This test was formerly known as "modified Micro-Deval“ [43]. In 2013 a German test with a similar name was introduced [18] for testing the aggregated loss. Therefore the subject test was renamed as “Micro Deval IMP”. The test has been used in various ASTRA national projects. This test was also used in the ASTRA user guide for low noise pavements [17]. Currently, it is used for special projects however the European standard Cantabro test is used internationally and MDI cannot be used in tenders.

In the Cantabro Test, asphalt specimens are placed in a Los Angeles drum. The particle loss is caused by the interaction of the sample with the drum or with a steel ball. However according to the experience gathered at IMP, this action does not duplicate what is happening in the field. In the case of MDI the drum described in EN 1097-1 [2] is used that is considerably smaller than the drum used in the Cantabro test, additionally the particle loss is simulated by the contact with the obstacle in the drum and not a ball.

Compared to the previous MDI tests, the test was compacted by preparing the test specimens accordingly following the steps below:

- Mixture aging: 85°C/ 120 hours
- Reduction of the number of blows in the Marshall compaction from 2x50 to 2x40 to represent the higher void content
- Water conditioning SN-EN 12697-12 [3]

***Tab. 10** Increase in mass loss due to various measures that were applied cumulatively*

SDA 4	Ageing	Reduced compaction	Water storage	Mass loss [g]	Mass loss [%]	Increase [%]	Increase factor
23-00388				19.9	1.9		
23-00389	x			29.2	2.9	51	1.5
23-00390	x	x		47.5	4.7	150	2.5
23-00391	x	x	x	52.1	5.2	174	2.7

In this way, the mass loss could be increased by 174 % (see example shown in Tab. 10). Higher mass losses in the test increase its informative value, especially its selectivity.

Compared to the previous MDI tests, the test was planned to store the test specimens appropriately prior to loading


.

Fig. 26 *Test setup for the MDI test. With every revolution, the sample has to roll over the obstacle*

The test procedure is as follows:

- Mixture aging: 85°C/ 120 hours
- Compaction of Marshall samples MPK with 2 x 40 blows
- Water conditioning SN-EN 12697-12 [3]
- Mass of samples before test: M1
- Testing of sample MPK (Fig. 26) at room temperature; 12’000 rotations
- Cleaning of sample MPK to remove loose pieces
- Weighing of sample MPK after test: M2
- Calculation of mass loss MV in % using the following formula:

$$MV = \frac{(M1 - M2)}{M1} . 100 \quad (10)$$

After exposure in the MDI drum, the abrasion partially adheres to the samples (see Fig. 27). To remove these particles, the test specimen was stored under water at room temperature for 24 hours. The remaining loose particles adhering to the sample were then removed with a fine brush.

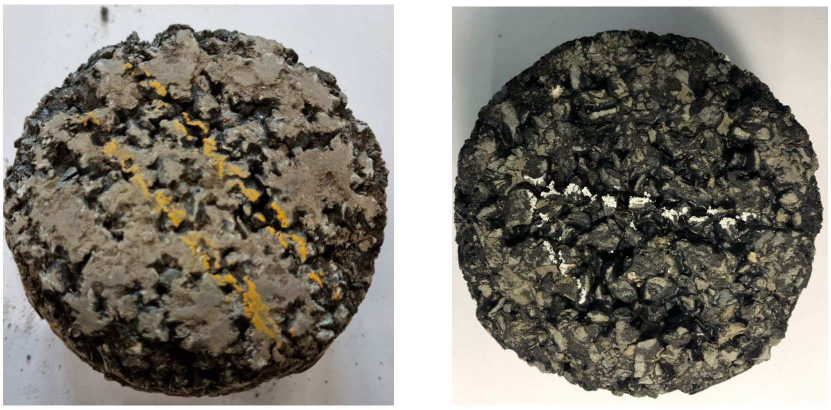

Fig. 27 *Test specimen after exposure in the MDI drum; the adhering abrasion particles were then removed; left before removing, right after removing*

7.4 Large scale experiments with Model Mobile Load Simulator (MMLS3)

The Mobile Model Load Simulator MMLS3 was used to upscale and validate the laboratory results obtained on cylindrical specimens. Specifically, this method allowed to obtain information about the mixtures in the wheel path and outside the wheel path. The production of slabs is shown in Fig. 28. The mixture is poured in a frame and compacted with a steel roller compactor manually. The MMLS3 is a downscaled traffic simulator with 4 pneumatic tires with tire pressure of 6 bar, that load the pavement with ca. 3600 unidirectional tire passes per hour over a length of about 1.2 m (Fig. 29). The design of the machine is such that only one tire is touching the pavement at a time at a speed of 1 Hz i.e. 60 wheel passes per minute, corresponding to a speed of about 4.5 km/h. The height of the device can be adjusted so each wheel is able to apply a load of about 2.1 kN. This type of test uses rolling tires to induce damage in asphalt slabs, in a similar way that traffic deteriorates pavements [38]. Depending on the temperature of the slab, it can also be used to study the rutting or cracking performance.

For this work, two slabs with dimensions 1600 x 430 x 50 mm were produced. Thereafter they were loaded in a temperature chamber at 40°C to study the rutting behavior. The slabs were laid directly on top of a concrete slab (Fig. 28). Deformation measurements in the wheel path were made at regular intervals.

Fig. 28 *Production of slabs for the MMLS3 traffic simulator tests*

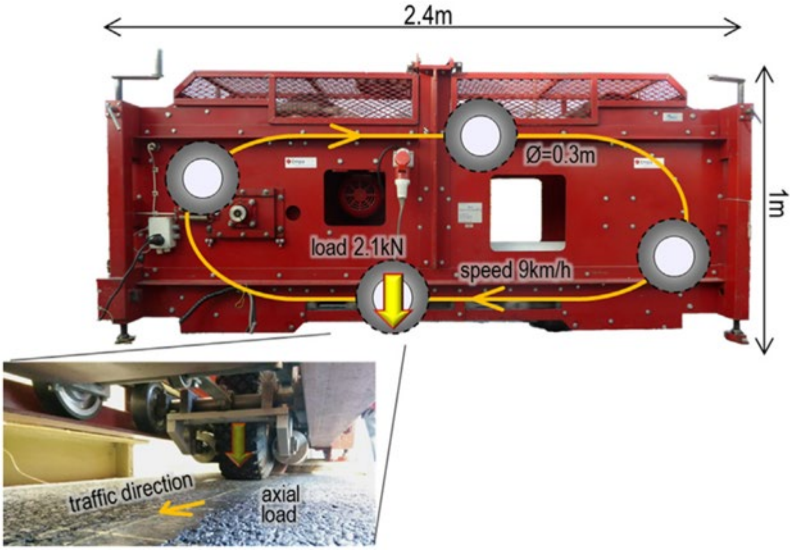

***Fig. 29** Experimental set up for the MMLS3 traffic simulator tests*

7.5 Acoustic tests on mixtures

In order to characterize the mixtures in terms of the (initial) acoustic performance, several tests were planned to describe the mixtures and to differentiate the mixtures and the optimized slabs. All acoustic characterizations were performed on the large slabs produced for the MMLS tests as the compaction with a roller compactor can represent the field compaction better than the gyratory compaction for the cylindrical laboratory specimens. This allowed to obtain data in the wheel path as well as outside of the wheel path thereby investigating the effect of loading cycles on the development of the material.

7.5.1 Surface texture

The surface texture of the MMLS3 asphalt samples was evaluated using an Ames Engineering 9400HD 3D laser scanner. The scanning was performed by placing the device horizontally on the slabs. The scanned region had an area of 102 x 50 mm^2 in the direction of the wheelpath, in and out of the wheelpath. The resolutions were 0.005 mm vertically, 0.006 mm along the length of the scan and 0.2 mm along the width. These scans were used to calculate the texture level ($L_{TX,\lambda}$, expressed in dB) as a function of center wavelength of the 1/3 octave band [67], λ, by taking the 1/3 octave band power spectral density $Z_{p,\lambda}$ of the surface profile amplitude along each scan line and by using Eq. (10) derived from ISO 13473-4:

$$L_{TX,\lambda} = 10 \cdot log\left(\frac{Z_{p,\lambda} \cdot 0.232/\lambda}{a_{ref}^2}\right) \quad (10)$$

where $0.232/\lambda$ is the corresponding bandwidth; and a_{ref} is the reference value of the surface profile amplitude (10−6 m according to ISO 13473-4).

Fig. 30 *Evaluation of asphalt slab with Ames Engineering 9400HD 3D laser scanner*

7.5.2 Computed Tomography (CT)

X-ray tomography was performed with an in-house developed tomograph located at Empa's Center for X-ray Analytics (*https://www.empa.ch/web/s499*). Such instrument consists of a high-energy, micro-focus, reflection-based X-ray source (by FineTec, model FOMR 300.03Y RT) and by a two-dimensional flat panel detector (by PerkinElmer, model XRD 1611-CP3) with 4096 × 4096 pixels, each with physical size of 100 µm. Each pixel is made of amorphous Si and is covered by a thin layer of CsI, acting as a X-ray scintillator, converting the respective photons into visible light ones, then detected by the amorphous Si element.

The X-ray source was operated at 180 kV and 500 µA. In front of it, a 1 mm-thick Cu disk was placed in order to reduce the content of low-energy photons in the X-ray source emission spectrum, thus respective beam hardening artifacts in the final tomogram [48] [50].

The detector was configured to exploit a 2 × 2 pixel binning, i.e., the signals from 2 × 2 adjacent pixels were averaged and the result assigned to a virtual pixel with double the size of the physical ones. This lead to a downsampling of the pixels' two-dimensional array by a factor of 2 along each dimension, leading to an actual physical pixel size p = 200 µm

Each tomography measurement consisted of 2700 radiographs acquired over 360° of specimen rotation around the specimen symmetry axis. At each specimen orientation angle, a respective radiograph was actually the result of averaging 5 successive radiographs, each acquired within 2 s.

Each averaged radiograph at any given angle was saved as a 2D TIFF image file with a 16-bit depth. The source-to-specimen distance, d_(S-s), was equal to 211.58, while the source-to-detector distance, d_(S-d), was equal to 1407.57. Because of the cone geometry of the X-ray beam, the radiographs were characterized by a geometrical magnification factor, $M \equiv d_{(S-d)}/d_{(S-s)}$, value of $\cong 6.65$, leading to an effective pixel size $\tilde{p} \equiv p/M \cong 0.03$ mm. $\tilde{p}$ is thus also the final size of the isotropic voxels each tomogram consists of. However, it is not equal to the spatial resolution of the tomograms, which is typically lower, i.e., it has a larger numerical value, due to different sources of image noise and response contribution of the whole imaging system. A ball-park value for an upper bound of the actual spatial resolution could be fixed at double the voxel size, i.e., 0.06 mm.

The final tomograms were reconstructed by a GPU processing-based implementation of the Feldkamp-Davis-Kress (FDK) cone beam filtered back-projection reconstruction algorithm [44], available within the XAct software (Ver. 1.1) by RX-Solutions (https://www.rx-solutions.com/).

7.5.3 Acoustic absorption

The sound absorption properties of a road surface are highly frequency-specific and depend on its layer thickness, porosity, pore shape, their degree of interconnection and the specific flow resistance. The sound absorption properties of a road surface can have a great influence on the extent of the horn effect and on sound propagation. Their metrological determination is of great importance in the closer analysis of the acoustic effectiveness of semi-dense and porous pavements.

The sound absorption properties are measured in-situ using the PU method. In this measurement method, a sound signal is emitted with a loudspeaker onto the test surface. In addition to the sound pressure, the sound velocity is also recorded. From this, the impulse response of the emitted signal and its reflection are calculated and the sound absorption coefficient of the test surface is determined. Compared to the determination of the absorption coefficient with the impedance tube method, the PU method can be used to determine the sound absorption coefficient for a wider range of the noise spectrum. Furthermore, it is possible to determine relatively low sound absorption properties in-situ with high accuracy.

The sound-absorbing properties of a road surface are best when the highest possible sound absorption coefficient is realised in the frequency range in which the most sound energy is generated when vehicle tyres roll over the road surface. This is typically the case in the middle frequency range between 800 Hz and 1250 Hz.

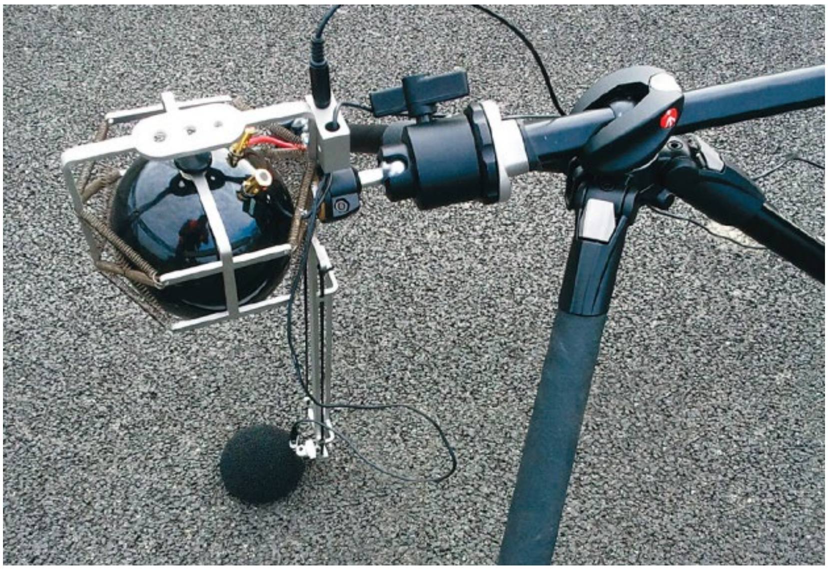

Fig. 31 *Sound absorption measurement device "PU-Probe" on a low noise road surface. The loudspeaker is shown on the upper left corner, while the PU-Sensor is situated on the road surface*

Normally, sound absorption reacts quite quickly to changes in the pore structure. Older pavements often have hardly any interconnected pores and the sound absorption coefficients are correspondingly low.

7.5.4 Air resistivity

Based on ISO 9053 [14] (this standard is also listed as EN 29053), the airflow resistance of a surface layer is determined using a non-destructive measurement in order to obtain information on the ventilation in the tyre/road contact area. These properties are of great importance with regard to the generation of noise when rolling over a surface layer.

To carry out the measurement, a chamber with an elastic sealing ring is pressed onto the pavement surface by means of a load. This is intended to create a situation similar to that which occurs when a tyre rolls over the surface. A constant flow q through a defined area A is generated with a pressurized air regulator. The pressure difference Δp generated by the flow through the surface is measured. The air flow resistance of a surface layer is defined as the ratio of the overpressure in the chamber Δp to the flow rate q. The specific flow resistance R_s is defined as the ratio of the overpressure to the flow velocity $u = \frac{q}{A}$ (A denotes the test area). This definition is explained in the following equation.

$$R_S = A\frac{\Delta p}{q} \text{ (Pa.s.m}^{-1}\text{)} \quad (12)$$

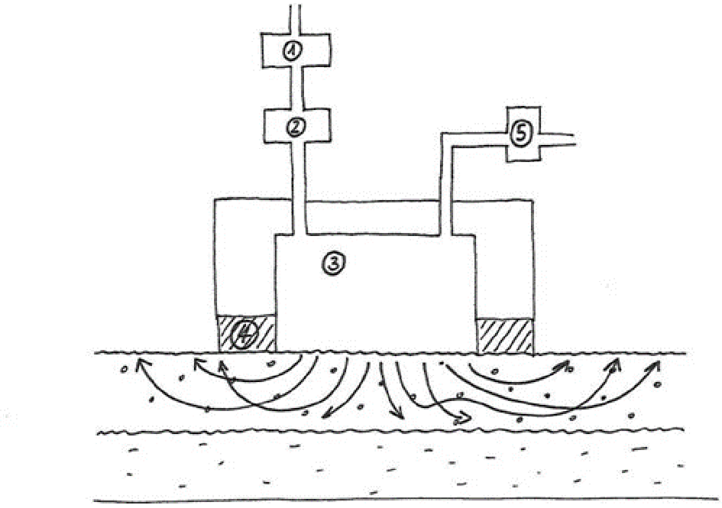

Fig. 32 *The measuring apparatus for determining the air flow resistance consists of (1) compressor, (2) flow controller, (3) chamber, (4) seal and (5) 2 differential pressure sensors*

A circular chamber with a diameter of 100 mm is used to determine the airflow resistance in situ. This geometry however is unfavourable for measurements on laboratory slabs; as was determined as part of a research project [23]. Therefore, the geometry was adapted for laboratory tests with a rectangular contact area (see Fig. 33).

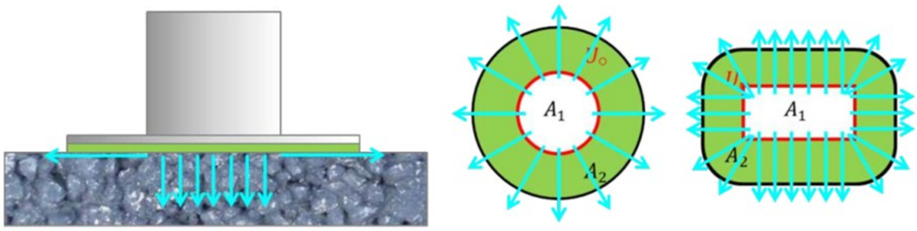

$U_{rund} = 31.4cm$ $\quad$ $U_{eckig} = 37.6cm$

Apparatur	A_1, cm^2	A_2, cm^2	U, cm
eckig	80.5	314.3	37.6
rund	78.5	308.5	31.4
Unterschied, %	2.5	1.9	19.7

Fig. 33 *Comparison of the measurement geometries for in-situ measurements (round) and for measurements in the laboratory (square), A= area, U= Circumference [23]*

As shown in Fig. 33, comparative measurements with both geometries, in the laboratory as well as in situ, proved in the previous project [23] that there was an excellent match.

7.5.5 Acoustic simulation of test slabs using SPERoN

The measurement methods described above are also used for acoustic simulations of tyre-road noise. SPERoN, a hybrid computational model, is used for this purpose. With SPERoN, predictions can be made about the force distribution in the tyre-road contact and predictions of tyre vibrations, flow noise in the tyre-road contact, friction effects, torus noise and aerodynamic vehicle noise. This makes it possible to compare the manufactured panels on the one hand with each other and on the other hand also in comparison with measurements in the field.

7.6 Summary of tests on mixtures

Tab. 11 shows the summary of all tests performed on the mixtures.

Tab. 11 *Summary of tests on mixtures*

Mixture/Test	**ITS**	**ITSR**	**Mod.**	**Fat.**	**CCT**	**SCB***	**MDI**	**MMLS3**				
								Def	**Air-Res**	**Abs**	**CT**	**Tex-ture**
Temp., Freq	**20°C**	**20°C**	**10°C 15°C 20°C**	**10°C 10Hz**	**50°C**	**0°C**	**-**	**40°C**	**-**	**-**	**-**	**-**
SDA 4-S	x	x	x	x	x		x	x	x	x	x	x
SDA 6-S	x	x	x	x	x		x					
SDA 8-S	x	x	x	x	x		x	x	x	x	x	x
SDA 4-M1	x	x	x	x	x	x	x					
SDA 4-M2	x	x	x	x	x	x	x					
SDA 4-M3	x	x	x	x	x	x	x	x	x	x	x	x
SDA 8-M3								x	x	x	x	x

8 Characterization of filler and mastic (mm scale)

Various combinations of mastic with bitumen filler and additives were investigated as listed in Tab. 12. The mastic was aged using the 2xPAV method.

***Tab. 12** Materials used in the project*

Step	Material combination	Description
1	Filler / Bitumen 1.16	Influence Filler-Bitumen ratio
2	Filler / Bitumen 2.05	
3	PmB 45/80-65 (CH-E) and Zeofill Filler/Bitumen 1.5	Basis with filler of „stiffening effect“
4	2 times ageing of PmB 45/80-65 with Zeofill	Basis aged
5	PmB 45/80-65 (CH-E) with Limestone unaged and 2 x aged	„softer filler“
6	PmB 45/80-65 (CH-E) with Zeobit unaged and 2 x aged	„highly stiffening effect“ of filler
7	PmB 45/80-80 with Zeobit unaged and aged	Unaged and aged
8	PmB 45/80-80 with Limestone unaged and aged	Unaged and aged
8	PmB 45/80-80 with Zeobit + Lime additive	Unaged and aged
9	PmB 45/80-65 (CH-E) with Zeobit + Lime additive	Unaged and aged

In order to simplify the captions in the graphics, the following Tab. 13 shows the designation of the mastics investigated. Furthermore, the phase angle is the dotted line, the IG*I line is solid.

***Tab. 13** Designation of mastic blends*

Designation	Description
B2U	Base Bitumen PmB 45/80-65 (CH-E) Unaged
B2-L-U/B2-L-A	Base Bitumen+Limestone unaged and aged
B2-ZF-U/B2-ZF-A	Base Bitumen+Zeofill unaged and aged
B2-ZB-U/B2-ZB-A	Base Bitumen+Zeobit unaged and aged
B2-ZB-L-U/B2-ZB-L-A	Base Bitumen + Zeobit + Lime aged and unaged
B1-L-U/B1-L-A	Highly modified PmB +Limestone unaged and aged
B1-ZB-U/B1-ZB-A	Highly modified PmB +Zeobit unaged and aged
B1-ZB-L-U/B1-ZB-L-A	Highly modified PmB +Zeobit+Lime unaged and aged

8.1 Characterization of the filler

3 Fillers with different stiffening effects were examined: 1) lime stone, a sedimentary rock CaCO, with low stiffening effect; 2) Zeofill with moderate stiffening effect, it is characterized as „phonolite“, Si-poor volcanic rock and 3) Zeobit it has high stiffening effect also characterized as „phonolite“, Si-poor volcanic rock. The Rigden voids corresponding to the stiffening effect of the three fillers are shown in Tab. 14.

Tab. 14 *Rigden voids of the fillers*

Filler Type	Rigden voids
Limestone	31
Zeofill	34
Zeobit	44

The use of an active filler such as hydrated lime can have antistripping effect, reduce ageing, and have a strong stiffening effect. As shown in Fig. 34, the additional voids in the filler can improve its performance.

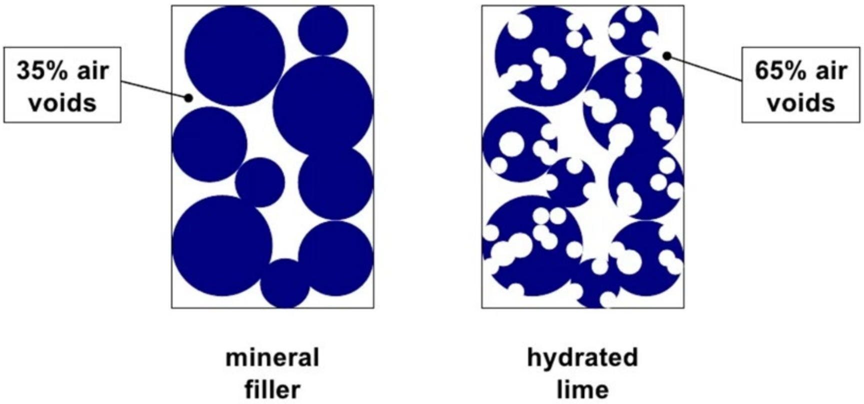

Fig. 34 *Visualization of the effect of hydrated lime [83]*

8.2 Characterization of the mastic

Various mastic combinations were investigated as outlined in the previous chapter. Unaged and aged mastic was investigated with all three fillers and two types of bitumen and an additive. The bulk of the results are presented in Appendix II. Below a summary of the findings is discussed.

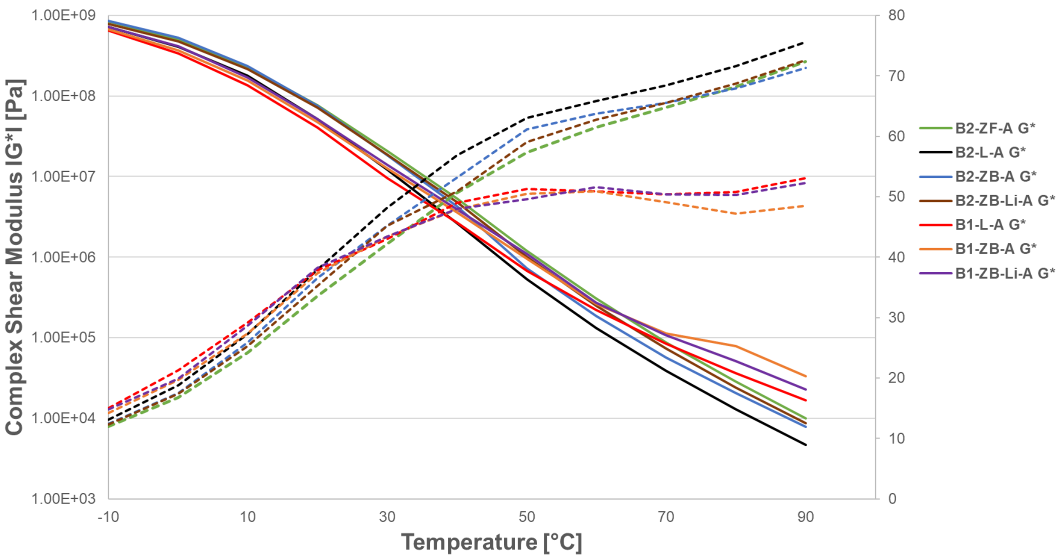

***Fig. 35** Effect of addition of different fillers on aged (A) mastic and comparison with bitumen PmB 45/80-65 (B2) and HM (B1). For the abbreviations see Tab. 13. The phase angle of the samples is the dotted line, the colour is the same as the complex shear modulus which is the solid line*

The results show that Zeobit (ZB), Limestone (L) und Zeofill (ZF) have similar results on both types of bitumen at -10°C, however at 30°C the influence of filler becomes apparent with a higher stiffening effect for Zeobit, this influence is larger as the temperature increases. The influence of filler at cold temperatures is minimal. Furthermore, the phase angle of HM with Zeobit and lime remains low indicating a more elastic response at higher temperatures.

The optimal curve for the shear modulus would be as low as possible at -10°C and high at high temperatures. As the Fig. 32 is in logarithmic scale the real differences between the curves are hard to judge. Therefore in Tab. 15 is a comparison of all the aged results to the aged B2-L (PmB-45/80-65 with Limestone). The table shows the ratio of the measured value of a mixture to the value of the mixture B2-L. For example, the value 2.1 for B2-ZF-A / 90 °C means that the B2-ZF-A mixture has a value 2.1 times higher than the B2-L mixture.

***Tab. 15** Comparison of all the aged mixtures to the PmB-45/80-65 Limestone (B2-L-A)*

[°C]	B2-ZF-A	B2-ZB-A	B2-ZB-Li-A	B1-L-A	B1-ZB-A	B1-ZB-Li-A
-10	1.2	1.2	1.1	0.9	0.9	1.0
30	1.7	1.5	1.6	0.8	1.0	1.2
60	2.3	1.4	1.9	1.7	2.0	2.1
90	2.1	1.7	1.9	3.6	7.0	4.8

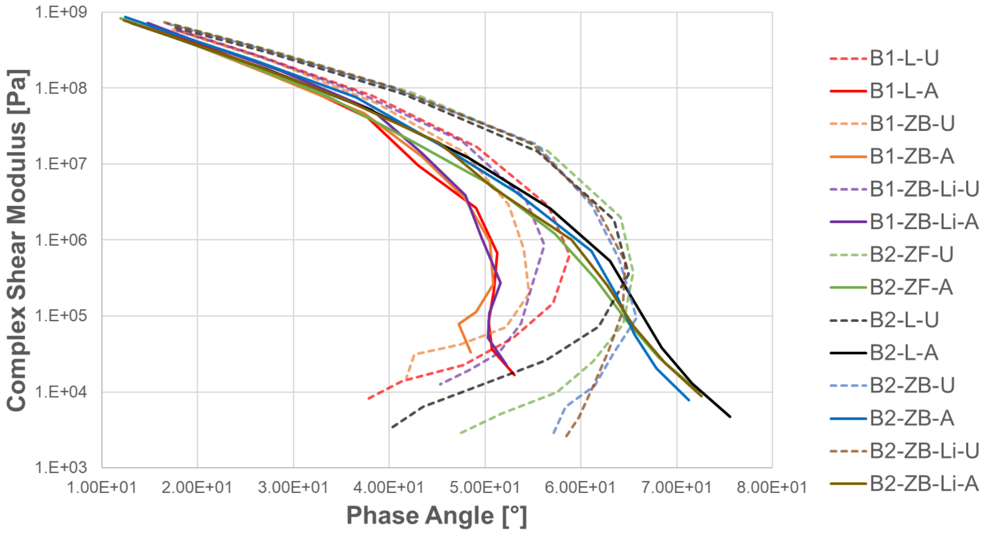

Fig. 36 *Black diagram showing the effect of the different fillers on unaged (dotted line) and aged (solid line) mastic and comparison with bitumen PmB 45/80-65 and HM*

Fig. 36 shows the Black Diagram with the complex shear modulus versus the phase angle. This type of diagram allows to compare the materials without the effect of temperature and frequency. The general pattern observed is a reverse C shape which is what is normally seen for an SBS polymer modified binder. This was true for all materials except aged PmB with the three fillers. The HM binder was able to retain its reverse C shape even after aging. In general aging resulted in shifting of the data towards the left i.e. lower phase angles indicating a more elastic response after aging, with the curves of aged HM with Zeobit and lime shifting the most indicating the lowest phase angle.

The main findings from the mastic experiments can be summarized as follows:

1. Addition of filler increases the complex modulus in the whole temperature range and the phase angle primarily above 30°C
2. The highly modified binder had a higher modulus and lower phase angle in comparison to the conventional PmB primarily above 30°C.
3. Aging increases the complex modulus in the whole temperature range and decreases the phase angle below 50°C and above which an increase is seen.
4. In unaged state and at cold temperatures, the influence of the three fillers on the conventional binder PmB 45/80-65 (B2) is similar. This is evident when results of Zeobit, Limestone und Zeofill at -10°C are compared.
5. In unaged state and intermediate temperatures, Zeobit was the stiffest and the highest phase angle above 30°C. At 90°C Sandstone filler had the highest modulus.
6. The influence of the different fillers at cold temperatures was minimal and its influence was highest at intermediate temperatures. This is understandable as at cold temperatures the composite material is elastic whereas as higher temperatures, the binder becomes soft and viscoelastic whereas the filler remains elastic and its influence becomes more apparent.
7. The aged highly modified bitumen with limestone filler and Zeobit and Zeobit with lime modifier show the best results and similar results in the mastic scale.
8. The additive lime did not influence the ageing process significantly. However, the ageing procedure used is only adding oxygen to the mix. Water and UV-Influence cannot be simulated with the PAV-procedure.

8.3 Fatigue testing of the mastic

The Linear Amplitude Sweep Analysis (LAS) (AASSHTO T 391-20 [80]) is a test that was developed to determine the long term damage of bitumen for different loads.

It was decided to try to use this test for the mastic mixtures. The tests were performed at 25°C. Not all results obtained could be used, as the failure was often not in the sample (cohesive failure) but the boundary between sample and plate (adhesive failure). The results can be seen in Tab. 16.

The deciding fatigue damage level was chosen at 35 %, as proposed in AASHTO, with a strain of 2.5 %. This means with the strain of 2.5 % it can survive N cycles before the modulus would reduce for 35 %. The tests showed that the highly modified binder was a lot more fatigue resistant.

Tab. 16 Linear Amplitude Sweep Analysis (LAS) shows, that the HM Binder (B1) shows better fatigue behavior whether it is aged or unaged.

Tab. 16 *Linear Amplitude Sweep Analysis (LAS) shows, that the HM Binder (B1) shows better fatigue behavior in aged or unaged state*

Mixture designation	unaged	aged
	Nf	**Nf**
B1-L	1'629'000	1'282'000
B1-Z	-	757'000
B1-ZB-Li	-	657'000
B2-ZB-Li	628'000	135'000

9 Mechanical characterization of mixtures (cm scale)

All mixtures were short term aged as discussed previously. Specimens were compacted using the gyratory compactor to target air voids and tested for various failure modes as described in detail below.

9.1 Indirect tensile strength of benchmark mixtures

Fig. 37 shows the Indirect tensile strength in dry state and after being water conditioned referred to as wet state. Three replicates were tested for each mixture and condition. As shown in the figure and as expected, the dry strength is higher than the wet strength. In addition the ranking of the mixtures is SDA 4>SDA 6>SDA 8 in all cases. It is to be noted that the repeatability of results should be 15% according to the standard and therefore the difference between SDA 4-S and SDA 6-S is negligible. It should be noted that SDA8 has performed better in situ. There difference here can be attributed to the fact that there is a lateral support exerted by the material in situ whereas in lab experiments this does not exist. In addition the larger void size also adds to the weaker strength seen in this example.

The dry and wet strength of SDA 4-S and the modified mixtures is shown in Fig. 37. This is discussed further in the next section.

9.2 Water sensitivity of benchmark mixtures

The water sensitivity values (ITSR) of the benchmark mixtures is shown in Fig. 37. All benchmark mixture pass the Swiss required ITSR of 70% minimum. Again as discussed in the case of ITS, the strength in SDA 8 war lower than SDA 4 and SDA 6 but the difference between wet and dry was less leading to higher ITSR values. As discussed above two factors contribute to the lower strength the larger voids compared to lab samples of SDA 4 and SDA 6 and lack f lateral support in comparison to in situ behavior.

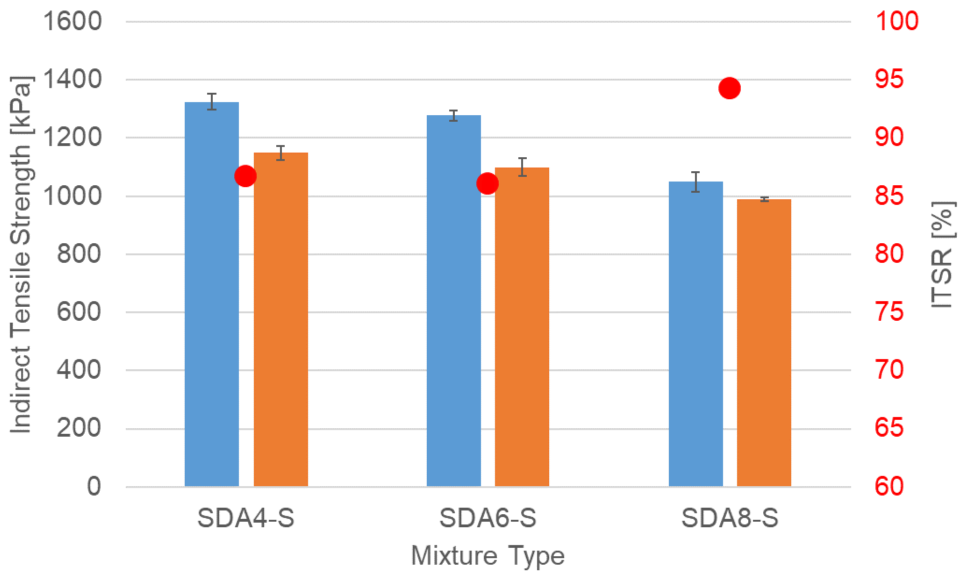

Fig. 37 *Dry and wet strength and Water sensitivity (red dots) of benchmark SDA 4, SDA 6, SDA 8*

Fig. 38 shows the water sensitivity of the SDA 4-S benchmark mixture in comparison to the three modified ones SDA 4-M1, SDA 4-M2 and SDA 4-M3. The figure shows that all mixtures satisfy the Swiss requirement of ITSR > 70%. Mixture SDA 4-M1 shows very similar dry and wet strength in comparison to the SDA-S mixture but slightly lower water sensitivity values. It can be seen from Fig. 38 that the binder and filler have reduced the wet strength and water sensitivity values of SDA 4. SDA 4-M3 has somewhat lower strength in comparison to SDA 4-S but very little difference between wet and dry strength leading to very high ITSR of 97%.

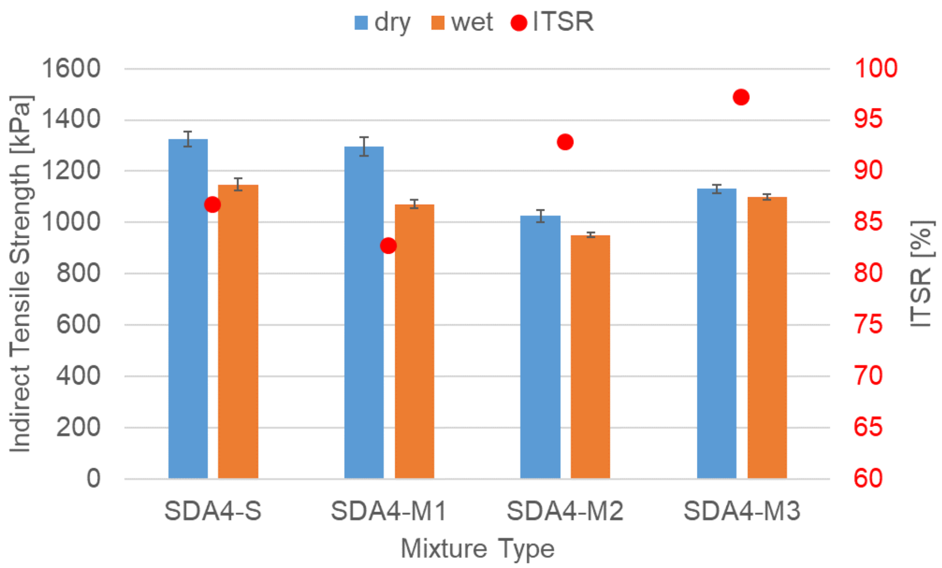

Fig. 38 *Dry and wet strength and Water sensitivity (red dots) of SDA 4-S and three modified mixtures SDA 4-M1, SDA 4-M2 and SDA 4-M3*

9.3 French rutting test

The French rutting test was performed on the modified mixtures. The requirement of the SN indicates that the value needs to be reported however, no threshold is defined. The lowest threshold for other types of mixtures is 7 %. Fig. 39 shows the SDA 4-M1 mixture after the French wheel tracking test and Fig. 40 reports the results of the three mixtures after 30'000 cycles. As shown the amount of rut is minimal at 4 % At 60°C. The ranking of the modified mixtures after 30'000 cycles is: SDA 4-M3 > SDA 4-M2 ≈ SDA 4-M1

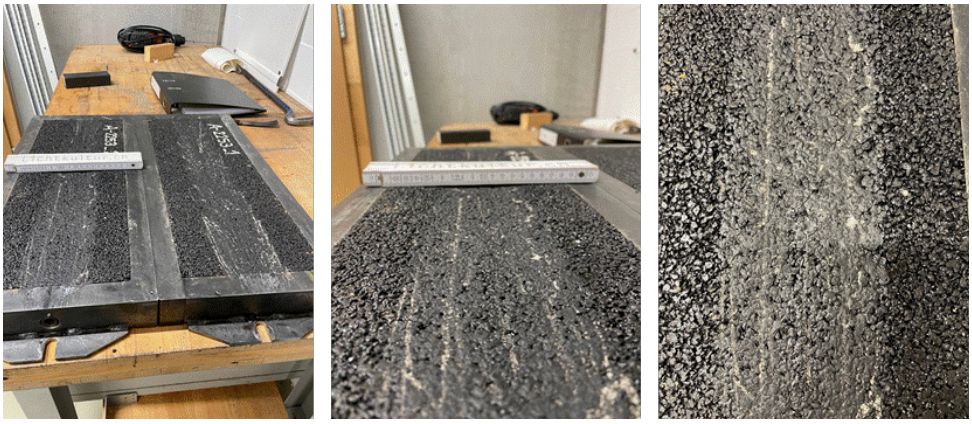

Fig. 39 *French rutting test for SDA 4-M1*

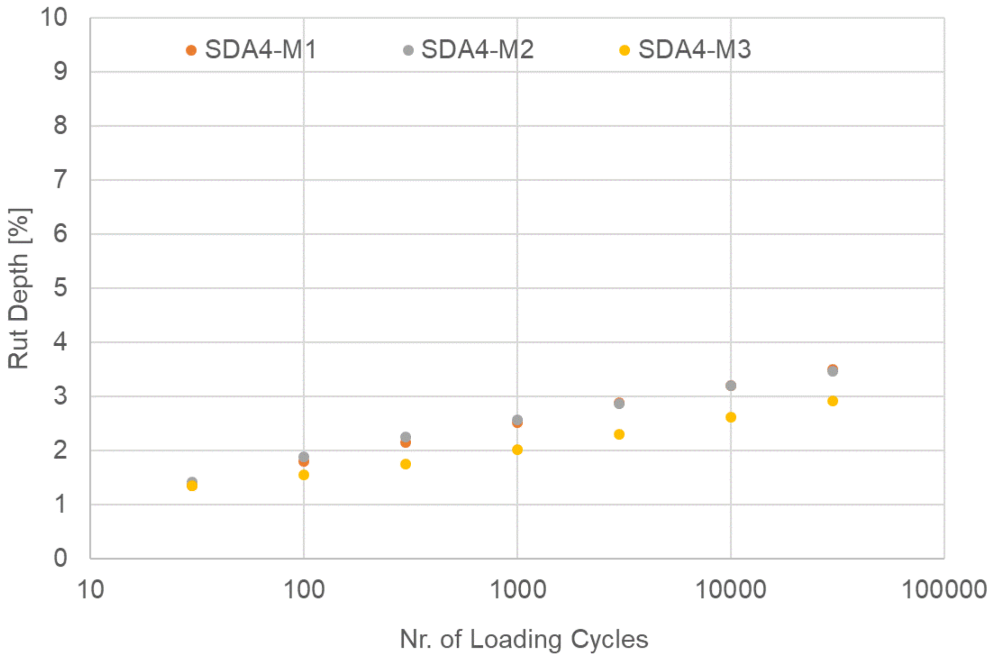

Fig. 40 *French rutting test results for SDA 4-M1, SDA 4-M2 and SDA 4-M3*

9.4 Cyclic compression test

Creep was tested using the cyclic compression tests (CCT) test at 50°C. The inflection point and cumulative axial strain at 2500 cycles for the three standard mixtures are shown in Fig. 41. In a parallel project an inflection point of ca. 2500 cycles was measured for SDA 4 mixtures [49]. It can be seen that SDA 8 reached the inflection point after much fewer cycles in comparison to SDA 6 and SDA 4. The cumulative axial strain was also much higher for SDA 8.

The ranking for the CCT test is as follows: SDA 4-S > SDA 6-S > SDA 8-S. Again as discussed above the higher void content and lack of lateral support have a strong effect on the results of this test.

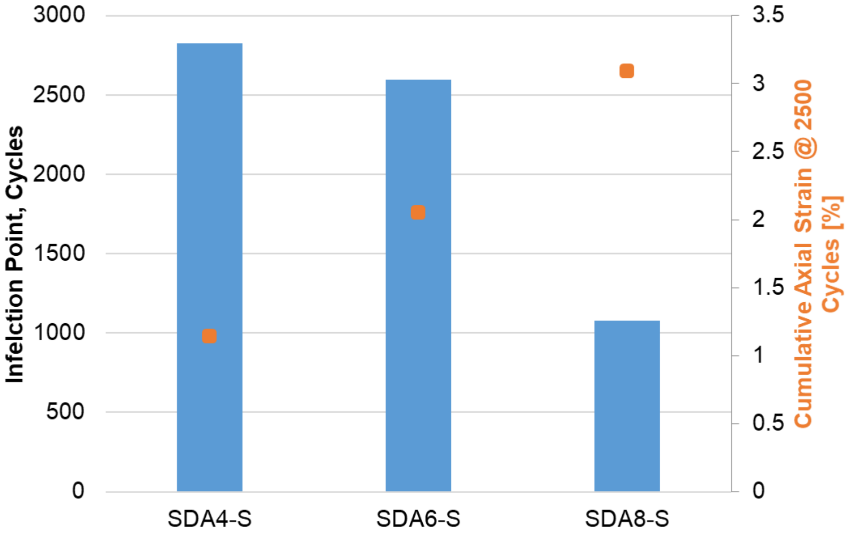

Fig. 41 *Inflection point and cumulative axial strain at 2500 cycles for SDA 4-S, SDA 6-S and SDA 8-S*

The results of the CCT test for the modified mixtures in comparison to the SDA 4-S is shown in Fig. 42. It can be seen that at higher temperatures the modified mixtures all had no inflection point and much lower cumulative axial strain in comparison to the standard mixture SDA 4-S. M1 and M2 had similar performance in this test however the performance of M3 was significantly better in terms of cumulative axial strain. The results of this test corroborate the mastic results that the modifications improve the creep performance of the mixtures.

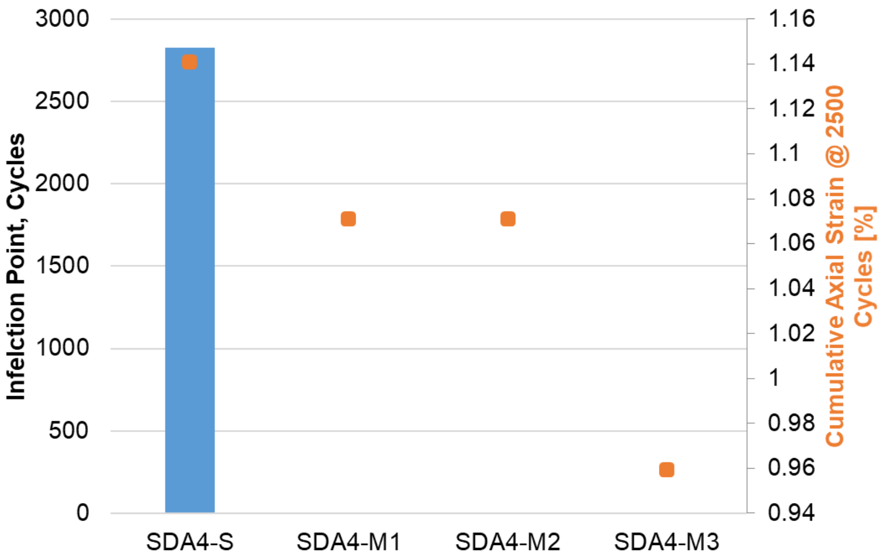

Fig. 42 *Inflection point and cumulative axial strain at 2500 cycles for SDA 4-S, SDA 6-S and SDA 8-S*

Fig. 43 shows the cumulative axial strain for a representative sample of the mixtures tested. It can be seen that at higher temperatures, the worst performing mixture was the SDA 8 and the best performing mixture was SDA 4-M3 with the three modified mixture performing similarly.

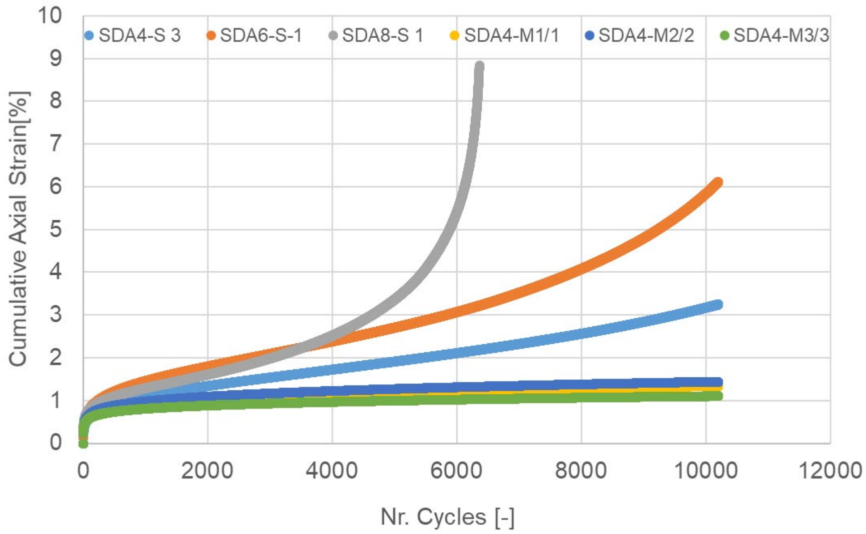

Fig. 43 *Inflection point and cumulative axial strain at 2500 cycles for SDA 4-S, SDA 6-S and SDA 8-S*

9.5 Semi-circular bend test

In order to test the resistance of the mixtures to low temperature cracking, four samples were tested at 0°C for each material type (Fig. 44). A sample of the results for the four test samples for SDA 4-M1 is shown in Fig. 45 and a summary of results in Fig. 46. The force vs. deformation curves show a brittle fracture of the samples. Fig. 46 shows that although the maximum force to failure was similar for the three mixtures, the deformation for M2 and M3 was larger indicating a slightly more ductile behavior that is positive in preventing catastrophic failure during cracking. Although in Switzerland no thresholds exist for the SCB test the order of magnitude of the maximum force to failure of ca 3.5 kN and deformation of ca 0.4mm is within the magnitudes that were seen in tests at Empa on SDA mixtures.

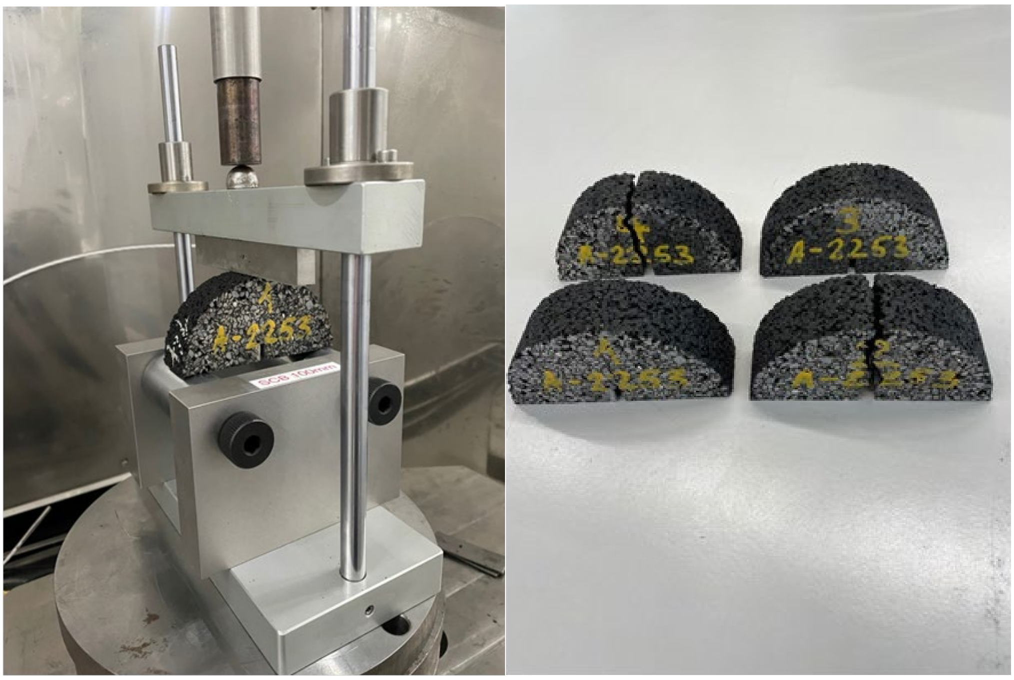

Fig. 44 *SCB test set up left, and SDA 4-M1 specimens after the test right*

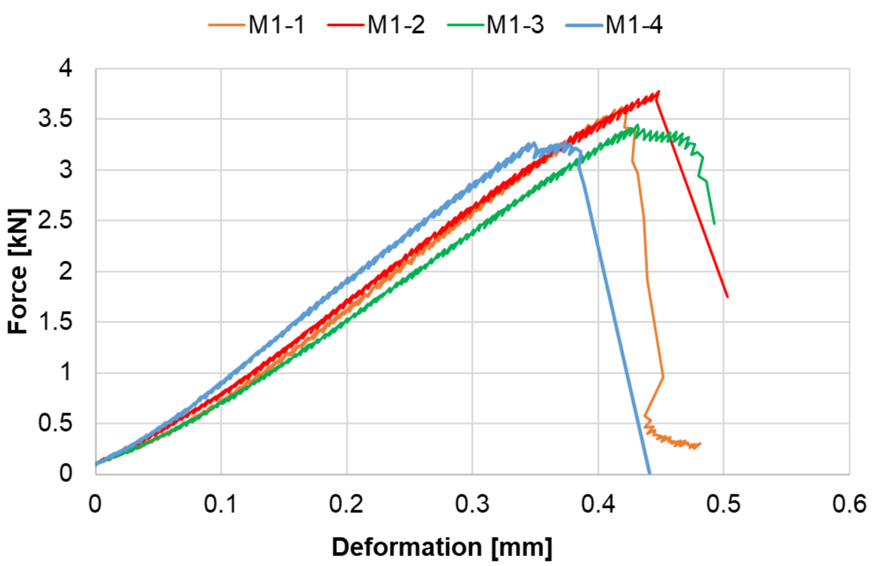

Fig. 45 *Force vs. deformation for the SCB test at 0°C of four samples for SDA 4-M1*

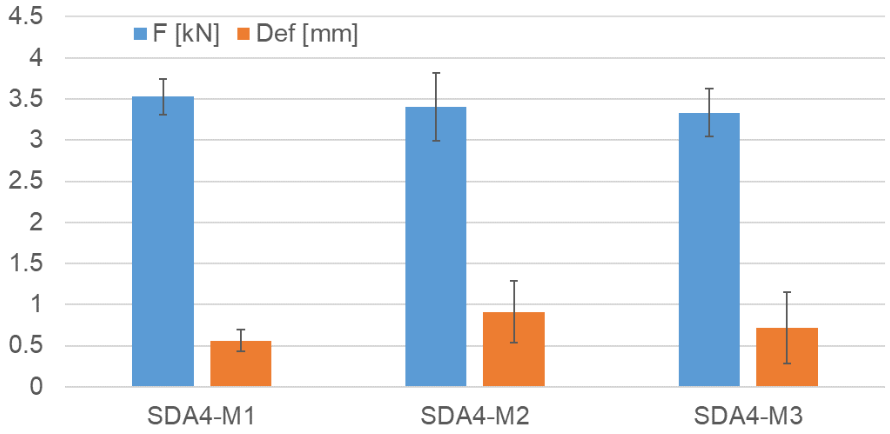

Fig. 46 *Maximum force and. maximum deformation for the SCB test at 0°C. The error bars indicate the standard deviation of the results for four samples*

9.6 Stiffness modulus

The stiffness modulus of the benchmark mixtures measured using the cyclic indirect tensile test on cylindrical samples under sinusoidal load (CIT-CY) is shown in Fig. 47. Four replicates were tested and three temperatures (10, 15 and 20°C) and three frequencies (0.1, 1 and 10 Hz) were used for these tests. The ranking of the tested benchmark mixtures were as follows: SDA 4 > SDA 6 > SDA 8 for all temperatures and frequencies tested. Here by ranking the higher value is meant as higher modulus is not necessarily better when we consider performance.

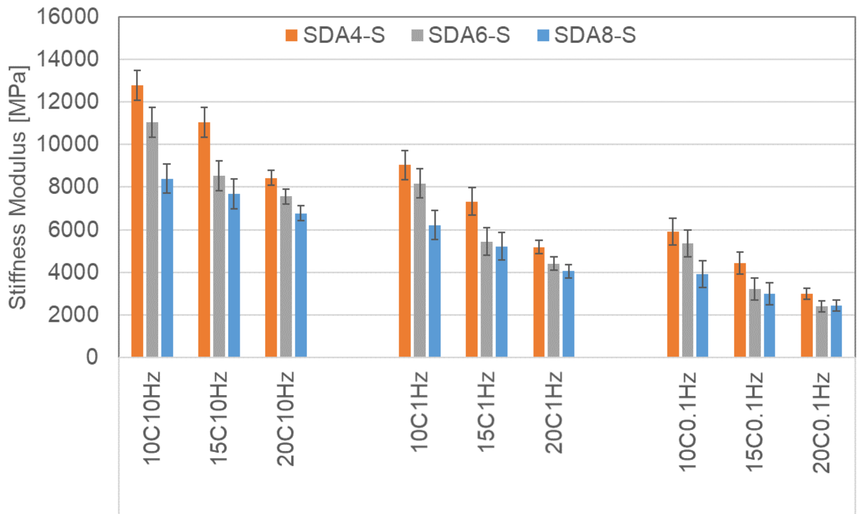

Fig. 47 *Stiffness modulus of benchmark SDA 4-S, SD6-S, SDA 8-S*

Fig. 48 shows the stiffness modulus of SDA 4 benchmark mixture in comparison to the modified ones SDA-M1, SDA 4-M2, and SDA 4-M3. The figure also shows the average air voids content for the four samples used for each mixture. The results show that even though the benchmark mixture S has the highest voids content, for all temperatures and frequencies the benchmark mixtures showed a higher modulus with this difference being smaller at lower frequency of 0.1 Hz and higher temperature 20°C. Amongst the modified mixtures M3 had on the average a higher modulus. As seen in the mastic results the highly modified binder used for M2 and M3 shows a difference with the other binders at higher temperatures. In the mixture scale also it can be seen that the modulus of the M3 mixture in comparison to M1 and M2 is the highest at 20°C. As M2 and M3 have the same highly modified binder this difference can be attributed to the fillers used in M3 i.e. a combination of Zeobit and lime.

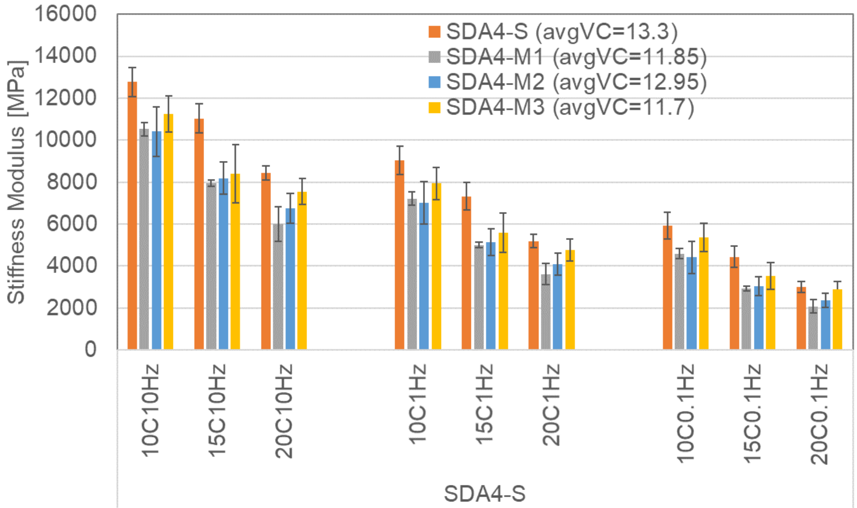

Fig. 48 *Stiffness modulus of benchmark SDA 4-S, and modified SDA 4-M1, SDA 4-M2 and SDA 4-M3*

9.7 Fatigue

The results of the fatigue experiments on cylindrical samples of the benchmark mixtures under sinusoidal load at 10°C and 10 Hz are shown in Fig. 49 and Fig. 50. As seen in the fatigue curve and ε_6 parameter, the fatigue performance of the benchmark mixtures reflects previous results with a similar ranking: SDA 4 > SDA 6 > SDA 8.

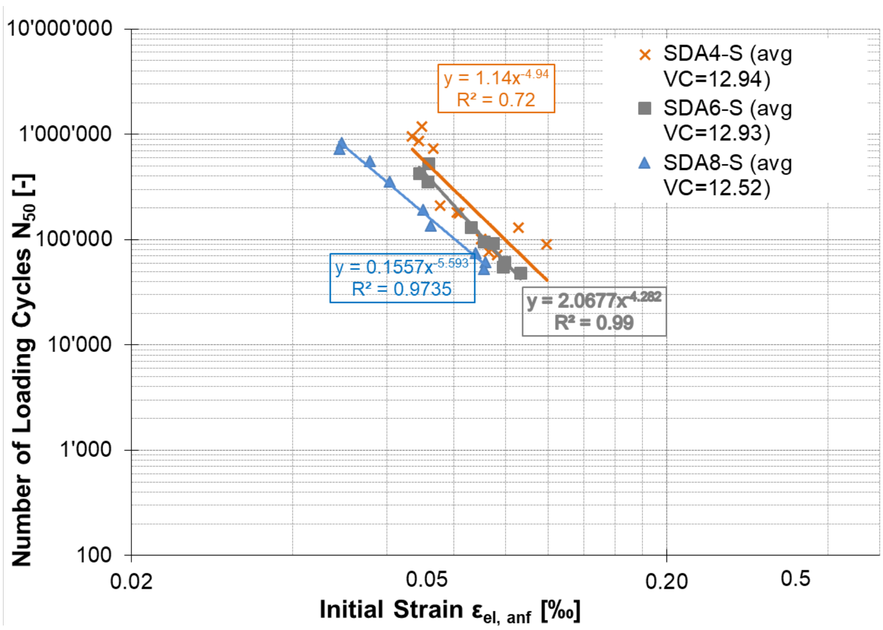

Fig. 49 *Fatigue curve of benchmark SDA 4, SD6, SDA 8*

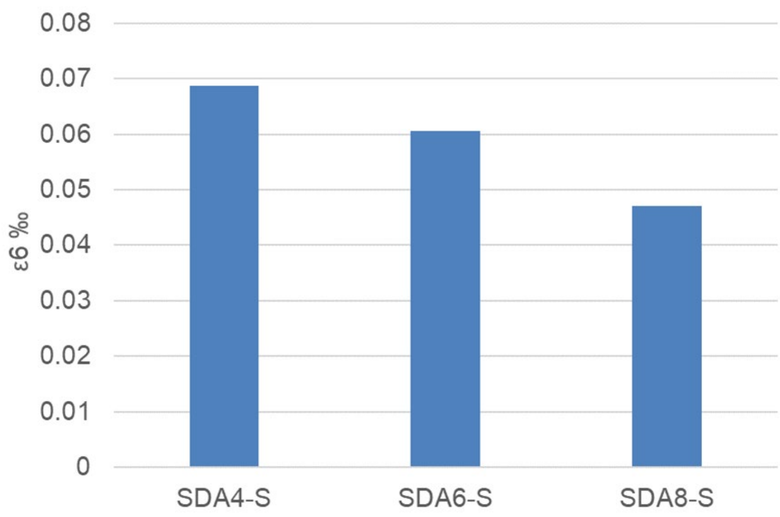

Fig. 50 *Fatigue performance of benchmark SDA 4, SD6, SDA 8*

The fatigue performance of the modified mixtures and comparison to SDA 4-S are shown in Fig. 51 and Fig. 52. A comparison of these values to ones obtained in previous projects using the IT-CY test setup indicate comparable fatigue performance for example SDA 8 mixtures showed a fatigue performance of 0.033 ‰ [68]. The Fig. 51 and Fig. 52 show that the fatigue performance of the modified mixtures is better than the standard mixtures. The e_6 parameter decreased for M1 (-4.6 %) and increased for M2 (7.4 %) and M3 (3.2 %) in comparison to SDA 4-S.

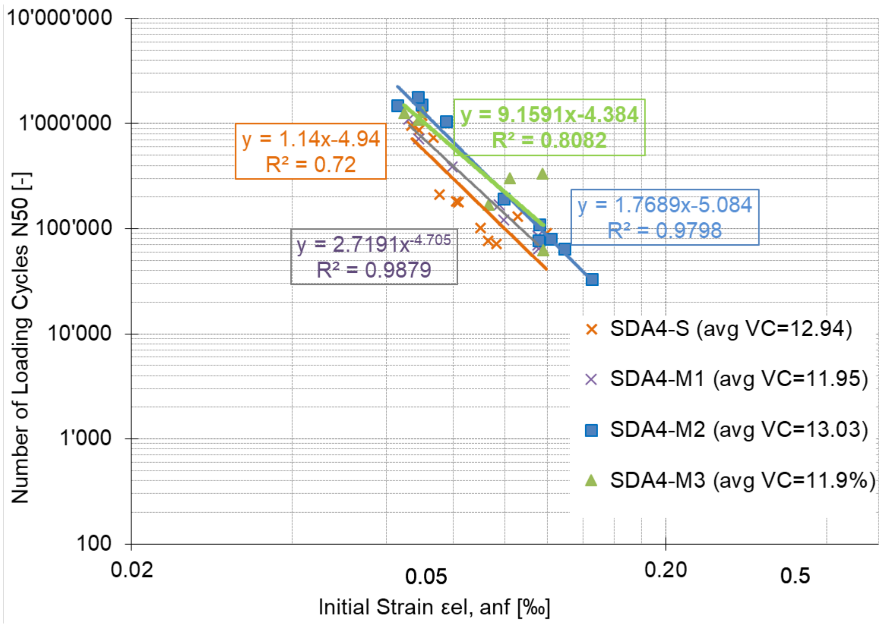

Fig. 51 *Fatigue performance of standard and modified mixtures SDA 4-S, SDA 4-M1, SDA 4-M2, SDA 4-M3*

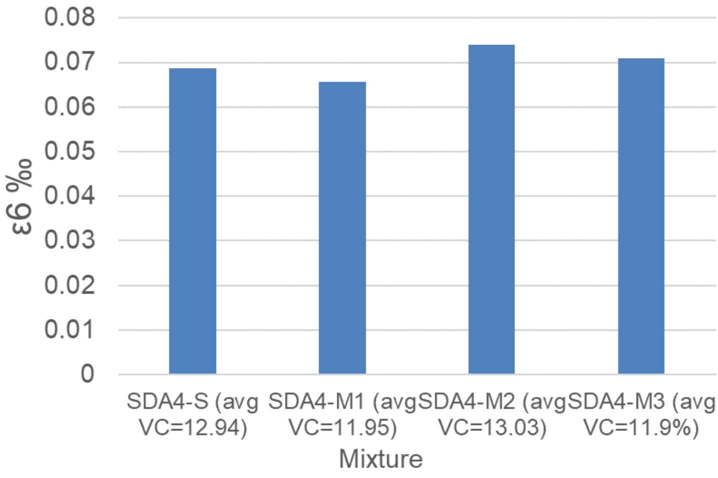

***Fig. 52** Fatigue performance of standard and modified mixtures SDA 4-S, SDA 4-M1, SDA 4-M2, SDA 4-M3*

9.8 Particle loss; MDI

The test was carried out on a total of 6 mixtures. As shown in the results listed in Tab. 17 and Fig. 53, The reference mixtures' particle loss ranking was as follows: SDA 4 < SDA 6 < SDA 8. This is partly due to the fact that the larger particles also have higher weights and result in a higher mass value. All mixtures with the exception of SDA 8 had particle loss values under 4% which is low in comparison to allowable values for the European standard Cantabro test which is normally 10 %.

***Tab. 17** Mixture ID and particle loss values*

Specimen	**PK1**	**PK2**	**Mean**
	Mass Loss [%]	**Mass Loss [%]**	**Mass Loss [%]**
SDA 4 - Reference	2.9	2.8	2.9
SDA 6 - Reference	3.5	4.2	3.8
SDA 8 - Reference	7.1	6.9	7.0
SDA 4- M1	3.8	4.1	4.0
SDA 4 - M2	2.6	2.8	2.7
SDA 4 - M3	3.5	3.2	3.3

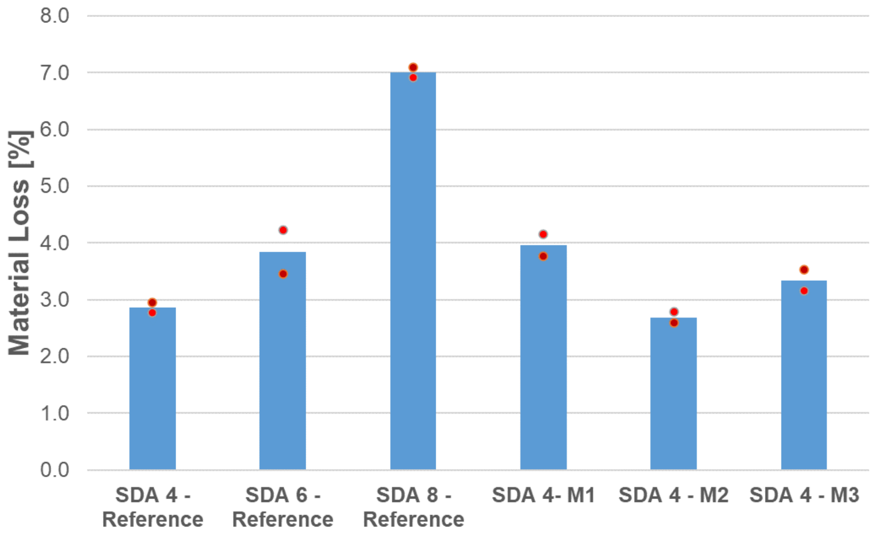

***Fig. 53** Particle loss according to the MDI test*

The following conclusions can be drawn from Fig. 53 :

- The differences between the materials are significantly greater than the dispersion of the two individual values. The differences are therefore mostly relevant.
- The reference mixtures clearly show that the loss in mass increases with increasing maximum grain size. However, it should be noted that in the laboratory test, the mass of the test specimens is the same for all mixtures. This means that fine-grained SDA 4 mixtures tend to be favored, as the loss of a single grain is significantly smaller than with an SDA 8.
- Based on experience with this test, differences in the order of 0.5 mass % are insignificant. This means that the SDA 4-M2 and SDA 4-M3 mixtures should be evaluated similarly to the reference mixture. SDA 4-M1 performs slightly worse than the reference mixture and the mixtures SDA 4-M2 and SDA 4-M3 in terms of grain loss.

10 Large scale durability testing of mixtures (m scale)

The mixtures that were tested at cm scale were further tested in a larger scale using slabs. In this case the mechanical durability is combined with acoustic performance. To this end mechanical durability was tested by recording the developing rut depth with the number of loading cycles using the MMLS3 vehicle simulator and on the other hand air resistivity, sound absorption and surface texture were measured to determine the acoustic behavior in the wheel path and outside the wheel path.

10.1 Measurement setup

Many of the tests performed on the test slabs are point measurements measuring a characteristic on an isolated spot. In order to have multiple measurements per plate and to isolate possible differences between the measurements following point test setup has been setup on all the reference plates (see Fig. 54). There were three points in the wheel path (P1, P2 and P3) and two points outside the wheel path (P4 and P5) which could be used as a reference. For the destructive tests, which are performed after the MMLS3 the points P1 and P4 are used.

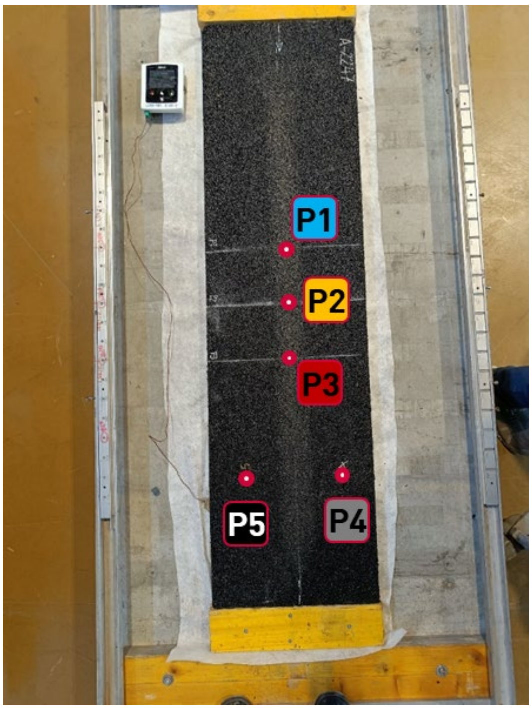

Fig. 54 *Measurement point setup of the MMLS3 plates*

10.2 MMLS3

Two slabs were tested in each case. Fig. 55 shows the development of the maximum deformation with number of cycles for SDA 4-S benchmark mixture and the modified mixture SDA 4-M3. Fig. 56 and Fig. 56 show the development of the maximum deformation with number of cycles for SDA 8-S benchmark mixture and the modified mixture SDA 8-M3. The results show that the behavior of the two slabs is not always following the same path. The difference in the two slabs can be partially attributed to the change in test temperature as the shorter experiments were interrupted regularly for up to an hour to make intermittent measurements, whereas the longer experiments stayed in the chamber while only deformation measurements were done, which take only a few minutes. It can be seen that most of the deformation occurs before 10'000 cycles and in absolute terms the value is very small at maximum of 4 mm to 4.5 mm for SDA 4 or SDA 8. Therefore, the longer experiments can be used to compare the two mixtures. These show that the modified mixtures shown in blue for both mixtures have lower deformation after 50k cycles compared to the benchmark standard mixtures (shown in red). Furthermore, the difference was much larger for SDA 8 compared to SDA 4. The large scale experiments show that there is no adverse effect in using the modified mixtures to the rutting properties, and possibly some improvement.

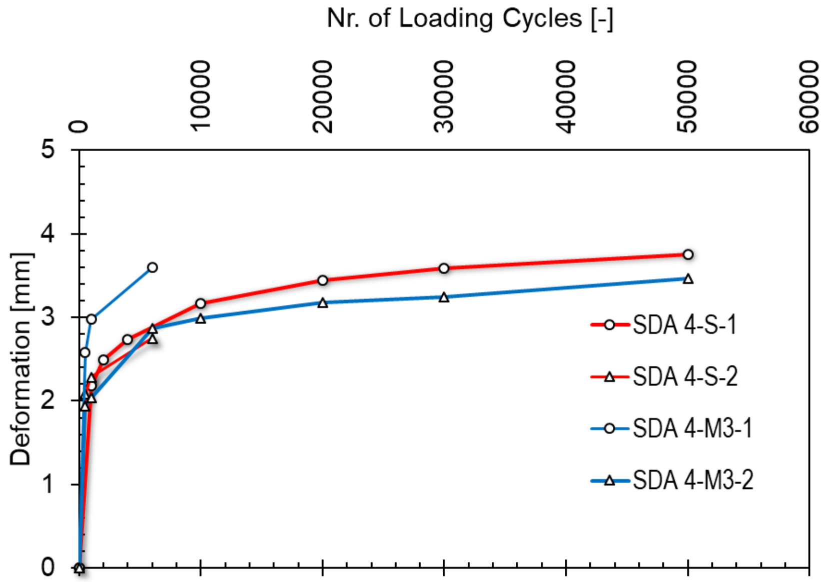

Fig. 55 *Development of rutting of two slabs of benchmark SDA 4-S and modified SDA 4-M3 using MMLS3*

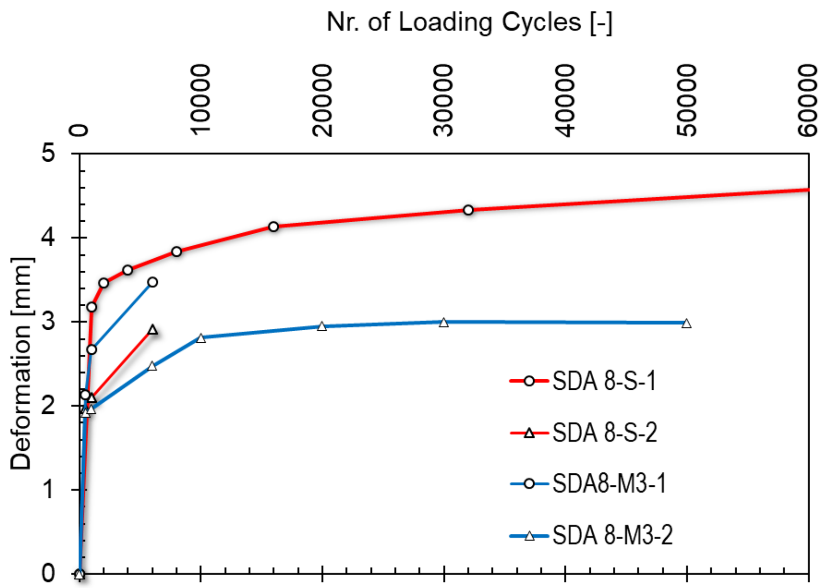

***Fig. 56** Development of rutting of two slabs of benchmark SDA 8-S and modified SDA 8-M3 using MMLS3*

10.3 Acoustic tests on mixtures

10.3.1 Surface texture

The surface texture data for the SDA 4 and SDA 8 MMLS3 slabs before loading are showing in Fig. 57. The texture level of the SDA 8 samples are higher than for the SDA 4. This is the case for the macrotexture where it would be expected given the higher aggregate size, but also in the microtexture.

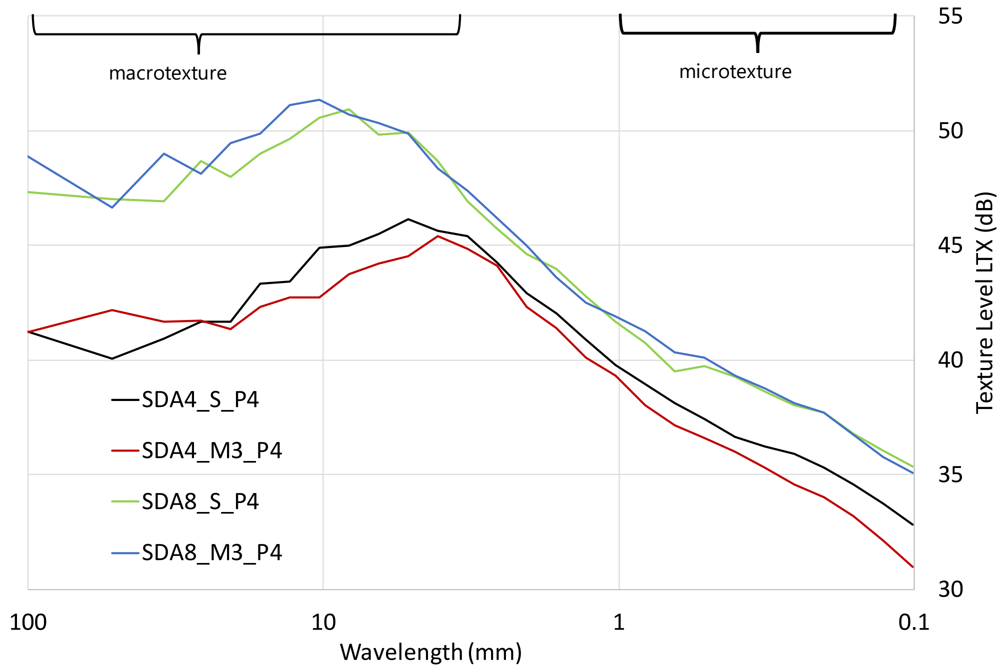

***Fig. 57** Surface texture level comparison of SDA 4 and SDA 8 slabs before MMLS3 loading*

Looking at the effects of the MMLS3 wheel loading, the texture level for the SDA 4 and SDA 8 samples are shown in Fig. 57 to Fig. 61, with the sample position and number of cycles indicated. The texture level in the wheelpath is reduced from the MMLS3 loading relative to the texture after compaction (P4 and P2_x cycles), which is indicative of the effect of the traffic on the surface texture of SDA, and has also been observed in field samples [53]. The texture reduction is more significant for the SDA 4 sample, where the modified SDA 4 seems to have more resistance to reduction in the microtexture. This could indicate better performance in skid resistance, as higher microtexture is correlated with this parameter [74]. However, we must keep in mind that this was only from comparing one slab per mixture and that the effect of the texture when including the effects of weathering in-situ are more complex [54]. Overall, the modification of the SDA mastic did not have a significant effect on the texture properties before and after wheel tracking.

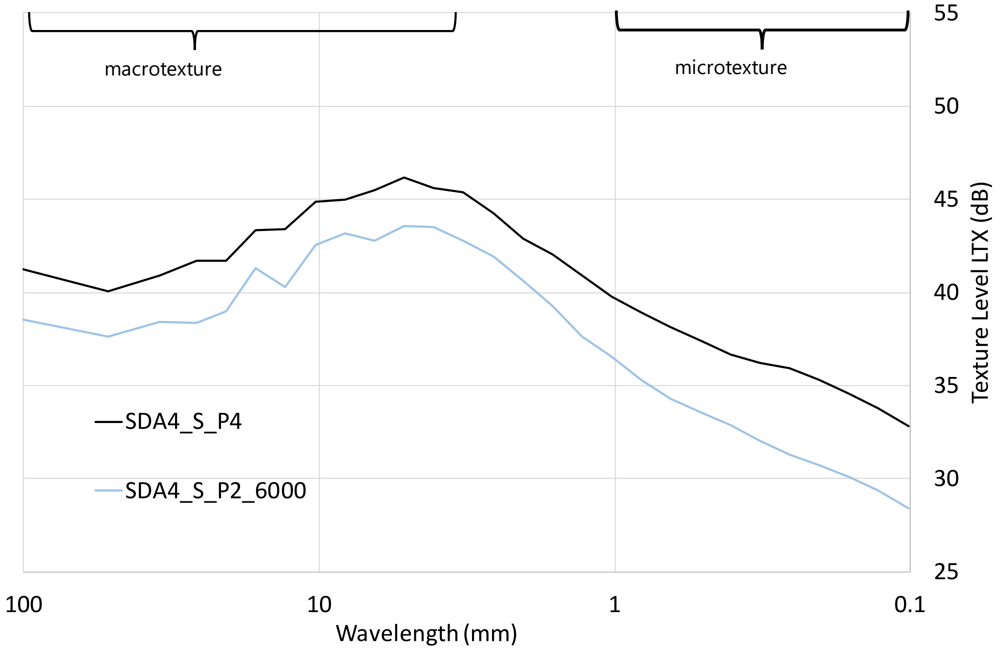

***Fig. 58** Surface texture level measurements for SDA 4 benchmark MMLS3 sample inside (P2) and outside (P4) of the wheel path*

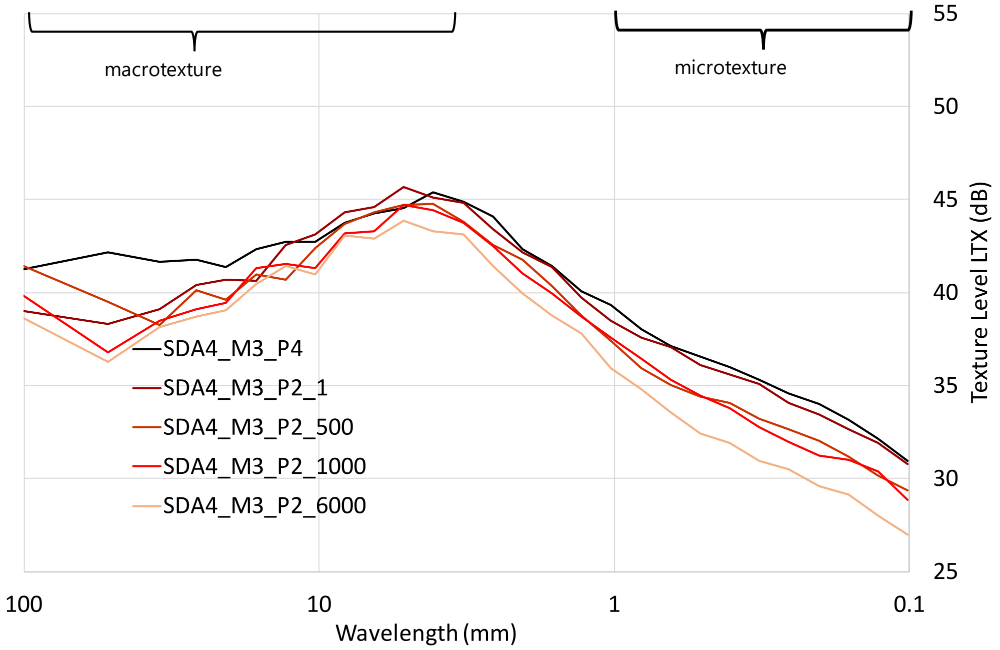

***Fig. 59** Surface texture level measurements for SDA 4 modified MMLS3 sample inside (P2) and outside (P4) of the wheel path*

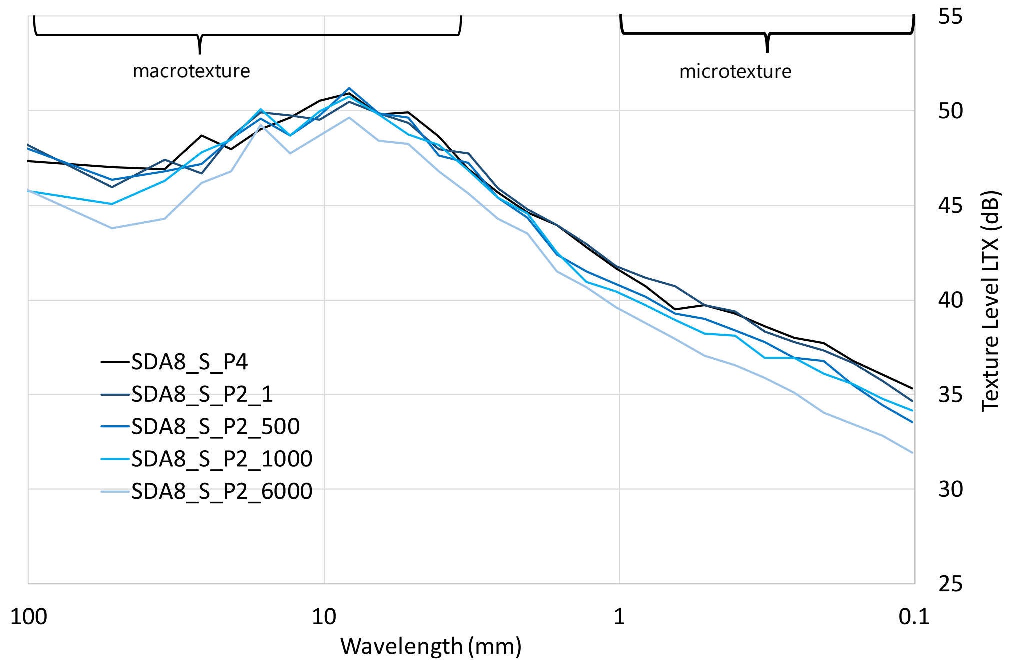

***Fig. 60** Surface texture level measurements for SDA 8 benchmark MMLS3 sample inside (P2) and outside (P4) of the wheel path*

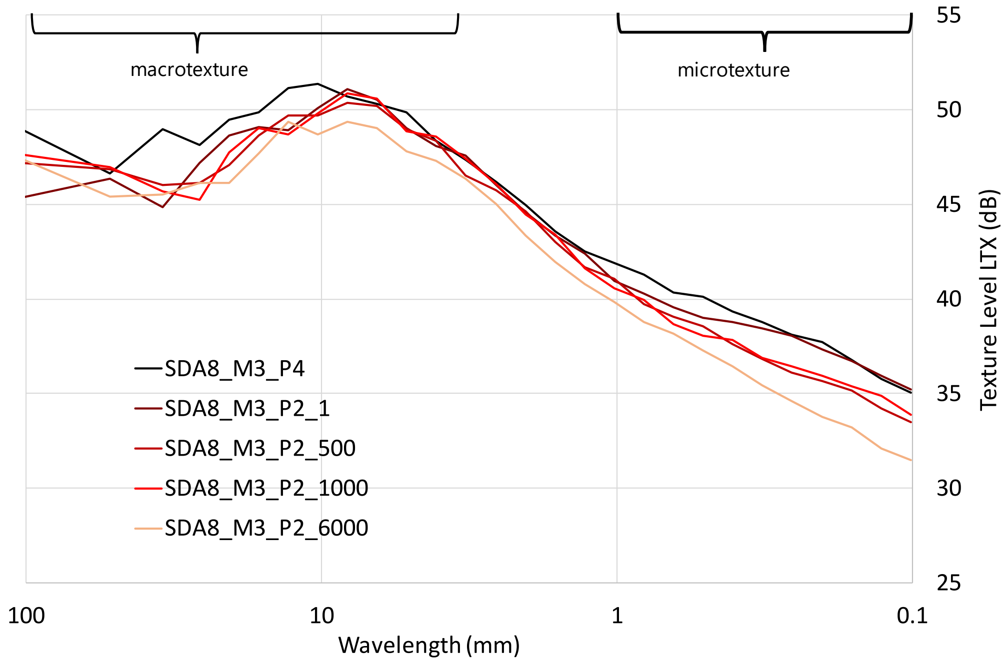

***Fig. 61** Surface texture level measurements for SDA 8 modified MMLS3 sample inside (P2) and outside (P4) of the wheel path*

10.3.2 Computed tomography (CT)

The following Fig. 62 and Fig. 63 show the profile of the connected void content over the depth of the drill core evaluated with the CT-method. Fig. 62 shows that the reference slab and the optimized slab can have very different behavior in terms of connected void contents. While connected void content of the reference slab on MP4 (outside the wheel path) is steadily decreasing over the depth over the core, the void content in the wheelpath stays more or less the same over the whole depth, indicating an improvement regarding acoustic performance.

It is also interesting to see that the reference slabs have in general lower void contents than the optimized mixtures.

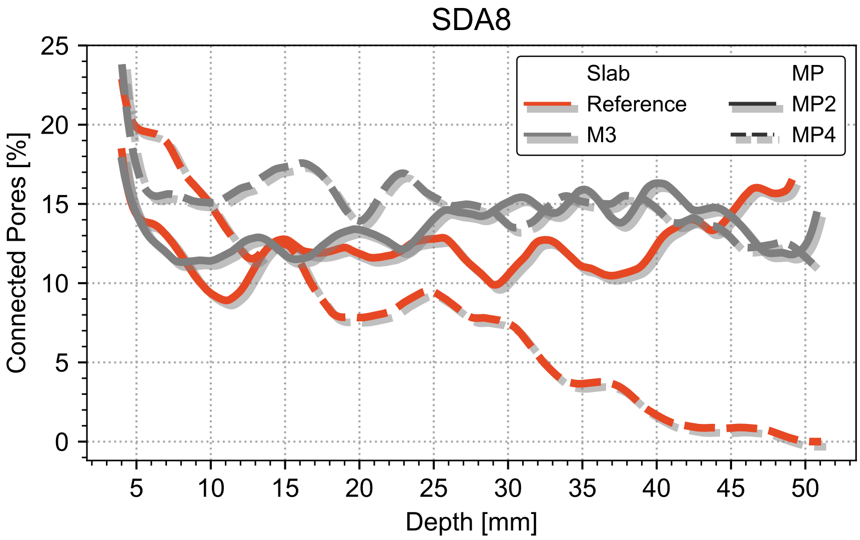

Fig. 62 *Connected pore network for the SDA 8-Slabs. Red: Reference Slab, gray: Optimized mixture (M3). Solid Lines: MP2, wheelpath after MMLS (6'000 cycles) and MP4, outside wheelpath (dotted lines)*

Additionally, a rather strong decrease in connected voids is observed for the reference slab SDA 4 in Fig. 63. In comparison, the optimized mixture M3 retains its connectivity throughout the depth indicating a favorable acoustic property. However, the comparability between the reference plate and the optimized mixture is limited.

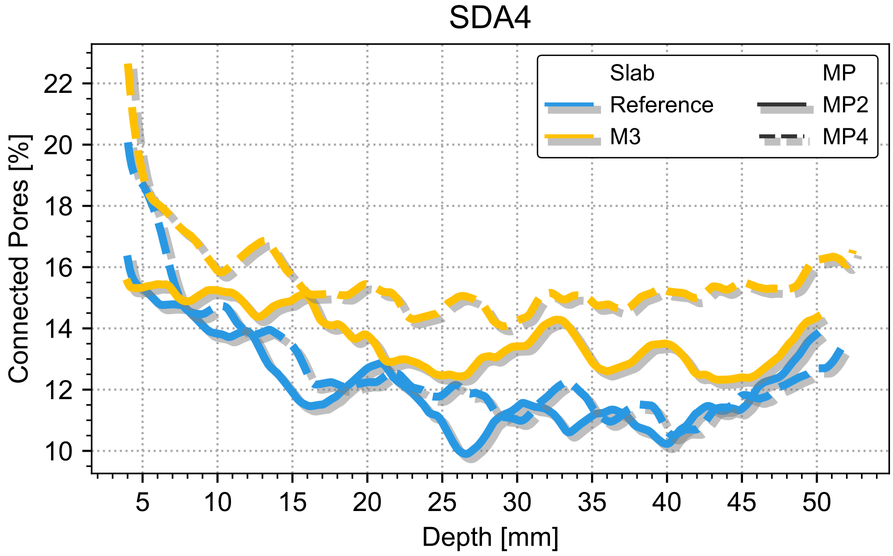

Fig. 63 *Connected pore network for the SDA 4-Slabs. Blue: Reference Slab, Yellow: Optimized mixture (M3). Solid Lines: MP2, wheelpath after MMLS (6'000 cycles) and MP4, outside wheelpath dotted lines*

10.3.3 Acoustic absorption

In Fig. 64, the averaged spectral sound absorption measurement is shown for the reference plate SDA 4-S after 0, 500, 1'000 and 6'000 cycles on the MMLS3. Detailed acoustic results for all the measurement points may be found in the Appendix I. Fig. 64 shows that outside the wheel track not very much has happened in terms of sound absorption between the cycles (except for low frequencies, which might be a measurement artefact).

Regarding the measurement in the wheel track a slight trend to lower sound absorption is shown between 0 and 500 cycles. However statistically significant differences (significance level $p < 0.05$) can only be observed for 1250, 2'000 and 4'000 Hz.

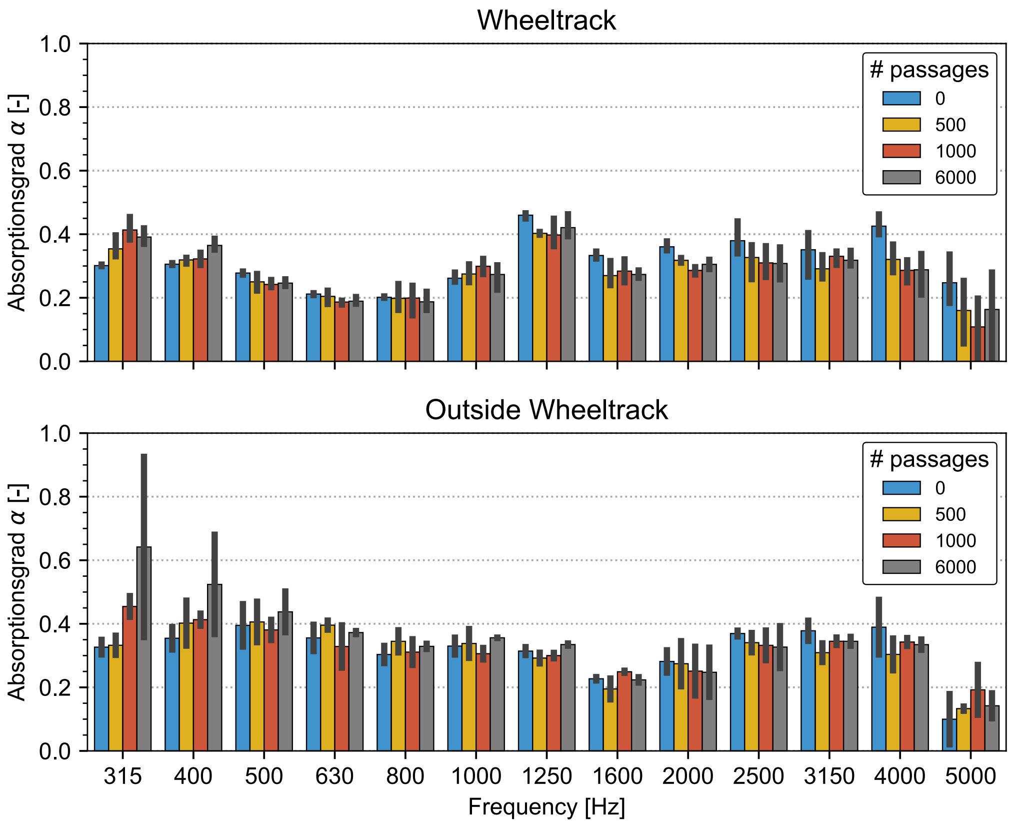

Fig. 64 *Comparison of sound absorption measurements of the reference plate SDA 4-S for measurements inside (up) and outside wheelpath (below); error bars indicate one standard deviation*

10.3.4 Air resistivity

Air resistivity development in the wheel path and outside the wheel path after exposure to loading cycles is shown in Fig. 65. After 6'000 loading cycles, the values have remained constant outside of the wheel path and they have been reduced in the wheel path. This effect has been observed for all four tested slabs. The SDA 4 slabs have higher air resistivity than the SDA 8 slabs and the modified mixtures (M3) have lower air resistivity than the benchmark. The lower air resistivity of SDA 8 is expected as the void size on average is larger due to large aggregates. The values observed corroborate values measured in the field for similar new mixtures [1] [24]. The reduction in the values after exposure to loads is the opposite effect that has been observed in field measurements where the aged pavements have an increased air resistivity [24]. The cause of the in-situ reduction can be primarily attributed to the compaction of the void structure due to traffic. The MMLS sample have shown little compaction as a result of the loading, this is especially the case for the M3 mixtures with the high modulus binder that keeps the structure intact even after the application of 6'000 loading cycles. This is also observed with the CT measurements that characterizes the void structure after loading and the surface texture showing less of a change in the surface texture. The consistent decrease in air resistivity in the current experiments in the wheel path can be attributed to the fact that due to the rut the device cannot form a sealed contact with the pavement surface and the air can escape causing a lower air resistivity. Therefore, for the noise modeling in the next chapter the air resistivity values outside of the wheel path are used.

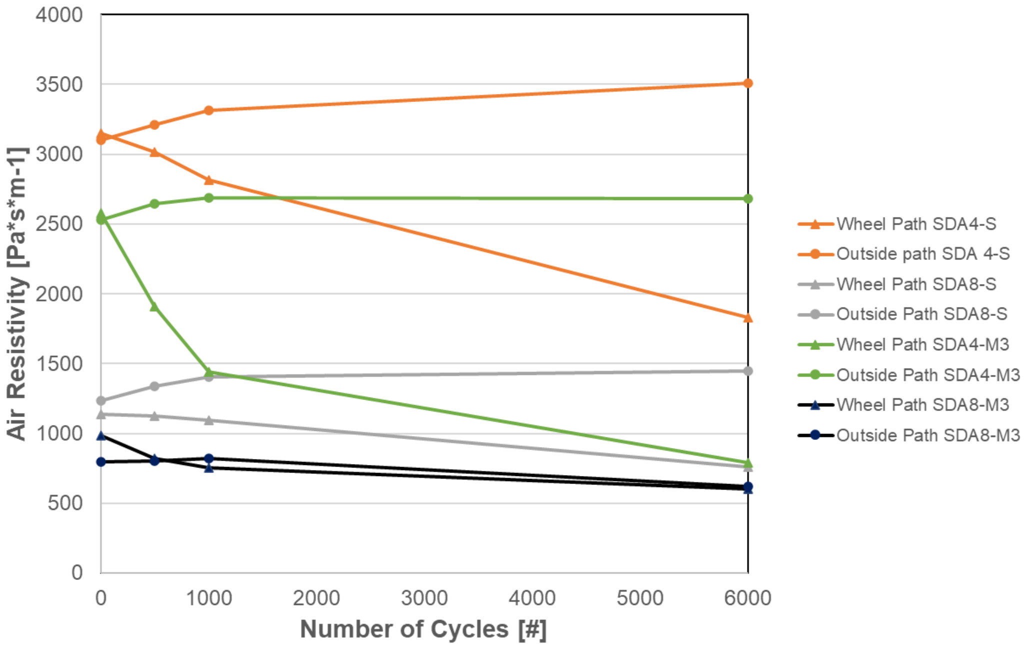

***Fig. 65** Air resistivity results of MMLS3 slabs for SDA 4 and SDA 8 samples*

10.4 Acoustic simulations of optimized mixtures (m scale)

The different noise contribution from the measurements of surface texture, absorption and air resistivity can be compared using the SPERoN-simulation. A more detailed description for the SPERoN is found in the chapter 7.5.5. Fig. 66 displays the simulated noise levels as total CPX-levels for the measurement points MP1-MP5 (see Fig. 54). The figure illustrates the differences between the loaded measurement points after 6'000 passages of MMLS3 (Yellow) and the unloaded measurement points (Blue). The figure shows that the loading from the MMLS3 has a direct impact on the simulated noise levels. After 6'000 cycles, the average sound emission in the wheel path was simulated to be 85.9 dB compared to 84.1 dB before being exposed to the loading. Thus, after the 6'000 cycles, the predicted sound pressure level is increased by 1.8 dB. In brackets are the values shown as a difference from the Swiss noise calculation reference model StL-86+.

The simulation shows that the initial noise levels for the Reference slab SDA 4 amounts to -7.5 dB, a very good initial level for SDA 4 road surfaces. After the application of MMLS3, the good acoustic characteristics have decreased by 1.8 dB. On the other hand, for the modified mixture SDA 4-M3 (Fig. 66) the simulated acoustic noise levels has remained more or less constant between the unloaded measurement points (0) and the loaded measurement points (6'000).

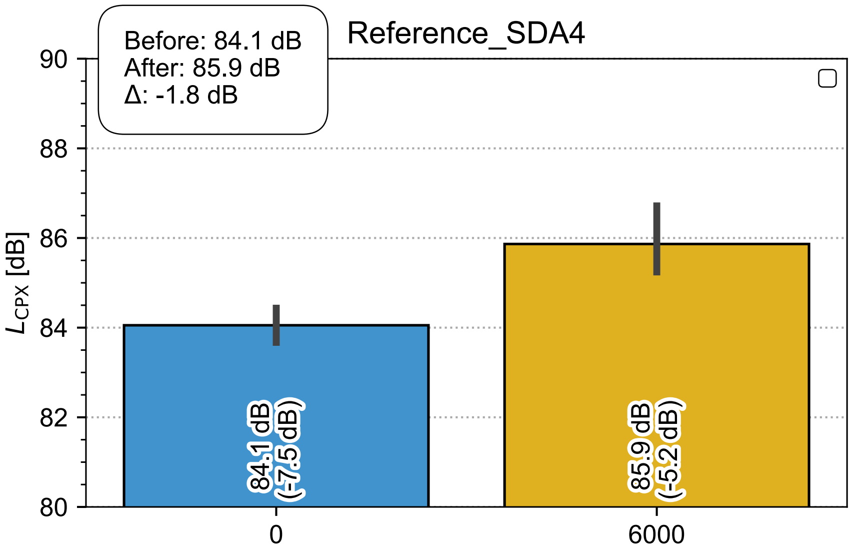

Fig. 66 *Comparison of the SPERoN simulated CPX-values for the reference mixture SDA 4-S. The brackets show the acoustic levels in comparison to the noise model StL86+*

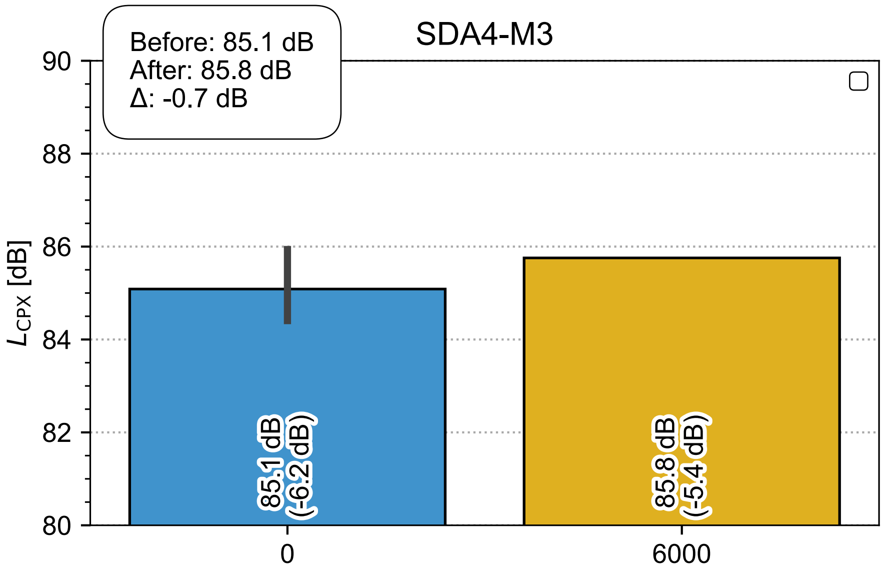

Fig. 67 *Comparison of the SPERoN simulated CPX-values for the optimized mixture SDA 4-M3*

Regarding SDA 8, the simulated initial noise levels of the reference surface were higher (-4.6 dB) compared to SDA 4 and lay in an expected range for newly laid SDA 8 road surfaces. This is due to the smaller grain size of SDA having a lower macrotexture, thereby reducing the magnitude of impact with the tyre as found previously [45] [69]. After the 6'000 loading cycles with MMLS3, the noise level decreased by 0.9 dB to -3.6 dB after 6'000 cycles.

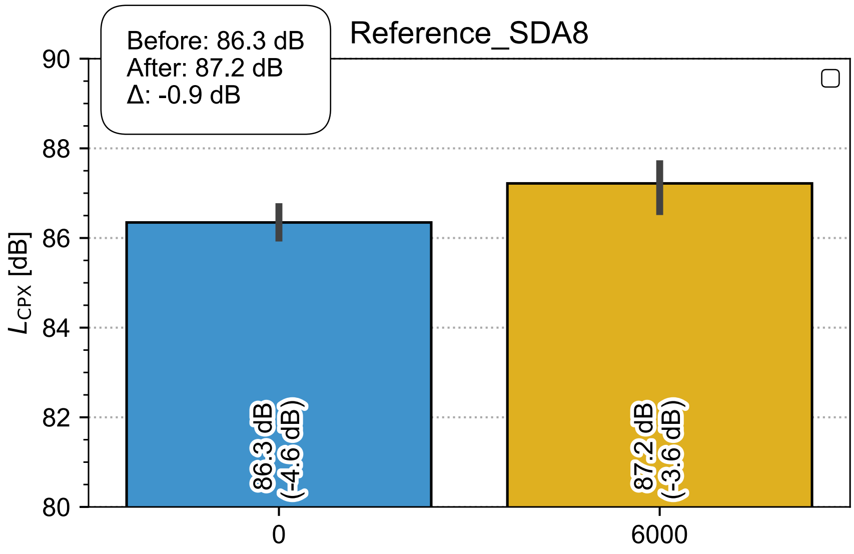

Fig. 68 *Comparison of the SPERoN simulated CPX-values for the reference mixture SDA 8-S*

The optimized mixture SDA 8-M3 has again shown better performance regarding durability compared to the reference, with the estimated pavement noise not increasing during the simulation.

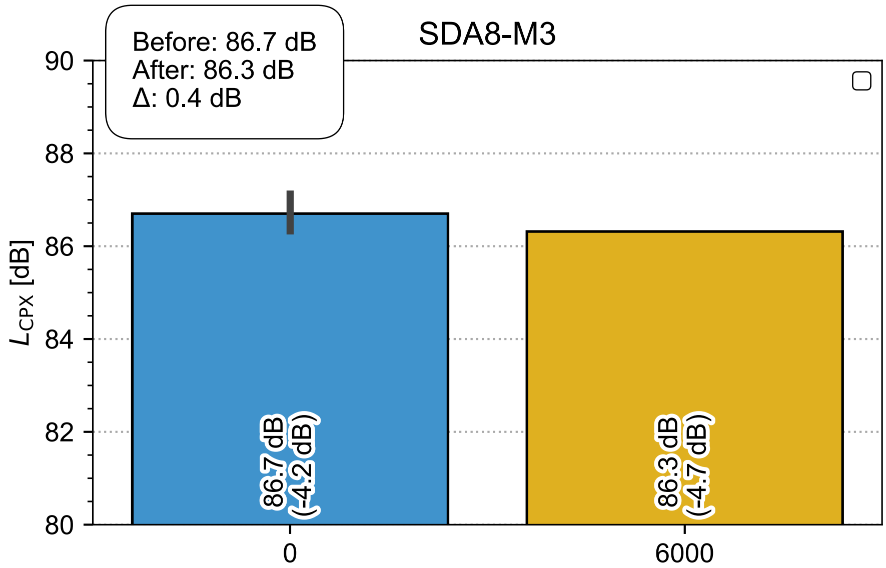

Fig. 69 *Comparison of the SPERoN simulated CPX-values for the optimized mixture SDA 8-M3*

When interpreting the results, it must be taken into account that the mechanical response and acoustical aging behaviour of the slabs in MMLS3 differs from the behavior in the field. This is because the load in the MMLS3 does not exhibit any shear forces and no dirt particles from the environment enter the samples. Therefore, the given acoustical ageing rate of the slabs can only be translated to reality to a limited extent.

In Fig. 70, the absolute levels for SDA 4 and SDA 8 are shown. This graph illustrates that SDA 4 has the better noise reduction potential initially as well as after the 6'000 MMLS3 cycles. It can also be seen that the acoustic performance decreases more for the SDA4 than for SDA8. However, this does not mean that it is performing better in field. The field from the past years data has show a different behavior (See Fig. 11). It has to be stressed, that the aging mechanism applied in the lab is more limited compared to the ageing mechanisms experienced in the field. In the field, clogging through dirt ingress is one of the main acoustical aging mechanisms. This was not incorporated in the current study, as a reliable method for simulating dirt ingress is not known. Also, the MMLS3 employs unidirectional loading. In the field, breaking, acceleration, turning of wheels apply more varied forces on the road surface than the controlled and consistent loading in a lab setting. These variations in loading conditions can significantly impact the aging mechanisms experienced by materials in real-world scenarios. The absence of dirt ingress and the lack of dynamic loading conditions in the lab can indeed result in a different aging profile compared to what is observed in actual field conditions.

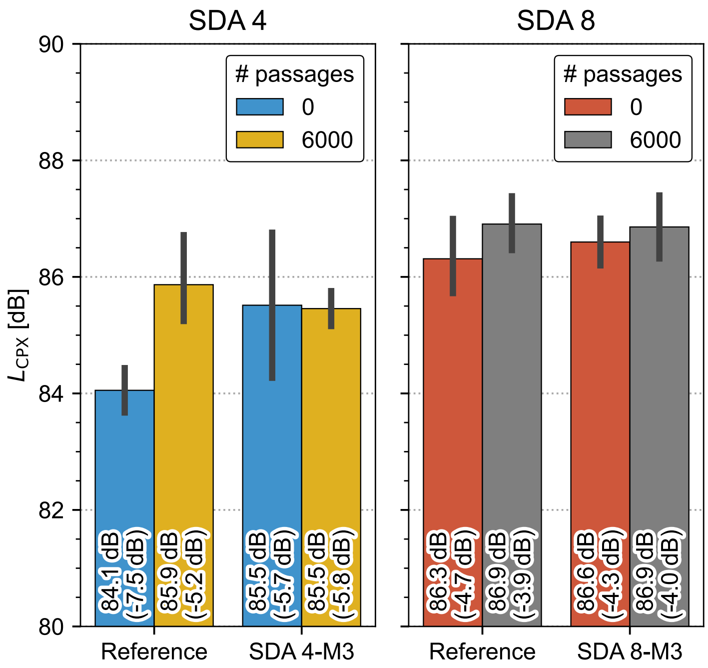

Fig. 70 *Summary of acoustic results of SDA 4 and SDA 8 for reference and optimized mixtures (M3) unaged and aged with MMLS3*

Fig. 72 shows the comparison of an aged sample (MP2 after 6'000 cycles) and an unaged sample (MP4, 0 cycles). In total, a reduction of 0.8 dB was observed. With the results from Fig. 72, the cause for the increase may be identified. It is evident that the vibration noise (red area) component is reduced in the upper frequencies (500 – 2'000 Hz). This corresponds well to the observation of reduced texture levels as indicated in the previous section 10.3.1. Furthermore, large differences are visible with the airflow noise (blue shaded region). Due to the effects of the loading wheel spreading the bitumen on the surface, smoothing the macrotexture and blocking part of the surface porosity, air has more difficulty escaping (Fig. 71). This leads to increased airflow sound, which is typically observed in the middle to the upper frequency range. The slightly reduced sound absorption observed in chapter 10.3.3, is another indication for this phenomena.

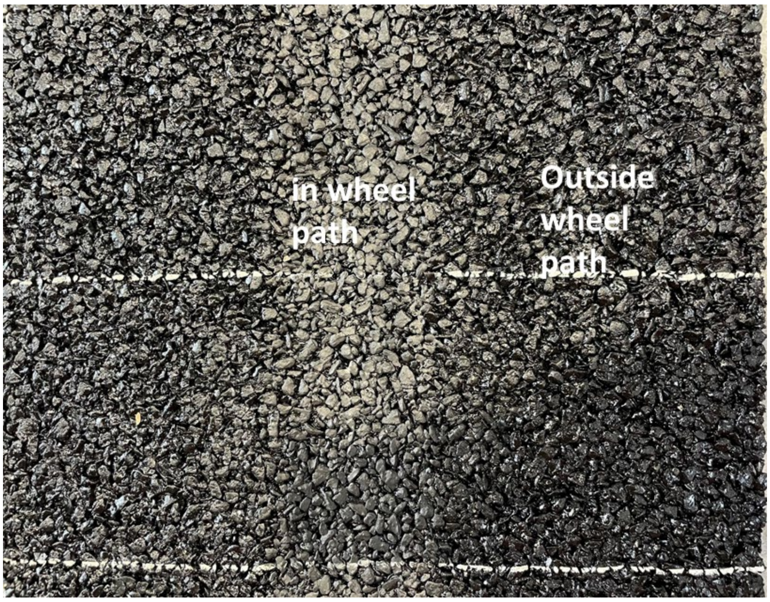

***Fig. 71** Change in surface properties as a result of wheel tracking in and outside of the wheel path*

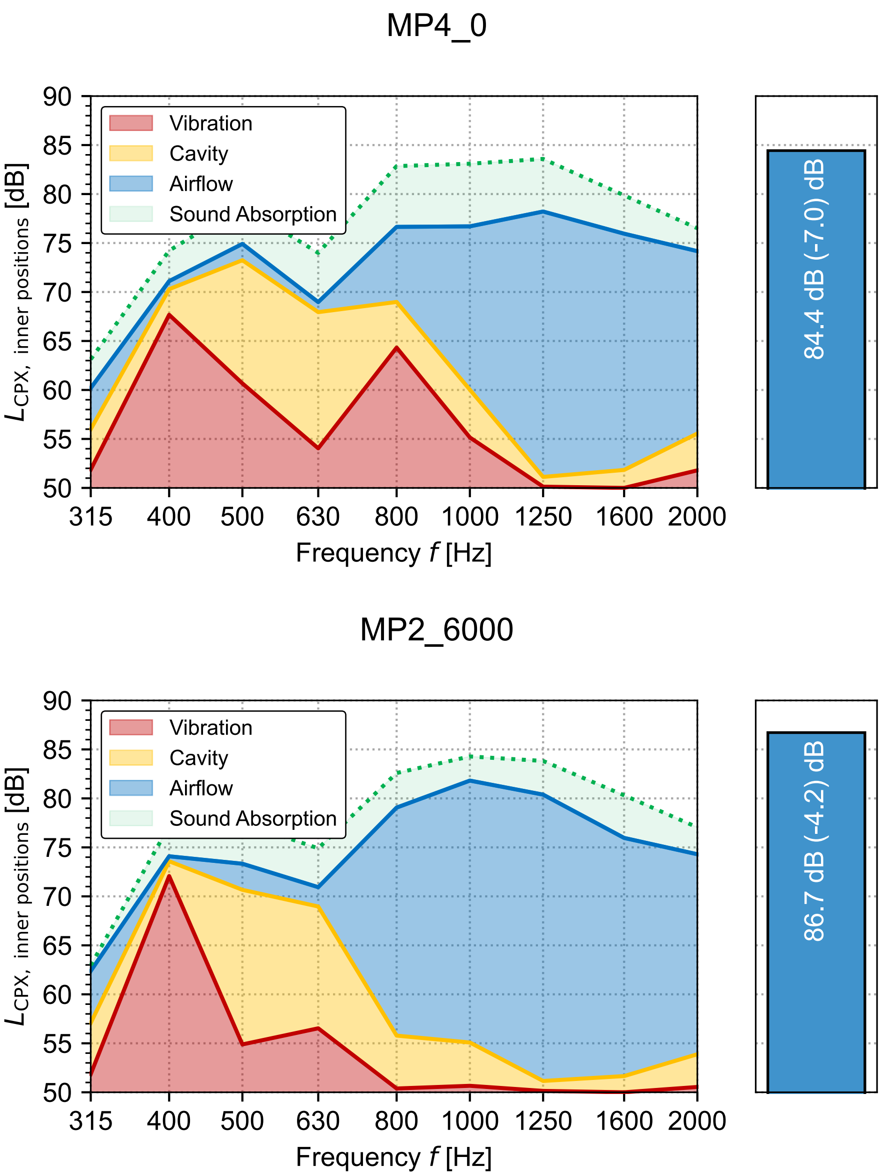

***Fig. 72** Spectral comparison of noise simulations for the SDA 4-S reference plate using SPERoN for and MP4 (unaged) MP2 (aged after 6'000 cycles)*

11 Summary and Conclusions

A multi-scale approach was implemented to investigate mechanical and acoustic performance of SDA 4, SDA 6 and SDA 8 mixtures from mm to km scale. Tab. 19 shows a summary of the critical results. Benchmark mixtures were developed using the optimum acoustic in-situ performance of these mixtures using 200 test sections. As a first step, the mechanical performance of the benchmark mixtures were investigated. It was shown that the overall ranking of the benchmark mixtures was as follows: SDA 4>SDA 6>SDA 8. As a second step, combinations of binder and filler and additives were used to characterize the mastic. The best performing mastic was used thereafter in producing the modified mixtures. The SDA 4 mixtures were first modified and tested mechanically using a wide variety of tests in order to determine their performance. Thereafter, the optimized modification was applied to SDA 8 slabs. From the experimental results the following conclusions can be drawn:

- At the mastic scale, it was observed that the filler primarily had a stiffening effect with higher complex modulus and lower phase angle at higher temperatures above 30°C, with Zeobit filler having a stronger effect.
- At the mastic scale, highly modified binder with limestone and Zeobit filler as well as a combination of Zeobit filler and hydrated lime had the best results that were also similar.
- The optimized modification for the mixtures was a combination of highly modified binder, stiffening filler (Zeobit) and hydrated lime to improve water sensitivity.
- It should be noted that hydrated lime has a relatively high environmental footprint and this aspect should be considered when choosing the optimum materials.
- Laboratory scale mixture performance tests have shown that the modification improved the water sensitivity, fatigue- and cyclic compression resistance and had similar low temperature cracking results in comparison to the benchmark.
- The micro-Deval IMP test has shown higher particle loss for SDA 8 mixtures. The modified SDA 4 mixtures showed similar particle loss to the benchmark mixtures.
- The large scale MMLS tests showed that after 50'000 loading cycles, the modified M3 mixtures showed less rutting in comparison to the reference. This effect was greater for the SDA 8 mixtures. The modified mixtures had similar changes in surface texture and acoustic performance to the benchmark mixtures before and after the wheeltracking.
- Using the MMLS3 load simulator and measurements before and after exposure to loads, the acoustic modeling has shown that the modified mixture SDA 4-M3 and SDA 8-M3 noise levels improved between the unloaded measurement points and the loaded measurement points. This indicates that the modification maintained the structural integrity of the mixture after loading. This was confirmed by the CT scans of the loaded and unloaded samples showing that the void connectivity of the modified mixtures was larger contributing to better noise absorption.

Tab. 18 *Summary of results: arrows indicate results in comparison to SDA 4-S standard mixture; green arrow=improved performance; yellow arrow=similar performance; red arrow=worst performance. SCB and rutting results are only for the modified mixtures; yellow arrow shows similar results and green arrow shows better performance in comparison to the modified mixtures*

Mixture / Test	**ITSR**	**Fatigue**	**CCT**	**Rut***	**SCB***	**MicoDeval**	**MMLS3**		
							Def	**Noise Abs**	**Air**
Temp.	20°C	10°C 10Hz	50°C	60°C	0°C		40°C	40°C	40°C
SDA4-S	REF	REF	REF				REF	REF	
SDA6-S	→	↓	↓				→		
SDA8-S	↑	↓	↓				↓		
SDA4-M1	↓	→	↑	→	→	→			
SDA4-M2	↑	↑	↑	→	→	↑			
SDA4-M3	↑	↑	↑		→	→	↑	→	↑
SDA8-M3							↑	→	↑

12 Acknowledgements

The authors would like to acknowledge the financial support of the Swiss Roads authority. The practical contribution and advice of the advisory committee (BK) throughout the duration of the project is acknowledged and appreciated. Michele Griffa and Martin Arraigada of Empa are gratefully acknowledged for performing the CT scans and the MMLS3 experiments. Pietro Luraschi from IMP is gratefully acknowledged for his cooperation in the project.

Appendix

I Appendix I: Test results MMLS3

Reference plate SDA 4-S Reference

Sound absorption measurements

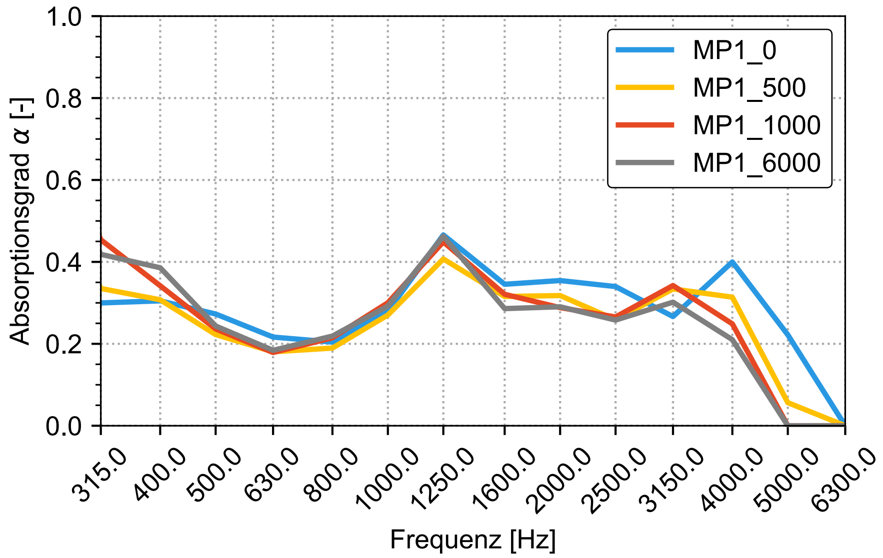

Fig. 73 *Measured sound absorption measurements for the reference plate SDA 4-S for MP1*

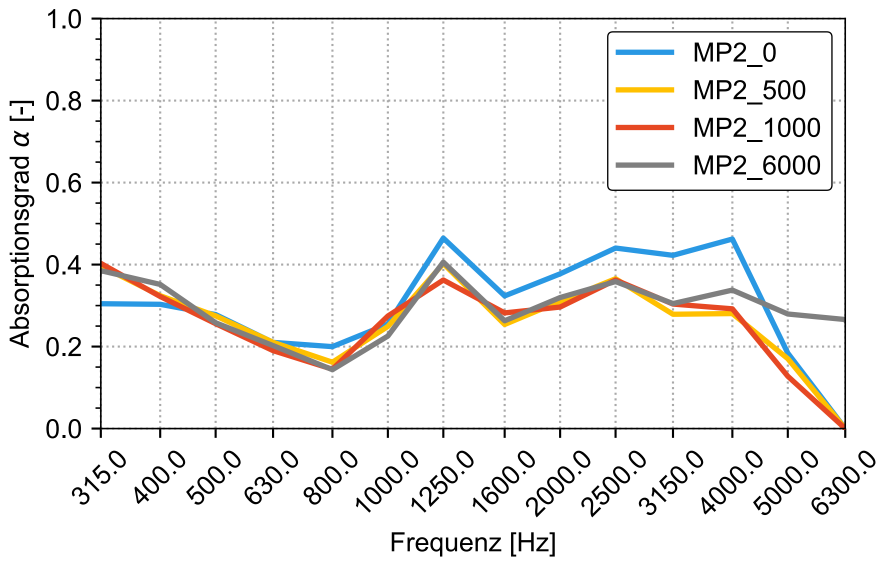

Fig. 74 *Measured sound absorption measurements for the reference plate SDA 4-S for MP2*

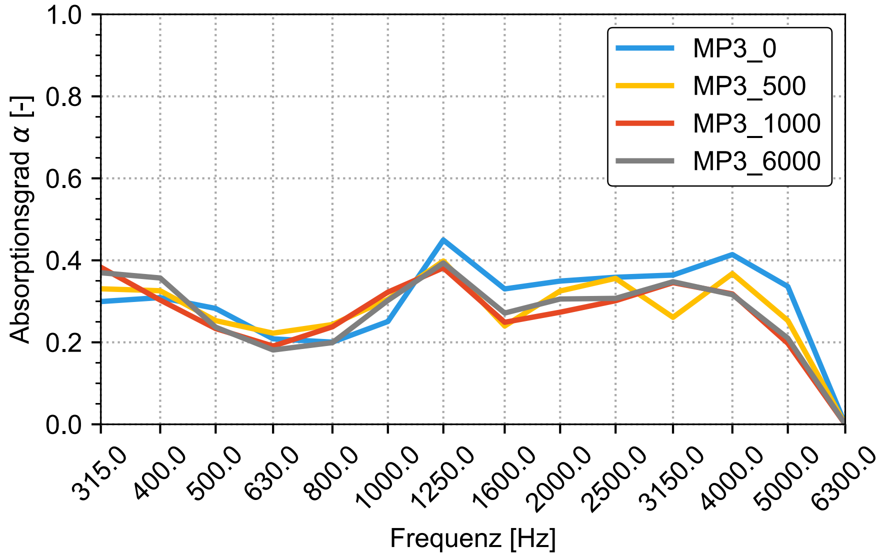

Fig. 75 *Measured sound absorption measurements for the reference plate SDA 4-S for MP3*

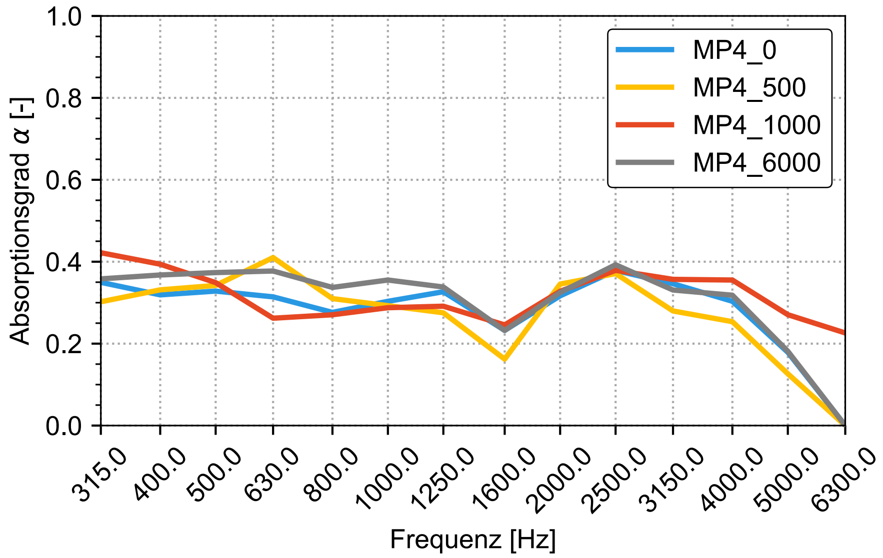

Fig. 76 *Measured sound absorption measurements for the reference plate SDA 4-S for MP4*

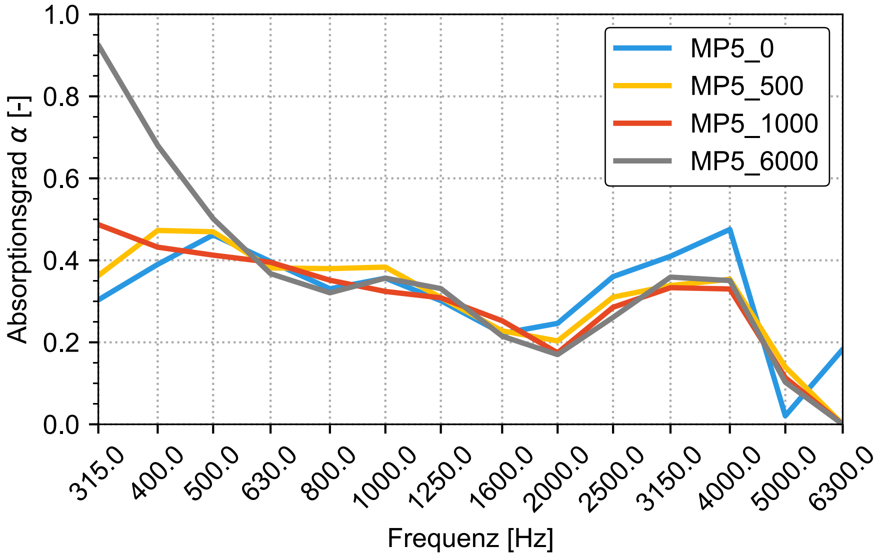

Fig. 77 *Measured sound absorption measurements for the reference plate SDA 4-S for MP5*

II Appendix II: Mastic

Various combinations of tests with bitumen filler and additive was investigated as listed below.

Complex modulus and phase angle of Bitumen with filler and additive

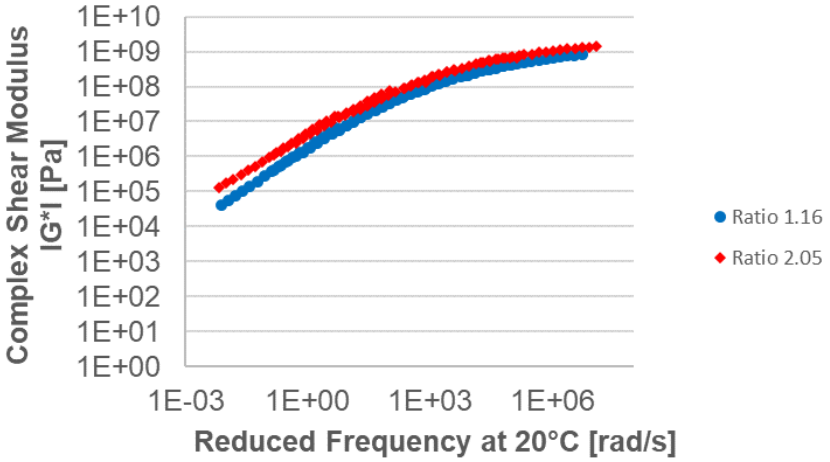

Fig. 78 *Comparison between two different Filler/Bitumen ratios. The influence for low temperatures is shown in Tab. 19.*

Tab. 19 *Ratio of the complex modulus for two different filler to bitumen ratios at 13.1 rad/s*

Temperature [°C]	Komplex Modulus 2.05 Filler / 1.16 Filler
-10	1.75
0	1.97
10	2.12
20	2.18
30	2.40

As seen before, the higher the temperature the higher the influence of the filler

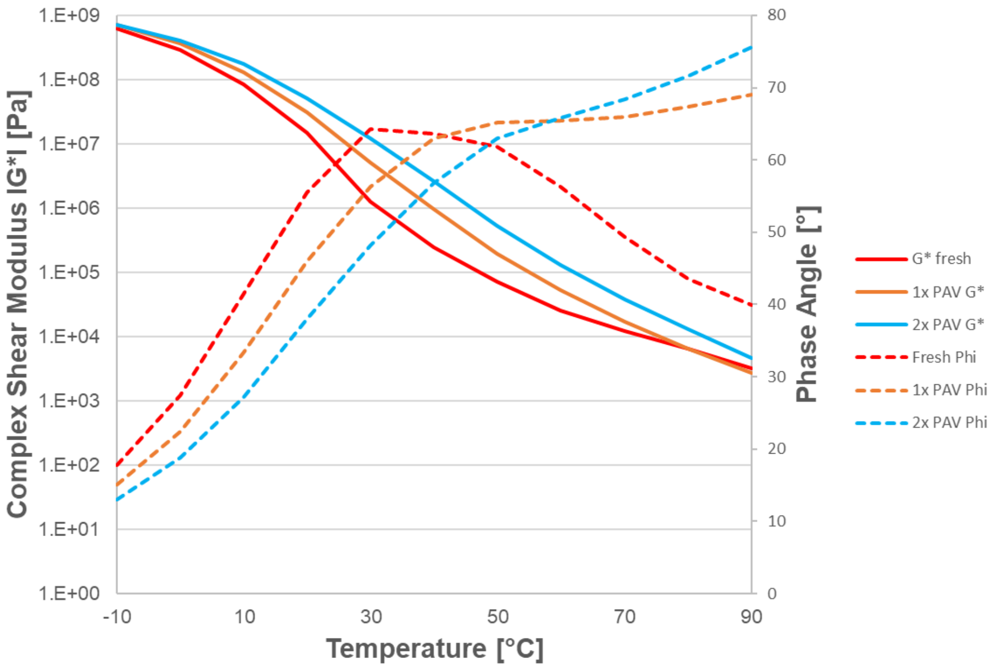

***Fig. 79** Lime filler with PmB 45/80-65 change with each ageing step. The Phase angle for high temperatures grows with each ageing step*

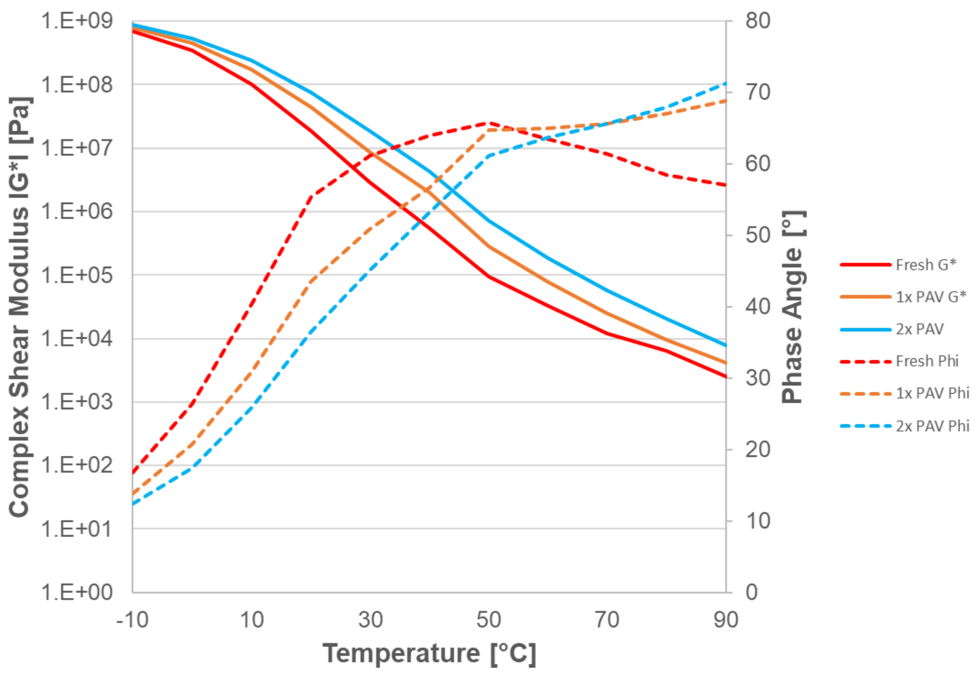

Fig. 80 *Zeobit Filler with PmB 45/80-65; change with each ageing step*

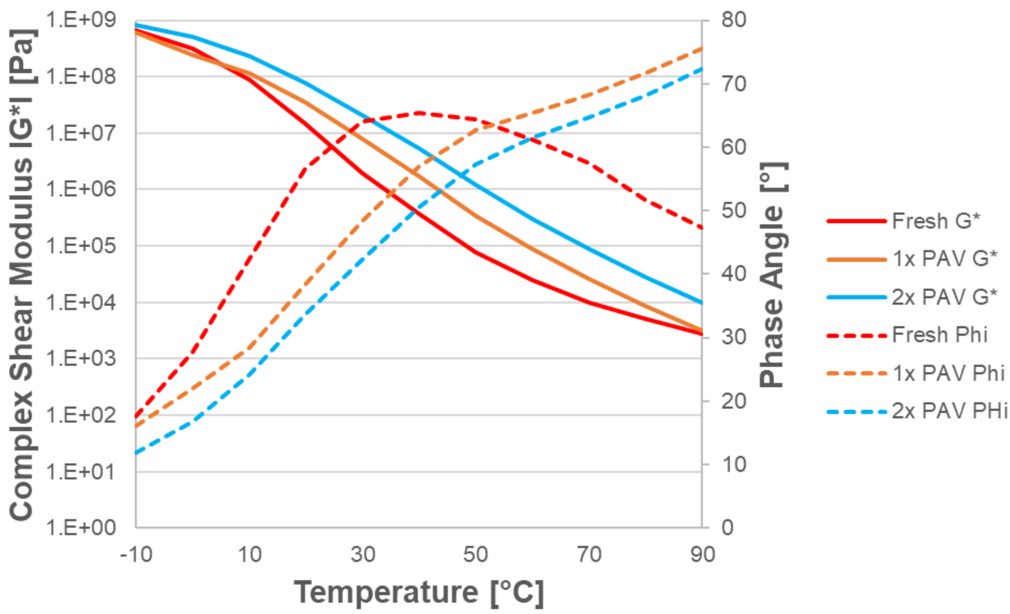

Fig. 81 *Zeofill filler with PmB 45/80-65, change with each ageing step*

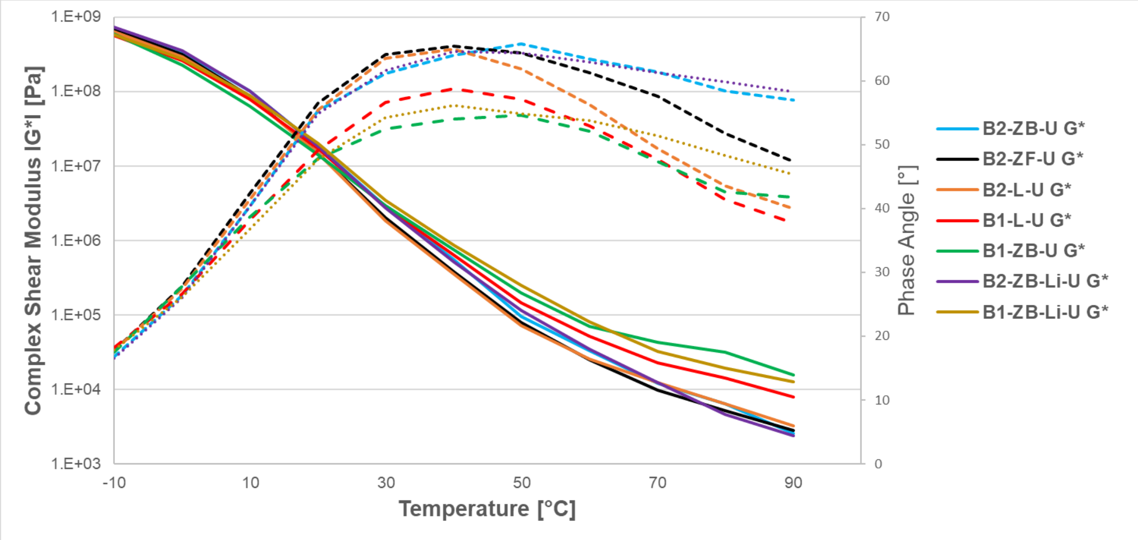

Fig. 82 *Two Bitumen (B1 and B2) with three fillers (ZB, ZF, L) and one additive (Li) in unaged (U) state*

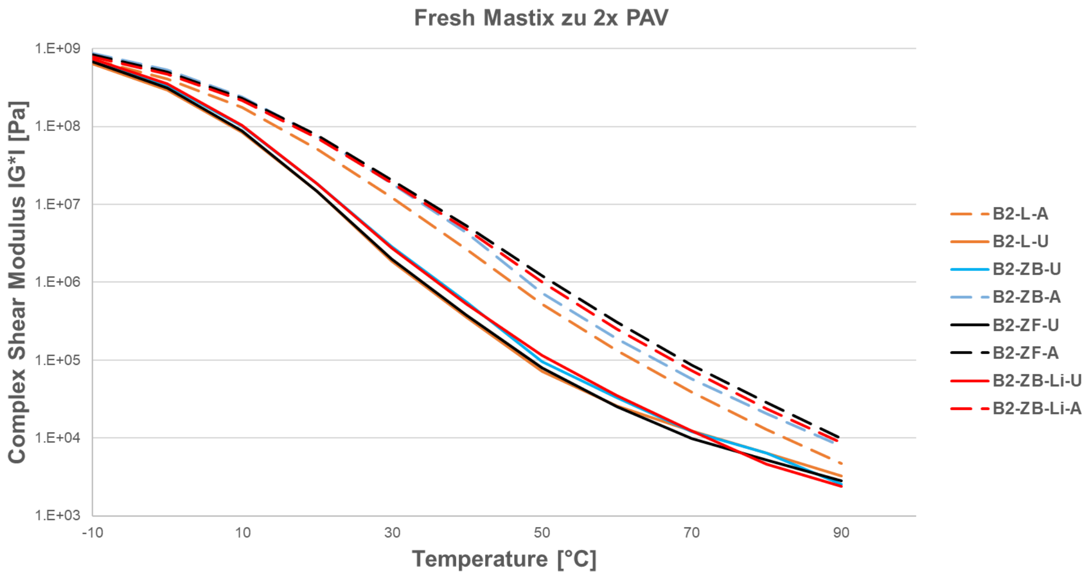

Fig. 83 *Comparison of the ageing effect on the complex shear modulus IG*I between PmB 45/80-65 (B2) and different fillers and one additive*

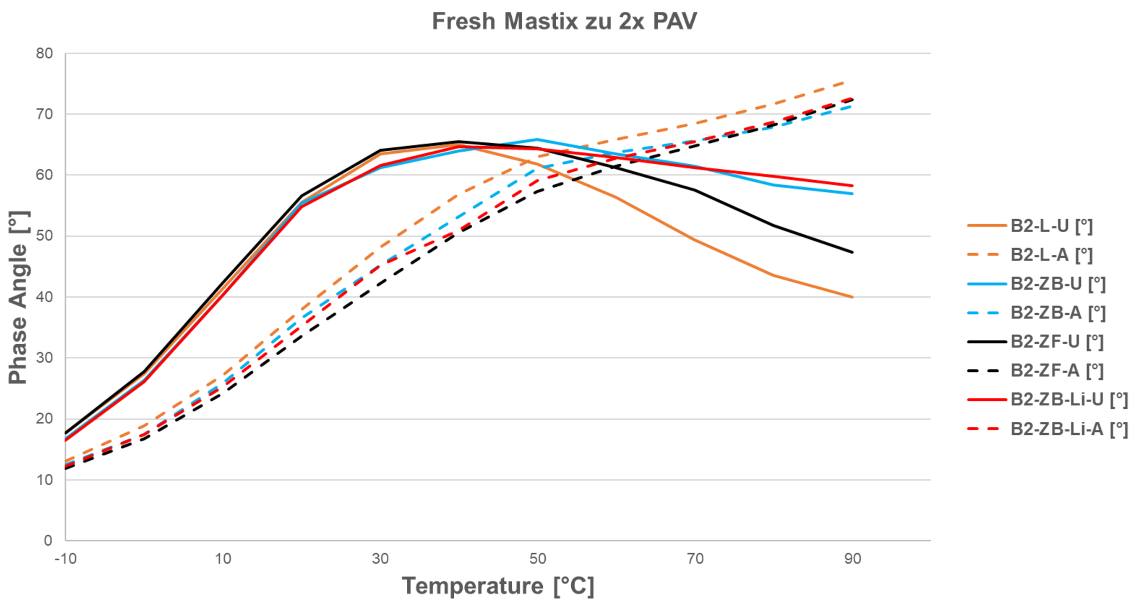

Fig. 84 *Comparison of the ageing effect on the phase angle [°] between PmB 45/80-65 with different fillers and one additive.*

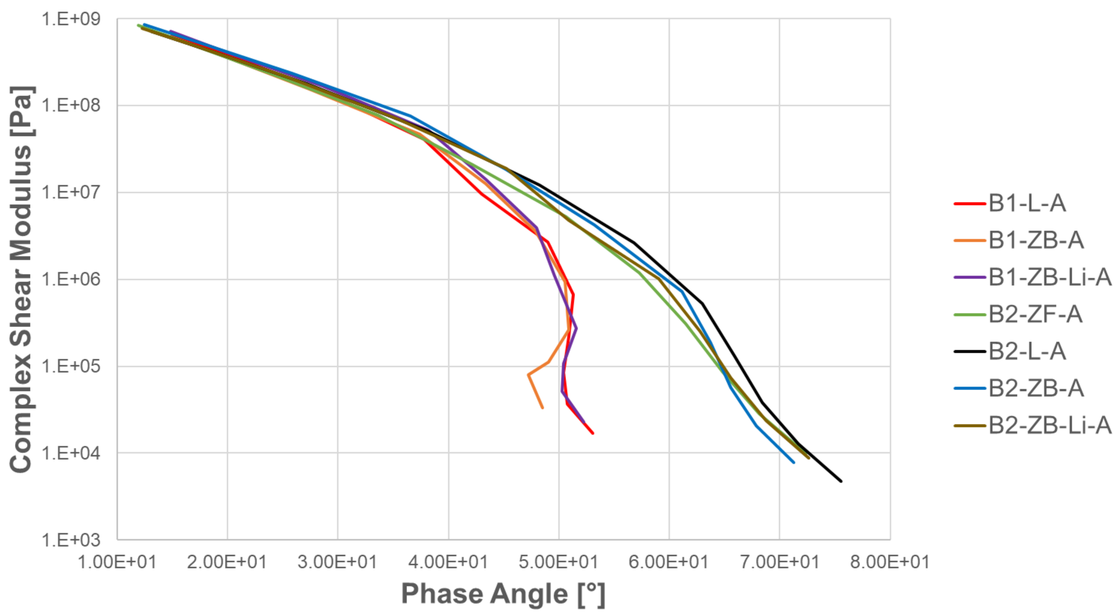

Fig. 85 *black diagram showing complex modulus vs phase angle of aged mastics*

Glossary

Abbreviation	**Meaning**
SDA	Semi Dense Asphalt
CPX	Close Proximity Method
PA	Porous Asphalt
SBS	Styrene Butadiene Styrene Polymer
EVA	Ethylene Vinyl Acetate polymer
ITS	Indirect Tensile Strength
ITSR	Indirect Tensile Strength Ratio
CCT	Cyclic Compression Test
MMLS3	Model Mobile Load Simulator

Bibliography

Standards

[1] American Association of State and Highway Transportation Officials (2020), „**Standard Method of Test for Estimating Fatigue Resistance of Asphalt Binders Using the Linear Amplitude Sweep**“, *AASHTO T 391-20.*

[2] Schweizerischer Verband der Strassen- und Verkehrsfachleute VSS (2011), „**Tests for mechanical and physical properties of aggregates - Part 1: Determination of the resistance to wear (micro-Deval)**", *SN-670903-1_EN-1097-1-E.*

[3] Schweizerischer Verband der Strassen- und Verkehrsfachleute VSS (2020), „**Bituminous mixtures - Test methods for hot mix asphalt - Part 12: Determination of the water sensitivity of bituminous specimens**", *SN_EN_12697-12_2020-01_EN.*

[4] Schweizerischer Verband der Strassen- und Verkehrsfachleute VSS (2018), „**Bituminous mixtures - Test methods - Part 17: Particle loss of porous asphalt specimens**", *EN-12697-17-D_SN-670417-NV*.

[5] Schweizerischer Verband der Strassen- und Verkehrsfachleute VSS (2020), „**Bituminous mixtures - Test methods for hot mix asphalt - Part 22: Wheel tracking**", *SN-EN-12697-22_2020-08_EN.*

[6] Schweizerischer Verband der Strassen- und Verkehrsfachleute VSS (2019), „**Bituminous mixtures Test methods - Part 23: Determination of the indirect tensile strength of bituminous specimens**", *SN_EN_12697-23_2019_EN.*

[7] Schweizerischer Verband der Strassen- und Verkehrsfachleute VSS (2019), „**Bituminous mixtures – Test methods for hot mix asphalt – Part 24: Resistance to fatigue**", *SN_EN_12697-24_2019_EN.*

[8] Schweizerischer Verband der Strassen- und Verkehrsfachleute VSS (2019), „**Bituminous mixtures – test methods for hot mix asphalt – Part 25: Cyclic compression test**", *SN_EN_12697-25_2019_EN.*

[9] Schweizerischer Verband der Strassen- und Verkehrsfachleute VSS (2023), „**Bituminous mixtures – Test methods for hot mix asphalt – Part 26: Stiffness**", *SN-EN-12697-26_A1_2023-04_EN*.

[10] Schweizerischer Verband der Strassen- und Verkehrsfachleute VSS (2020), „**Bituminous Mixtures - Test Methods for Hot Mix Asphalt - Part 44: Crack Propagation by Semi-circular Bending Test**", *SN_EN_12697-44_2020-01_EN.*

[11] Schweizerischer Verband der Strassen- und Verkehrsfachleute VSS (2016), „**Bitumen and bituminous binders. Determination of needle penetration**", *SN-670511_EN-1426-E*

[12] Schweizerischer Verband der Strassen- und Verkehrsfachleute VSS (2013), „**Bitumen and bituminous binders - Accelerated long-term ageing conditioning by a Pressure Ageing Vessel (PAV)**", *SN-670558-E_EN-14769-E*

[13] Schweizerischer Verband der Strassen- und Verkehrsfachleute VSS (2013), „**Bitumen and bituminous binders - Determination of complex shear modulus and phase angle - Dynamic Shear Rheometer (DSR)**", *SN-670559-E_EN-14770-E.*

[14] International Organization for Standardization [ISO] (2018), „**Acoustics - Determination of airflow resistance - Part 1 Static airflow method**", *ISO 9053-1.*

[15] Schweizerischer Verband der Strassen- und Verkehrsfachleute VSS (2022), „**Bituminous mixtures; Material specifications – Part 1: Asphalt Concrete**", *SN-EN-13108-1_2022-09_EN.*

[16] Schweizerischer Verband der Strassen- und Verkehrsfachleute VSS (2019), „**Semidichtes Mischgut und Deckschichten; Festlegungen, Anforderungen, Konzeption und Ausführung**", *VSS-40436.*

[17] ASTRA (2006), „**Technisches Merkblatt für offenporige, lärmarme Beläge auf Autobahnen**", Bern, Switzerland.

[18] Forschungsgesellschaft für Strassen- und Verkehrswesen e.V., Köln FGSV (2013), „**Bestimmung der mechanischen Festigkeit an der Gesteinskörnung 0/5.6mm - modifiziertes Micro-Deval-Verfahren**", *TP Gestein-StB, Teil 5.5.3*

[19] Schweizerischer Verband der Strassen- und Verkehrsfachleute VSS (2022), „**Semidichtes Mischgut und Deckschichten; Festlegungen, Anforderungen, Konzeption und Ausführung**", *VSS-40436_2022-09*

Reports

[20] Angst, Ch., Bosshard, D., Clavien Ch., Grolimund, H.-J. & Pestalozzi, H. (2004, 2005, 2006), „**Lärmarme Beläge innerorts**“, *Jahresbericht, BAFU/ASTRA.*

[21] Angst, Ch., Beltzung, F., Bosshardt, D., Grolimund ,H. J., Pestalozzi, H. & Bühlmann, E. (2010), „**Lärmarme Strassenbeläge innerorts**“, *Forschungsauftrag ASTRA 2004/06, Bern, Switzerland.*

[22] Angst, Ch., Bürgisser, Ph. & Beckenbauer, Th. (2016), „**Lärmarme Beläge innerorts EP 2: Labortechnische Bestimmung der Dauerhaftigkeit lärmarmer Beläge**", *Forschungsauftrag VSS 2010/011, Bern, Switzerland.*

[23] Beckenbauer, T., Belcher D., Kneib, G. & Angst, Ch. (2016), „**Forschungspaket: lärmarme Beläge innerorts / EP 4: Labormethoden für die Bestimmung akustischer Eigenschaften lärmarmer Beläge**", *Forschungsauftrag ASTRA 2010/013, Bern, Switzerland.*

[24] Bühlmann, E., Bürgisser, P., Ziegler, T., Angst, C. & Beckenbauer, T. (2017), „**Report TP3 long-term monitoring, Research Package on low-noise road pavements in urban areas**", *end report, Oberbuchsiten, Bern, Allschwil: IMP Bautest AG, Grolimund + Partner AG, Müller-BBM Schweiz AG.*

[25] Bühlmann, E, Egger, S., Hammer, E. & Ziegler, T. (2017), „**Basic information for assessing noise effects at speed limit 30 km/h**", *VSS2012/2014, Bern, Switzerland.*

[26] Bühlmann, E., Hammer, E., Bueche, N. & Perret, J. (2017), „**Ausführungsbestimmungen Akustik für semidichte Asphalte – Auswertung physischer Parameter**", *Report G+P 21.10.2017, Forschungsauftrag BAFU A4852, Bern, Switzerland*

[27] Catillaz, A. & Fischer, F. (2018), „**Lärmbelastung in der Schweiz, Ergebnisse des nationalen Lärmmonitorings sonBASE, Stand 2015**", *BAFU, Bern, Switzerland.*

[28] Kuijpers, A., Peeters, B., Kropp, W. & Beckenbauer, T. (2007), „**Acoustic Optimization Tool RE4 – Modelling refinements in the SPERoN framework**", *Report M+P*, http://www.innovatieprogrammageluid.nl.

[29] Perret, J., Bolli, J.-P. & Arn, T. (2017), „**Forschungspaket lärmarme Beläge innerorts: Synthesebericht**", *Forschungsprojekt ASTRA 2010/004, Bern, Switzerland.*

[30] Pestalozzi, H., Grolimund, H.-J. & Angst, Ch. (2003), „**Lärmarme Strassenbeläge innerorts**", *Statusbericht BUWAL/ASTRA 2004, Bern, Switzerland.*

[31] Poulikakos, L. D., Gubler, R., Partl, M. N., Pittet, M., Arnaud, L., Junod, A., Dumont, A. G. & Simond, E. (2006), „**Mechanical Properties of Porous Asphalt, Recommandations for Standardization**", *Forschungsauftrag VSS 1999/280; Bern, Switzerland.*

[32] Schlatter, F., Schweizer, D., Bühlmann, E. (2023), „**Präzisierung Ausführungsbestimmungen Akustik SDA-Beläge 2022, Auswertung Bauparameter & Akustik**", *Forschungsauftrag A6142, Bundesamt für Umwelt (BAFU), Bundesamt für Strassen (ASTRA), Kanton Aargau, Kanton St. Gallen, Switzerland.*

[33] Wehr, R., Fuchs, A., Schlatter, F., Bühlmann, E., Männel, M., Beckenbauer, T., Wistuba, M., Grönniger, J. & Weninger-Vycudil, A. (2020), "**Akustische Dauerhaftigkeit larmmindernder dichter oder ¨ semi-dichter Asphaltdeckschichten ADURA**", , https://projekte.ffg.at/anhang/60797daa0cb02_ADURA_Ergebnisbericht.pdf, *last accessed 13.11.2024.*

[34] World Health Organization (2011), „**Burden of disease from environmental noise, Quantification of healthy life years lost in Europe**", *report available at:* https://www.who.int/publications/i/item/9789289002295, *last accessed 13.11.2024.*

[35] World Health Organization (2017), „**Metrics: Disability-Adjusted Life Year (DALY)**", report available at http://www.who.int/healthinfo/global_burden_disease/metrics_daly/en/, *last accessed 22.09.2017*

Scientific publications and thesis

[36] Angst, Ch. (1982), „**Morphologische Beurteilung verdichteter bituminöser Mischungen**“, *Diss ETH 7002.*

[37] Airey, G. D. (2011), „**Use of Black Diagrams to Identify Inconsistencies in Rheological Data**“, *Road Materials and Pavement Design, Vol. 3, No. 4, pp. 403–424.*

[38] Arraigada, M., Pugliessi, A., Partl, M. N. & Martinez, F. (2014), “**Effect of full-size and down-scaled accelerated traffic loading on pavement behavior**“, *Mater Struct, 47, 1409–1424.*

[39] Bennert, T., Hanson, D., Maher, A. & Vitillo, N. (2005), „**Influence of pavement surface type on tire/pavement generated noise**", *ASTM International. J. Test. Eval., 33(2): 94–100.*

[40] Bueno, M., Hugener, M. & Partl, M. N. (2015), „**Fracture toughness evaluation of bituminous binders at low temperatures**", *Mater Struct, 48, 3049-3058.*

[41] Bühlmann, E. & Ziegler, T. (2012), „**Interpreting measured acoustic performance on Swiss low-noise road surfaces using a tyre/road interaction model**", *Proc. Conference: Acoustics Hong-Kong, China*

[42] Bühlmann, E. & Hammer E. (2017), „**Towards semi-dense asphalt mixtures that guarantee acoustic performance and durability**", *Proc. Conference: Internoise, Hong Kong, China.*

[43] Clavien, Ch. & Angst, Ch. (2005), „**Enrobé drainant oui ou non?**", *Journée technique LAVOC.*

[44] Feldkamp, L. A., Davis, L. C. & Kress, J. W. (1984), „**Practical cone-beam algorithm**", *J. Opt. Soc. Am. A. 1, 612-619.*

[45] Freitas, E. F. (2012), „**The effect of time on the contribution of asphalt rubber mixtures to noise abatement**", *Noise Control Engineering Journal, 60, 1-8.*

[46] Gorkem, C. & Sengoz, B. (2009), „**Predicting stripping and moisture induced damage of asphalt concrete prepared with polymer modified bitumen and hydrated lime**", *Construction and Building Materials, 23 (6), 2227-2236.*

[47] Gruber, I., Zinovik, I., Holzer, L., Flisch, A. & Poulikakos, L. D. (2012), „**A computational study of the effect of structural anisotropy of porous asphalt on hydraulic conductivity**", *Construction and Building Materials, 36, 66-77.*

[48] Herman, G. T. (1979), „**Correction for Beam Hardening in Computed tomography**", *Phys Med Biol., 24, 81-106.*

[49] Kakar, R. M., Mikhailenko, P., Piao, Z. & Poulikakos, L. D. (2022), „**High and low temperature performance of polyethylene waste plastic modified low noise asphalt mixtures**", *Construction and Building Materials, 348, 128633.*

[50] Ketcham, R. A. & Hanna, R. D. (2014), „**Beam hardening correction for X-ray computed tomography of heterogeneous natural materials**", *Computers & Geosciences. 67 49-61.*

[51] Knabben, R. M., Trichês, G., Gerges, S. N. Y. & Vergara, E. F. (2016), „**Evaluation of sound absorption capacity of asphalt mixtures**", *Applied Acoustics, 114, 266-274.*

[52] Liao, G., Sakhaeifar, M. S., Heitzman, M., West, R., Waller, B., Wang, S. & Ding, Y. (2014), „**The effects of pavement surface characteristics on tire/pavement noise**", *Applied Acoustics, 76, 14-23.*

[53] Mikhailenko, P., Griffa, M., Pieren, R., Pachale, U. & Poulikakos, L. D. (2024), „**Pore Space of In-Situ Semi-Dense Asphalt: A Characterization by X-Ray Tomography**", *Construction and Building Materials, 453, 139091.*

[54] Mikhailenko, P., Piao, Z., Kakar, M.R., Bueno, M., Athari, S., Pieren, R., Heutschi, K. & Poulikakos, L. (2020), „**Low-Noise pavement technologies and evaluation techniques: a literature review**", *International Journal of Pavement Engineering, 23(6), 1911–1934.*

[55] Molenaar, A. A. A., Scarpas, A., Liu, X. & Erkens, S. M. J. G. (2002), „**Semi-circular bending test; simple but useful?**", *Journal of the Association of Asphalt Paving Technologists, 71.*

[56] Paje, S. E., Bueno, M., Teran, F., Vinuela, U. & Luong, J. (2008), „**Assessment of asphalt con-crete acoustic performance in urban streets**", *Journal of the Acoustical Society of America, 123(3), 1439-1445.*

[57] Paje, S. E., Luong, J., Vazquez, V. F., Bueno, M. & Miro, R. (2013), „**Road pavement rehabilitation using a binder with a high content of crumb rubber: Influence on noise reduction**" *Construction and Building Materials, 47, 789-798.* doi:10.1016/j.conbuildmat.2013.05.008

[58] Poulikakos, L. D., Buttlar, W., Schüwer, N., Lo Presti, D., Balmer, T. & Bueno, M (2021), „**Can crumb rubber modifier effectively replace the use of polymer- modified bitumen in asphalt mixture?**", *Sustainable and Resilient Infrastructure, 7(5), 515–530.*

[59] Poulikakos, L. D. & Partl, M. N. (2009), „**Evaluation of moisture susceptibility of porous asphalt con-crete using water submersion fatigue tests**", *Construction and Building Materials, 23(12), 3475-3484.*

[60] Poulikakos, L. D. & Partl, M. N. (2011), „**Micro Scale Tensile Behaviour of Thin Bitumen Films**", *Experimental Mechanics, 51(7), 1171-1183.*

[61] Poulikakos, L. D. & Partl, M. N. (2012), „**A multi-scale fundamental investigation of moisture induced deterioration of porous asphalt concrete**", *Construction and Building Materials, 36, 1025-1035.*

[62] Poulikakos, L. D., dos Santos, S., Bueno, M., Kuentzel, S., Hugener, M. & Partl, M. N. (2014), „**Influence of short and long term aging on chemical, microstructural and macro-mechanical properties of recycled asphalt mixtures**", *Construction and Building Materials, 51, 414-423.*

[63] Poulikakos, L. D., Heutschi, K. & Soltic, P. (2013), „**Heavy duty vehicles: Impact on the environment and the path to green operation**", *Environmental Science & Policy, 33, 154-161.*

[64] Poulikakos, L. D., Morgan, G. C. J., Muff, R., Partl, M. N., Doupal, E. & Calderara, R. (2008), „**Interpretation of accelerated laboratory testing of the prototype Modulas stress in motion sensor with the MMLS3 load simulator"**, *Journal of Transportation Engineering-Asce, 134(10), 414-422.*

[65] Poulikakos, L. D., Pittet, M., Dumont, A. G. & Partl, M. N. (2014), „**Comparison of the two point bending and four point bending test methods for aged asphalt concrete field samples**", *Materials and Structures, 48(9), 2901-2913.*

[66] Poulikakos, L. D., Tiwari, M. K. & Partl, M. N. (2013), „**Analysis of failure mechanism of bitumen films**", *Fuel, 106, 437-447.*

[67] Poulikakos, L. D., Athari, S., Mikhailenko, P., Kakar, M. R., Bueno, M., Piao, Z., Pieren, R. & Heutschi, K., (2022), „**Effect of waste materials on acoustical properties of semi-dense asphalt mixtures**", *Transp. Res. Part Transp. Environ. 102, 103154.*

[68] Poulikakos, L. D. & Hofko, B. (2020), „**A critical assessment of stiffness modulus and fatigue performance of plant produced asphalt concrete samples using various test methods**", *Road Materials and Pavement Design, 22(11), 2661-2673.*

[69] Praticò, F. G. & Briante, P. G. (2020), „**Prediction of surface texture for better performance of friction courses**", *Construction and Building Materials, 230, 116991.*

[70] Rigden, P. J. (1965), „**The Use of Fillers in Bituminous Road Surfacing : A Study of Filler-Binder Systems in Relation to Filler Characteristics**", *Jour. Society of Chemical Industry, 66, 299-309.*

[71] Rinaldini, E., Schuetz, P., Partl, M. N., Tebaldi, G. & Poulikakos, L. D. (2014), „**Investigating the blending of reclaimed asphalt with virgin materials using rheology, electron microscopy and computer tomography**", *Composites Part B-Engineering, 67, 579-587.*

[72] Schaffer, B., Schlittmeier, S. J., Pieren, R., Heutschi, K., Brink, M., Graf, R. & Hellbruck, J. (2016), „**Short-term annoyance reactions to stationary and time-varying wind turbine and road traffic noise: A laboratory study"**, *Journal of the Acoustical Society of America, 139(5), 2949-2963.*

[73] Schlatter F. & Bühlmann E. (2020), „**Acoustic optimization of asphalts using Acoustic Void Content Analysis AVCA on drill cores**", *Proceedings of 2020 International Congress on Noise Control Engineering, InterNoise 2020, Seoul, Korea.*

[74] Skov, R., Cesbron, J. & Bendtsen, H., (2015), „**Laboratory measurements on poroelastic test slabs from full scale test sections**", *Euronoise 2015, Maastricht, Netherlands.*

[75] Soenen, H., Besamusca, J., Fischer, H. R., Poulikakos, L. D., Planche, J. P., Das, P. K. & Chailleux, E. (2014), „**Laboratory investigation of bitumen based on round robin DSC and AFM tests**". *Materials and Structures, 47(7), 1205-1220.*

[76] Sonderegger, T., Dewulf, K., Fantke, P., Maia de Souza, D., Pfister, S., Stoessel, F., Verones, F., Vieira, M., Weidema, B. & Hellweg, S. (2017), „**Towards harmonizing natural resources as an area of protection in Life Cycle Impact Assessment**", *Int J Life Cycle Assess 22, 1912-1927.*

[77] Steiner, S., Bühlmann, E. & Hammer, E. (2018), „**Milestones in establishing low-noise asphalts as a widely used, effective and durable noise abatement measure in Switzerland**", *Proceedings of 2018 International Congress on Noise Control Engineering, InterNoise 2018, Crete, Greece.*

[78] Steiner, S., Schlater, F. & Bühlmann, E. (2022), „**Achieving a better match between ordered and actual performance of urban low-noise asphalts -exploring better solutions for noise abatement**", *Proceedings of 2022 International Congress on Noise Control Engineering, InterNoise 2022, Glasgow, UK.*

[79] Tonin, R. (2016), „**Quiet Road Pavements: Design and Measurement-State of the Art**", *Acoust Aust 44, 235-247.*

[80] Zaumanis, M., Cavalli, M. C. & Poulikakos, L. D. (2020), „**Effect of rejuvenator addition location in plant on mechanical and chemical properties of RAP binder**", *International Journal of Pavement Engineering, 21 (4), 507-515.*

Books

[81] Sandberg, U. & Ejsmont, J. A. (2002), „**Tyre/road noise reference book**", *INFORMEX, Kisa, Sweden.*

Media and Internet

[82] Federal Council (2017), „**Neuer Massnahmenplan zur Bekämpfung von Lärm**", *News release,* https://www.bafu.admin.ch/bafu/de/home/themen/laerm/mitteilungen.html *(in German/French), last accesed: 2.10.2024, Bern, Switzerland.*

[83] Lesueur, D. (2009), „**The Benefits of Hydrated Lime in Asphalt Mixtures**", *Presentation at the Pennsylvania Asphalt Pavement Association PAPA annual meeting, available at:* https://www.slideshare.net/slideshow/benefits-of-hydrated-lime/4080003, *last accessed 13.11.2024.*

Project sign off

Schweizerische Eidgenossenschaft
Confédération suisse
Confederazione Svizzera
Confederaziun svizra

Eidgenössisches Departement für
Umwelt, Verkehr, Energie und Kommunikation UVEK
Bundesamt für Strassen ASTRA

FORSCHUNG IM STRASSENWESEN DES UVEK

Version vom 09.10.2013

Formular Nr. 3: Projektabschluss

erstellt / geändert am: 01.03.2024

Grunddaten

Projekt-Nr.:	TRU_20_01D_01
Projekttitel:	Improving the durability of low-noise SDA through a multi-scale optimization
Enddatum:	30.04.2024

Texte

Zusammenfassung der Projektresultate:

This project aimed to improve mechanical and acoustic durability of various low noise pavements, namely : SDA 4, SDA 6 and SDA 8. These mixtures as well as the corresponding mastic (filler+bitumen+additive) were tested for their mechanical and acoustic performance partially in non-aged and aged states using a multi-scale approach (mm to m).

In WP1, the mechanical properties of benchmark mastics and mixtures were examined.
In WP2, the mixtures that had good low-noise properties in situ were identified;
In WP3 the mastic and mixtures were modified and characterized;
Mixtures selected in WP4 were mechanically and acoustically examined on a m-scale;
The results were published in WP5.

As a result of this research project the following is recommended:
• This investigation has shown that using highly modified binder with stiffening Zeobit filler improves the mechanical performance of SDA mixtures and without harming the acoustic performance.
• A voids content of 15% was recommended for SDA in order to strike a balance between acoustic and mechanical performance.
• Using the MMLS3 load simulator, and measurements before and after exposure to loads, the acoustic modelling has shown that the noise levels improved between the unloaded and loaded measurement points for the modified mixtures SDA 4 and 8 with the highly modified binder and Zeobit. This indicates that the modification resulted in similar resistance to mechanical aging from wheel tracking.

Forschung im Strassenwesen des UVEK: Formular 3 — Seite 1 / 3

Schweizerische Eidgenossenschaft
Confédération suisse
Confederazione Svizzera
Confederaziun svizra

Eidgenössisches Departement für
Umwelt, Verkehr, Energie und Kommunikation UVEK
Bundesamt für Strassen ASTRA

Zielerreichung:

According to the proposal, the main objectives were to improve the acoustic and mechanical durability of SDA 4, SDA 6 and SDA 8 by optimizing and adapting the mixtures to different traffic and climatic conditions present on the Swiss national and main road network using a multi-scale approach.
The laboratory results allowed the highly modified binder and Zeobit filler to be identified as ingredients to SDA mixtures for improving the mechanical performance without compromising the acoustic performance. Moreover, targeting 15% voids content in these types of mixtures was identified as a volumetric value to strike a balance between acoustic and mechanical performance. According to the results, we consider the general objectives of the project have been successfully accomplished.

Folgerungen und Empfehlungen:

Future project should continue focusing on the improvement of the long term mechanical and acoustic properties of low noise asphalt mixtures. The ingredients identified in highly modified binder and Zeobit filler should be evaluated for their cost effectiveness and environmental effects compared to the ingredients they are replacing. Further possible projects should include the addition of RAP in order to improve the sustainability of the mixtures without compromising its performance.

Publikationen:

Mikhailenko, P., Schlatter, F., Poulikakos, L., Angst, C., Huber, L., Bühlmann, E., 2024. Optimizing the acoustical durability of semi-dense asphalt from statistical analysis of in-situ performance based on mixture data. Presented at the 10th International Conference on Maintenance and Rehabilitation of Pavements—Mairepav10, Guimarães, Portugal.

Additional journal paper currently in preparation.

Der Projektleiter/die Projektleiterin:

Name: Lily Vorname: Poulikakos

Amt, Firma, Institut: Empa

Unterschrift des Projektleiters/der Projektleiterin:

i.V. Martin Arraigada

Forschung im Strassenwesen des UVEK: Formular 3 Seite 2 / 3

Schweizerische Eidgenossenschaft
Confédération suisse
Confederazione Svizzera
Confederaziun svizra

Eidgenössisches Departement für
Umwelt, Verkehr, Energie und Kommunikation UVEK
Bundesamt für Strassen ASTRA

FORSCHUNG IM STRASSENWESEN DES UVEK

Formular Nr. 3: Projektabschluss

Beurteilung der Begleitkommission:

Beurteilung:

The project has been performed in agreement with the project description and each project partner contributed to the project success. The final report has been validated by BK and the various comments taken into account by research partners.

The project results provided some insight in the field of the improvement of SDA mechanic and acoustic optimization.

Umsetzung:

The results can be used in order to provide some guidelines for the future optimization of SDA mixtures. Tests and results related to filler, bitumen and mastic are some interesting optimization points for such asphalt mixtures. The implementation is mainly expected through construction companies or road owners that are willing to improve the (acoustic and mechanic) service life of SDA.

weitergehender Forschungsbedarf:

Some future researches could be performed in the field of SDA optimization (acoustic and mechanic) and also in the field of rehabilitation strategies of fuch mixtures. Considering the various reserarches performed in that field in the last 10-15 years, it could be suggested to summarize the results and then organized a more global research projects with some specific WP dedicated to relevant aspects.

Einfluss auf Normenwerk:

No major influence on standards. The project is mainly related to mixture optimization.

Der Präsident/die Präsidentin der Begleitkommission:

Name: Bueche Vorname: Nicolas

Amt, Firma, Institut: IMP Bautest AG

Unterschrift des Präsidenten/der Präsidentin der Begleitkommission:

Bueche.